MAMMALIAN MISMATCH REPAIR: HOTSPOTS AND PROTEIN COMPLEXES

By

Nancy Matton

RECOMMENDED:

Advisory Committee Chair

Department Head

APPROVED:

Dean of the College of Science, Engineering and Mathematics

Dean of the Graduate School

Date

MAMMALIAN MISMATCH REPAIR: HOTSPOTS AND PROTEIN COMPLEXES

A

THESIS

Presented to the Faculty

of the University of Alaska Fairbanks

in Partial Fulfillment of the Requirements

for the Degree of

DOCTOR OF PHILOSOPHY

By

Nancy Matton B.S., A.M.

Fairbanks, Alaska

May 2000

ABSTRACT

Deficiencies in DNA mismatch repair have been found in hereditary cancers as well as in sporadic cancers, illustrating the importance of mismatch repair in maintaining genomic integrity. To determine if inefficient mismatch repair can contribute to hotspots of mutation, repair rates were determined *in vivo* in mammalian cells for mismatched nucleotides located at H-*ras* codon 10 and compared to previously determined repair rates at a nearby activating hotspot of mutation, H-*ras* codon 12. Repair rates for H-*ras* codon 10 are significantly improved over repair rates at codon 12. This indicates that inefficiencies in mismatch repair are responsible, at least in part, for the well-documented hotspot of mutation at codon 12 and that surrounding sequence context can effect repair of mismatches. Gel-shift analysis demonstrates that the degree of binding by the initial mismatch recognition factor hMutSα (heterodimer of hMSH6 and hMSH2) correlates with *in vivo* repair rates for each mismatch tested at the codon 12 location. UV cross-linking of nuclear proteins to G:A and G:T mismatches at codon 10 or codon 12 generally confirm these results. Overall this suggests that there is lowered efficiency in the kinetics of mismatch repair at codon 12, perhaps in the initiation step, rather than inaccurate repair leading to mutation.

The interactions of specific mismatch repair proteins in human nuclear extracts were then examined to determine the proteins binding to mismatched DNA. Immunoprecipitation followed by Western blotting indicates two novel complexes that exist in the absence of ATP: one consisting of hMSH2, hMSH6, hMLH1 and hPMS2 and the other consisting of hMSH2, hMSH6, hMLH1 and hPMS1. Furthermore, the

protein complexes specifically bind to mismatched DNA and not to a similar homoduplex oligonucleotide. The protein complex-DNA interactions occur primarily through hMSH6, although hMSH2 can also become cross-linked to the mismatched substrate. In the presence of ATP, the binding of hMSH6 to mismatched DNA is decreased. In addition, hMLH1, hPMS2 and hPMS1 no longer interact with each other or with the hMutSα complex. However, the ability of hMLH1 to co-immunoprecipitate mismatched DNA *increases* in the presence of ATP, suggesting a role for hMLH1 in subsequent ATP-dependent repair processes.

TABLE OF CONTENTS

LIST OF FIGURES page

LIST OF TABLES page

I. Introduction

A. DNA Damage, Mutations and Cancer

Faithful maintenance of the genome is crucial for an individual's health and for propagation of the species. Unfortunately, DNA is constantly under attack, both from within and without, with the large genomes of mammalian cells making them especially vulnerable (for review of DNA damage see 1, 2). There are a number of sources of potential damage, one of which is mis-copying by the DNA replication enzymes (3). Although the main mammalian replicative polymerase, DNA polymerase δ, includes its own 3' –> 5' exonucleolytic proofreading capability, occasionally deletions, insertions and misincorporated nucleotides occur. As well, the DNA molecule itself exhibits some intrinsic instability, with tautomeric shifts, deaminations and depurinations/depyrimidinations constantly occurring. Perhaps most insidiously, necessary endogenous reactions such as those of aerobic respiration, produce reactive oxygen species and free radicals which can damage DNA through oxidative chain reactions. These reactions produce strand breaks, base loss and potentially mispairing residues such as thymine glycol and 8-hydroxyguanine. Finally, exogenous agents such as UV light, benzopyrene, aflatoxin, and cisplatin can attack DNA, both directly and indirectly, causing helix-distorting DNA lesions.

These damaging events take their toll on DNA. Overall, a single mammalian DNA molecule is estimated to undergo approximately 100,000 modifications per day (4).

However, in spite of this constant assault, the spontaneous mutation rate in normal cells is low (approximately 2×10^{-7} mutations/gene/cell division) (1,5). Obviously, efficient cellular mechanisms exist to repair most DNA damage. Sometimes though, mutations do occur despite the cell's best efforts. If they accumulate in several specific oncogenes and/or tumor suppressor genes a cell can acquire a transformed phenotype. Considering the rate of mutation, this has been calculated to be extremely unlikely to occur, leading to the hypothesis that an early event in tumorigenesis may be a gene mutation conferring a mutator phenotype (genome-wide elevation in mutation) (6). Evidence for the resulting genomic instability has recently been discovered in studies of sporadic tumors where 12-15% were found to contain thousands of mutations in microsattelite sequences (7).

Even more compelling evidence for the mutator theory comes from studies of 'cancer families', for example hereditary non-polyposis colon cancer (HNPCC) kindreds (for reviews see 8 - 11). HNPCC is an autosomal dominant disease in which family members are pre-disposed to early-onset colon cancer as well as tumors in the ovary, endometrium, stomach, pancreas, small intestine, skin and urinary tract. In these families germ-line mutations have been found in the genes associated with a specific DNA repair mechanism; long-patch mismatch repair. The individual's DNA contains a germline defect in one allele, while in tumor cells the remaining wild-type allele is typically lost or mutant (12). The result is a measurable elevation of the genome-wide mutation rate in the tumor cells (13), leading to the accumulation of mutations in genes that provide the selective advantages needed for a cell to give rise to a tumor. Further analysis has revealed that many spontaneous tumors that display increased mutation rates and

microsattelite instability also contain mutations in one of the long-patch mismatch repair genes (14, 15). This exciting research has forged a direct link between mutations in DNA repair genes, elevated mutation rate, and a predisposition to cancer, and has led to an increased interest in the mechanisms of mismatch repair. It is hoped that future developments in the field of DNA repair will lead to better diagnosis, treatment and perhaps, eventually, prevention of cancer.

B. DNA Repair

1. Damage reversal

Of the DNA repair mechanisms the simplest is direct damage reversal, for example ligation of strand breaks by DNA ligase (1). Another direct damage reversal system functions to photoreactivate UV damage. Although this system is extremely common it does not appear to occur in mammalian cells, perhaps reflecting our evolution from hair-covered nocturnal ancestors. Placental mammals can, however, directly reverse damaged O^6-methylguanine residues and to a lesser extent O^4-alkylthymine residues (for review see 1, 16). These are generated endogenously due to reactive cellular catabolites that act as monofunctional alkylating agents (17). O^6-methylguanine residues are highly mutagenic as they can pair with approximately equal ability to both C and T nucleotides, causing transition mutations. These mispairs attract the attention of the long-patch mismatch repair system (see below), which attempts repeatedly to repair

the mispair leading to a futile cycling that can result in cell death. To prevent this from occurring, alklytransferase enzymes remove deleterious methyl and larger alkyl groups from damaged nucleotides by transferring them covalently to one of their own cysteine residues (18). Interestingly, the alkyltransferase enzymes, which are also called "suicide enzymes", are themselves consumed in this process. As the entire protein molecule is sacrificed for each lesion corrected, this mode of repair is obviously only suitable for removing rare but highly mutagenic DNA lesions. The energetic expense involved in such a system demonstrates the cellular importance of DNA repair mechanisms. It is also interesting to note that the gene for the alkyltransferase enzyme is one of the few DNA repair genes that can be transcriptionally activated by treatment with a DNA damaging agent, in this case by alkylating agents, UV light or X-rays (1, 19). This induction appears to be limited to liver cell lines (19 - 21), presumably reflecting the increased exposure that can occur in this organ.

2. Base excision repair

The base excision repair pathway removes common DNA modifications, such as those caused by endogenous agents. It is thought to be, quantitatively at least, the most active repair system and is characterized by a small repair tract (1 - 6 nucleotides) and by restricted repair specificities (for review see 1, 22, 23). The initiating enzyme in standard base excision repair is a DNA glycosylase. Eight human DNA glycosylases have now been identified (22), many of which have *Escherichia coli* homologs. Two of these can

function to repair the mismatched nucleotides examined in these studies. Specifically, in HeLa cell extracts a thymine DNA glycosylase specialized for G:T mismatches has been identified which removes thymine in G:T mispairs to form G:C (24). hMYH, the mammalian homolog of *E. coli* mut Y, has also been identified. This removes adenine from A:G mismatches and A:^{8}OH-G (25). In each case the glycosylase moves by facilitated diffusion along the minor groove of DNA until it recognizes its specific type of damaged nucleotide. The glycosylase enzymes are believed to then kink the DNA by compression of the strand and to "flip" out the abnormal residue into a recognition pocket (26). Cleavage of the N-glycosidic bond between the base and the deoxyribose occurs leaving behind an apurinic or apyrimidinic (AP) site (see Figure 1) (27 - 29). The DNA strand is cleaved by the glycosylase 3' to the AP site if the glycosylase is bifunctional (30, 31). If the glycosylase is monofunctional it complexes with a separate AP endonuclease (APE1/HAP1) which cleaves the DNA 5' to the AP site (32). From this point the repair process can occur via two pathways. In short-patch base excision repair (one nucleotide repair patch) DNA polymerase β joins the base excision repair complex and the remaining deoxyribosephosphate residue (dRP) is completely excised by a phosphodiesterase activity (dRP lyase) of DNA polymerase β (32). The one nucleotide gap is filled in by DNA polymerase β using the intact complementary strand and the nick is sealed by DNA ligase III complexed together with XRCC1 (33). XRCC1 has been shown to interact with DNA polymerase β, and presumably acts as an adaptor molecule, bringing DNA ligase III to the site of repair (33, 34). The other base excision pathway is the so called long-patch base excision repair (2 - 6 nucleotide repair patch). In this

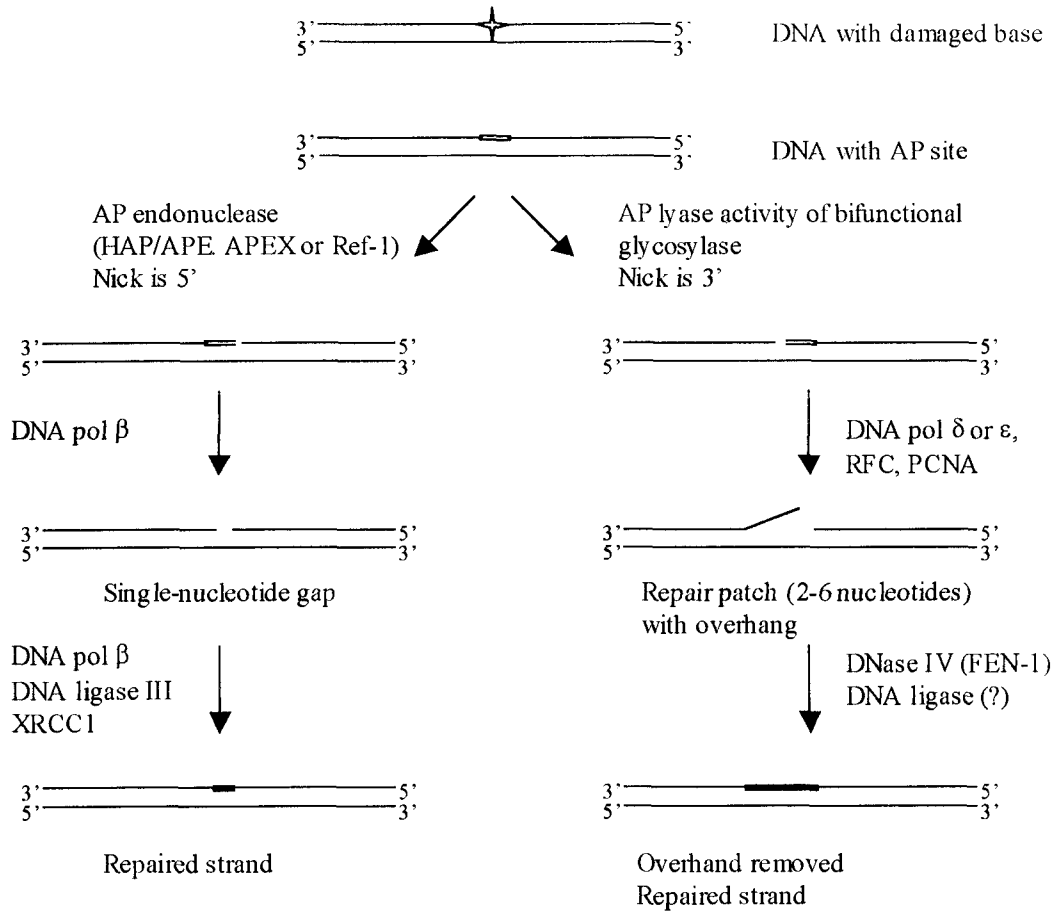

Figure 1 – Human Base Excision Repair. See text for description of the processes. Figure is adapted from Krokan et. al., 1997 (22).

process DNA polymerase δ or ε replicates a short repair patch in the presence of PCNA (Proliferating Cell Nuclear Antigen) and RFC (Replication Factor C) (35 - 37). DNAase IV (FEN1) acts to excise the resulting overhang containing the dRP residue (38). DNA ligase I is then believed to complete the repair process by sealing the final nick (22). Interestingly, recent evidence has shown that base excision repair occurs more efficiently on transcribed DNA and that this may be of critical importance in repair of oxidative lesions (39, 40). This type of interaction suggests a potential physical correspondence between the DNA glycosylases and the transcription machinery.

One consideration in base excision repair is the use of DNA polymerase β, which unlike DNA polymerase δ or ε, does not have a 3' –> 5' exonuclease activity, and as such shows a relatively high error frequency (1 in every 3000 to 5000 nucleotides) (3, 41, 42). Two mechanisms are currently known to serve to protect against such replication errors. First, DNA ligase III has been shown to be relatively inefficient at joining nicks with a 3' mismatched residue, leaving time for excision of the mismatched nucleotide (43). Secondly, a new mammalian 3' exonuclease has been found that is believed to function in editing of DNA polymerase β replication (44, 45). Together, these mechanisms could serve to produce the high degree of repair fidelity necessary for mutation avoidance.

Apurinic/apyrimidinic sites that occur due to spontaneous hydrolysis are also repaired by the base excision repair system with the AP endonuclease (APE1/HAP1) recognizing and initiating repair (46, 47). Abasic sites generated in this way may indeed outnumber those produced by DNA glycosylases as knockout mice for the various DNA glycosylases so far investigated are viable, whereas knockouts for APE/HAP1 are not

(48). Although base excision repair pathways are believed to be primarily responsible for repair of the most commonly damaged nucleotides, as yet no direct link has been found between loss of base excision repair and increased cancer incidence.

3. Nucleotide excision repair

The nucleotide excision repair system acts to repair helix-distorting DNA lesions and is characterized by a 24-32 nucleotide repair tract (for reviews see 1, 16, 49). It responds to a large range of damage that produces local distortions in the DNA, including the bulky chemical adducts, alkylating chemical adducts and cross-links that are caused by exogenous DNA damaging agents, ionizing radiation and endogenous reactions. Also, nucleotide excision repair in humans removes the pyrimidine dimers caused by UV light, which may indeed be its most important function (see below).

Reduced levels of nucleotide excision repair is associated with three recessive genetic disorders in humans: Cockayne's syndrome (CS), trichothiodystrophy (TTD) and xeroderma pigmentosum (XP) (50). In Cockayne's syndrome patients exhibit growth retardation, neurological deficiencies, skeletal abnormalities and shortened lifespan. Trichothiodystrophy patients have brittle hair, short stature, scaly skin, mental underdevelopment and shortened lifespan. Of these disorders only XP is associated with an increased incidence of cancer, perhaps due to the relatively normal lifespan of these individuals. XP patients display a 2000-fold increased risk of skin cancer and an approximately 10-fold increased risk of common internal cancers (16). This incremental

risk of internal cancers compared to the much higher incidence of skin cancers reflects the importance of nucleotide excision repair in removal of the pyrimidine dimers caused by UV radiation. XP is a rare but heterogenous disease in which seven genetic complementation groups have been identified (XPA –> XPG). Study of the protein products of these genes has shed considerable light on the basic pathways in nucleotide excision repair.

The general mechanisms of human nucleotide excision repair appear to be biochemically similar to those in the *E. coli* UvrABC pathway (for review see 16, 51), demonstrating through evolutionary conservation the importance of DNA repair mechanisms. Essentially, nucleotide excision repair involves dual incision by ATP-dependent nucleases followed by excision of the oligomer and filling in and ligation of the resulting gap. However, the eukaryotic pathway involves a far greater number of protein products, many of which do not show homology to the *E. coli* proteins (52 - 54). In humans, six core factors comprising 15 –18 polypeptides appear to be involved in the dual incision. An additional 10-14 polypeptides are then necessary for the repair synthesis. It appears that in eukaryotes the basic pathways have been evolutionarily expanded upon with proteins involved in other cellular mechanisms taking on roles in nucleotide excision repair. In fact, many of the proteins involved in nucleotide excision repair have essential functions in other disparate cellular events. For example, RPA (Replication Protein A) functions in replication and recombination as well as in nucleotide excision repair (47). The ERCC1-XPF heterodimer functions in repair of

double-stranded breaks (55) and the XPG gene promotes the activity of the hNth DNA glycosylase in base excision repair (39, 40).

The first step in global genome nucleotide excision repair appears to be recognition of a helix distortion by the XPC-hHR23B complex in an energy-independent manner (see Figure 2) (56). Although this is somewhat controversial (57), XPC-hHR23B has the greatest affinity among the nucleotide excision repair enzymes for damaged nucleotides (56) and it is not required in transcription-coupled repair where a separate damage recognition activity is believed to exist (see below). A multi-protein repair complex then forms involving XPC-hHR23B, XPA (possibly involved in damage verification), the single-stranded binding heterodimer RPA (also possibly involved in damage verification), the XPG nuclease, the heterodimeric ERCC1-XPF nuclease, and the TFIIH complex, which includes the XPB and XPD proteins (58 - 60). A key intermediate in nucleotide excision then forms with the DNA unwinding to form an open "bubble" structure surrounding the lesion. This process uses the ATP-dependent helicase activities of the XPB and XPD proteins (both part of the TFIIH complex). Mutations in XPD are also the causative factor in TTD patients (61). Formation of the open bubble structure creates sites for excision by the XPG and ERCC1-XPF nucleases (62, 63). These recognize junctions between single-stranded and double-stranded DNA with different polarities (XPG –> 3', ERCC1-XPF –> 5'). A 24 to 32 residue oligonucleotide is thus released. The resulting gap is then filled in by the DNA polymerase δ or ε holoenzymes in an RPA, RFC and PCNA-dependent manner, and the nicks are sealed, presumably by DNA ligase 1 (64, 65).

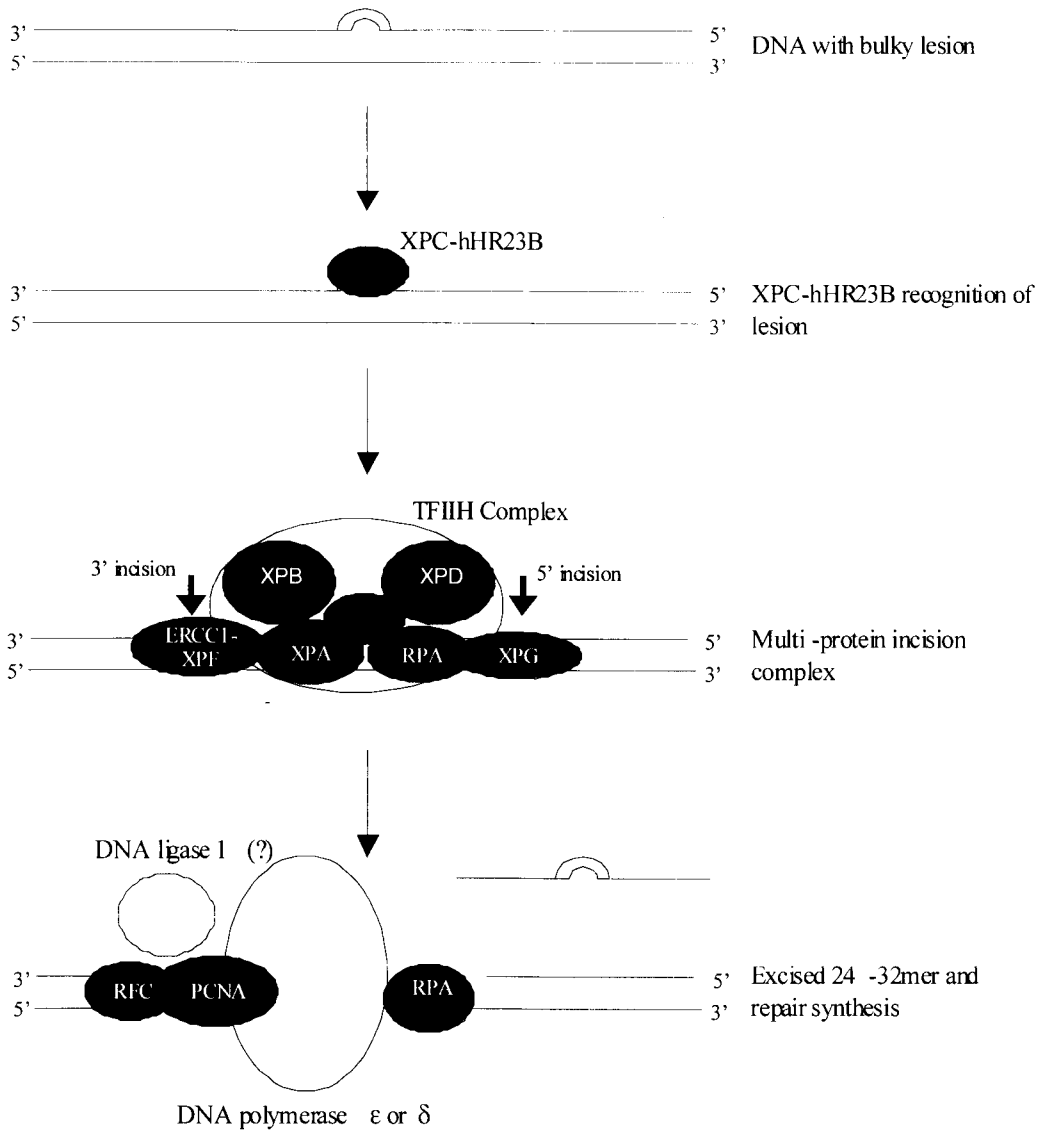

Figure 2 – Human Nucleotide Excision Repair. See text for description of processes. Figure is adapted from Lindahl and Wood (47).

The one XP complementation group not discussed so far is XPE. These cells harbor mutations in the UV-DNA damage binding factor E (UV-DDE) and although XPE cells are moderately UV sensitive, the function of this gene is not clearly understood (66 - 69). It has been suggested that it may have a specialized function in detection and/or repair of DNA damage in chromatin where specialized nucleotide excision repair systems may exist (70).

This general model for nucleotide excision repair represents the reactions as they are believed to occur on non-transcribed DNA, which is indeed the bulk of the genome. Interestingly, a distinctive type of nucleotide excision repair has been demonstrated to occur on transcribed DNA, with transcribed genes being repaired faster than complementary non-transcribed sequences and the template strand of transcribed genes being repaired faster than the complementary non-template strand (71 - 74). Nucleotide excision repair that is modulated by transcription is now called transcription-coupled repair and has been shown to function similarly to the process described above, but without the need for the XPC-hHR23B gene products (75 - 77). While XPC-hHR23B is required in global genome repair, probably for recognition of the initial helix distortion and recruitment of the nucleotide excision repair complex, RNA polymerase II arrest at a lesion is believed to serve this role in transcription-coupled repair (78). RNA polymerase II is then thought to recruit the other necessary nucleotide excision repair factors as well as recruiting the CS-A and CS-B proteins (71, 78, 79). Mutations in these proteins are the causative agents in Cockayne's syndrome and are thought to couple RNA polymerase II arrest to repair. The nucleotide excision proteins, both those involved in global

genome and transcription-coupled repair are critical in maintaining genomic integrity and normal metabolism as graphically illustrated by the severity of the human diseases associated with their mutation.

4. Mismatch repair

a. Mismatch repair in E. coli

Long-patch mismatch repair (hereafter referred to as mismatch repair) is a broad specificity mispair correction mechanism believed to be responsible for repair of most mismatches generated during replication and recombination (for reviews see 80 - 82). Although the precise functions of the human mismatch repair proteins are just beginning to be understood, they are homologous to those in the relatively well-characterized *E. coli* MutSLH strand-specific mismatch repair pathway (for review see 83). Indeed, the degree of conservation between such divergent species reflects the essential role of mismatch repair. In bacteria, the proteins involved in mismatch repair have been isolated to near homogeneity and the entire system has been reconstituted *in vitro* (84). The first step in the repair process is recognition of and binding to a mismatch by a homodimer or tetramer of the 95 kDa MutS protein, which initiates the repair process (see Figure 3) (85 - 87). Next, the DNA-bound MutS interacts with a homodimer of the 68 kDa MutL protein to form a complex in a reaction that depends on ATP binding, but not on ATP hydrolysis (88 - 90). This complex translocates along the DNA strand, forming an α–loop structure with the proteins resting at the crossover point (91). This process

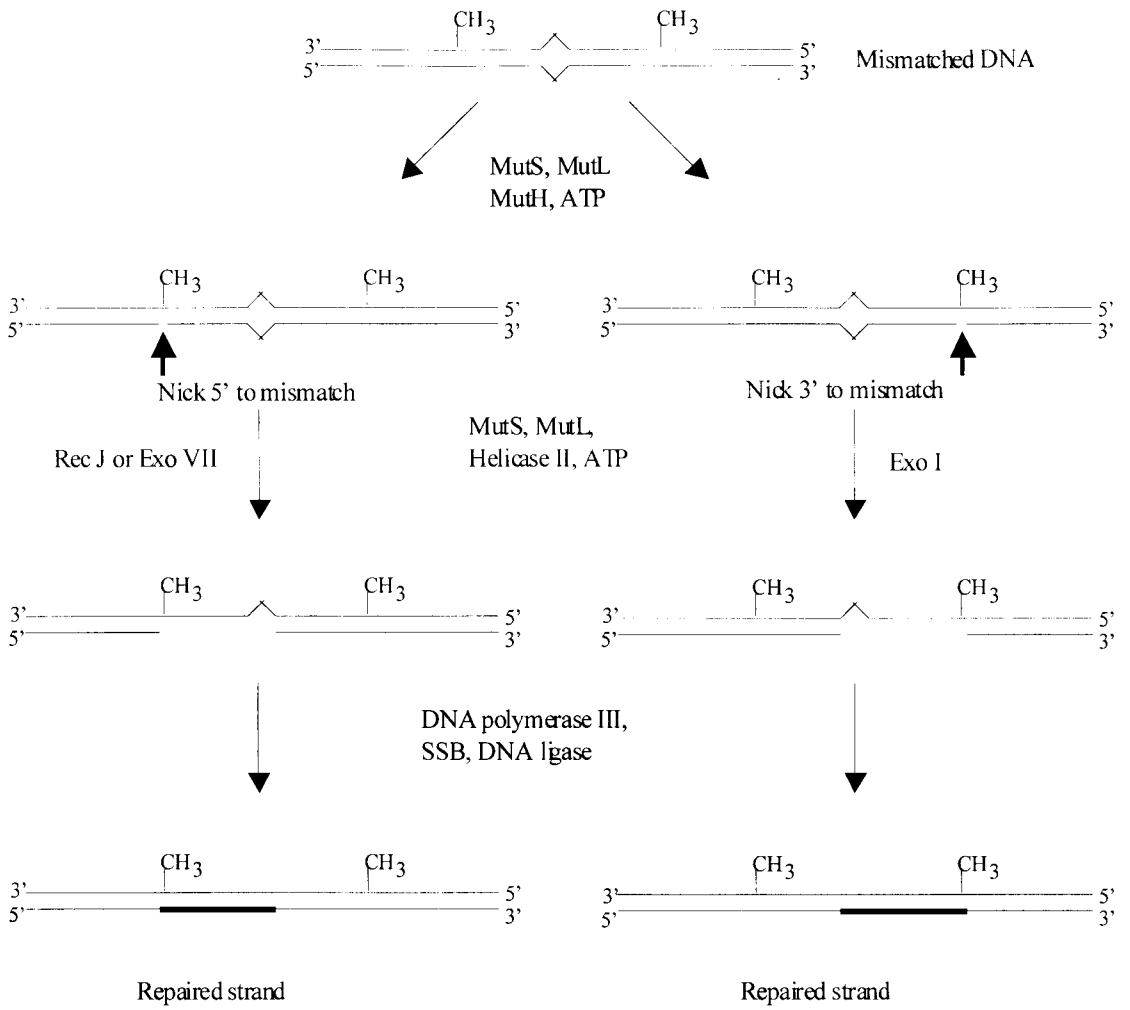

Figure 3 – *E. coli* MutS/L/H Mismatch Repair. See text for description of the processes. Figure is adapted from Modrich and Lahue, 1996 (80).

requires ATP hydrolysis by MutS and although the exact role MutL plays is unclear, it does enhance MutS binding (92) and increase the rate of loop growth (91). The MutS/Mut L complex is then believed to associate with the 25 kDa MutH protein, although the exact chronological order of association events has not been conclusively demonstrated. Assembly activates a latent endonuclease activity of MutH, which incises the unmethylated DNA strand at the nearest d(GATC) site either 3' or 5' to the mismatch (the process is bi-directional) (93 - 96). MutL helps to load DNA helicase II (MutU/UvrD) onto the site and the helicase is activated in a MutS/MutL/mismatch-dependent manner (96 - 98). A segment of DNA is then unwound by the helicase (99) and excised by Exo I (when the nick is 3' to the mismatch), or RecJ/Exo VII (when the nick is 5' to the mismatch) (100, 101). The resulting single-stranded tract extends from the strand break to several discrete sites 100 to 150 nucleotides beyond the mismatch and is stabilized by single-stranded binding protein (SSB) (87). The segment of DNA is finally re-synthesized by the DNA polymerase III holoenzyme and the remaining nick is sealed by DNA ligase (84).

Although this working model of *E. coli* mismatch repair is generally agreed upon, a few mysteries remain. One of the most important of these concerns the unknown biochemical function of MutL. One suggestion is that MutL serves as a "molecular matchmaker", facilitating the interaction between MutS and MutH (83, 92). Evidence for this comes from studies utilizing electron microscopy where a ternary complex of MutS, MutL and MutH was observed on the α-loop structure (91). Two-hybrid studies identified the interaction between MutL and MutH and protein affinity chromatography

experiments confirmed that MutL, and not MutS, physically associates with MutH (96). Furthermore, MutL can stimulate the endonuclease activity of MutH in the absence of MutS and a mispaired base (96). MutL has also been suggested to play a role in loading the helicase onto the nicked strand (98, 99). Another suggestion for a biochemical function for MutL arises from MutL's observed homology to class II DNA topoisomerases and the molecular chaperone molecule Hsp90 (102). Similar to Hsp90, MutL binds ATP and has a weak ATPase activity that is stimulated by ATP (103, 104). This suggests that MutL may also act as a molecular chaperone, perhaps facilitating the conformational changes necessary for the mismatch repair proteins to function.

b. Human MutS homologs

In humans, the mismatch repair pathway is homologous to but more complex than that of *E. coli*. For example, six MutS homologs (MSH1-MSH6) have now been demonstrated to be involved in eukaryotic mismatch repair (see Table 1) (for review see 105). All of these display a high degree of homology in the C-terminus helix-turn-helix domain that is involved in protein-protein interactions (106) and are nearly invariant in the Walker Type A nucleotide binding domain (107). As in *E. coli*, the MutS homologs appear to function in the initial recognition step of mismatch repair, but unlike *E. coli* where they act as homodimers, in eukaryotes they function as heterodimeric complexes, (108, 109). Thus, there is an inherent asymmetry in the eukaryotic mismatch repair system that is presumed to be reflected in protein function.

Table 1 - Relationships between MutS and MutL homologs.

E.coli protein	*S. cerevisiae* protein	Human protein	Size of human protein (kDa)	HNPCC kindreds
MutS	MSH1	Not reported	N/A	N/A
	MSH2	hMSH2	102	~ 36 %
	MSH3	hMSH3 (DUG1, MRP1)	127	None known
	MSH4	hMSH4	Not reported	None known
	MSH5	hMSH5	93	None known
	MSH6	MSH6 (GTBP)	160	2 known families
MutL	MLH1	MLH1	70	~ 60 %
	MLH2	PMS1	115	1 known family
	MLH3	Not reported	N/A	N/A
	PMS1	PMS2	116	2 known families

Of the MutS homologs, hMSH2 was the first gene to be associated with the HNPCC cancer syndrome, with approximately 36% of kindreds now known to carry mutations in this gene (8, 11, 110, 111). It encodes a protein of 102 kDa and like its *E. coli* homolog, purified hMSH2 homodimers have been shown to bind specifically *in vitro* to DNA substrates containing mismatches or small insertion-deletion loops, although the possible function and/or relevance of an hMSH2 homodimer is unknown (106, 112, 113). Tumor cell lines deficient in hMSH2 have been found to display high rates of mutation

(114 - 116), and, extracts from these cells have been shown to be deficient in repair of mismatches and small insertion-deletion loops of 1 to 5 bases (108, 116).

Mismatch repair in hMSH2 deficient cell lines can be restored by a protein activity that was found to contain both hMSH2 and the 160 kDa hMSH6 protein (also known as GTBP), in a complex that is referred to as the hMutSα heterodimer (108, 117). Interestingly, hMSH6 had been isolated previously based on its ability to bind preferentially to G:T mispairs (hence GTBP for G:T binding protein) (118). It was subsequently demonstrated that the binding activity that was believed to be the 160 kDa hMSH6 protein and a 100 kDa breakdown product of hMSH6 was actually the hMutSα heterodimer of hMSH6 and hMSH2 (117). Further work with purified proteins has demonstrated that hMSH6 does not bind heteroduplex DNA on its own, but must be complexed with hMSH2 (117, 119).

Much current analysis has focused on the biochemical function of hMutSα. As stated previously, the most highly conserved area of both hMSH2 and hMSH6 is the Walker Type A nucleotide binding fold. Both hMSH2 and hMSH6 have been shown to possess intrinsic ATPase activity (118, 120, 121) and this ATPase activity has been shown to be required for function (120 - 122). Mutations in the consensus site for nucleotide binding of either hMSH2 or hMSH6 results in decreased ATPase activity and a decreased capacity to promote mismatch repair *in vitro* (120, 122). The ATPase activity is stimulated by DNA and has been shown in some cases to be stimulated more efficiently by DNA containing mismatched bases (119, 121, 123, 124). Thus it can be

concluded that the ATPase activity of hMutSα is central to its biochemical function in mismatch repair.

The hMutSα heterodimer binds specifically to heteroduplex DNA *in vitro* in the absence of additional ATP (108, 117, 119) with the K_d for hMutSα binding to homoduplex DNA estimated to be approximately 20-fold lower than for heteroduplex DNA (120). Due to the asymmetry of the heterodimers, it is reasonable to assume that each subunit will play a specific role in the repair process. It appears that the interaction with the DNA occurs via hMSH6, as it alone is capable of becoming UV cross-linked to oligonucleotide substrates (120). Conversely, ATP has been found to become cross-linked with increased efficiency to hMSH2 as compared to hMSH6 (120), and studies using mutants have shown that disruption of the ATPase activity of hMSH2 has a greater effect on *in vitro* repair than do ATPase mutants of hMSH6 (121, 122). Therefore, hMSH2 appears to play the predominant role in ATP binding and hydrolysis.

Numerous studies have demonstrated that the hMutSα heterodimer releases from oligonucleotide substrates upon addition of ATP (108, 119 - 121). This reaction has been shown to be dependent upon ATP binding but not on ATP hydrolysis, as it can be facilitated by non-hydrolyzable analogs of ATP and by mutants deficient in ATP hydrolysis but not ATP binding (120, 121, 125). Based on these reports it has been postulated that hMutSα acts as a molecular switch, analogous to G-proteins such as Ras (121). In this model the hMSH2-hMSH6 molecular switch is 'on' (bound to a mismatch) in the ADP-bound form and 'off' in the ATP-bound form. In a more refined version of this model the 'off' form has recently been described as a sliding clamp whereby the

hMutSα heterodimer dissociates from the mismatch but remains bound to the DNA (126). Hydrolysis of the ATP molecule results in the recovery of the mismatch binding capability whereas ADP-ATP exchange results in dissociation away from the mismatch. Exchange of ADP –> ATP is provoked by mismatch recognition and/or binding, and thus regulates the hMutSα molecular switch.

A second model has also been proposed to describe the action of ATP on hMutSα. In the translocation model, binding by ATP causes the heterodimer to translocate along the DNA in a mechanism driven by ATP hydrolysis, similar to the process as demonstrated in *E. coli* (91, 125, 127). In *in vitro* experiments the translocation results in hMutSα falling off of the relatively small oligonucleotide substrates used. Evidence for this model includes kinetic analysis suggesting that simple diffusion is unlikely to be the mechanism for the heterodimers release (127). ATP hydrolysis and not ATP binding has also been shown to be involved in the rate determining repair step (125). As well, experiments using end-blocked substrates have demonstrated that these inhibit hMutSα release from the oligonucleotide (125). The suggested model is that ATP binding reduces the affinity of the hMutSα heterodimer for a mispair, but activates secondary DNA binding site(s) that are used to move the protein along the helix in a reaction that is dependent on ATP hydrolysis. Although the details of ATP action on hMutSα are currently hotly debated it is clear that ATP binding results in a conformational change which affects DNA interactions, protein interactions and subsequent steps in the repair process.

HNPCC kindreds with mutations in the gene for hMSH6 have been found, but there are only two known families making this extremely rare (128 - 130). As well, study of hMSH6 deficient cell lines has shown that the mutator phenotype is not as pronounced as in hMSH2 deficient cells (4, 129). This genetic evidence is now believed to be explained by a functional redundancy in the MutS homologs, with hMSH2 able to pair with hMSH6 to form the hMutSα heterodimer or with hMSH3 to form the hMutSβ heterodimer (109, 131). *In vitro*, hMutSβ has been shown to bind with greatest affinity to insertion-deletion loops of up to 16 bases although it can also bind to some extent to the various mismatches (132 – 134). Studies have also demonstrated that hMutSβ specifically supports the repair of insertion/deletion loops of 2 - 8 nucleotides (131) and as well, the hMutSβ complex been shown to be modulated by ATP binding, similar to hMutSα (135). As of yet there are no known reports of HNPCC kindreds with mutations in the gene for hMSH3 (11) and MSH3 deficiency has been shown to *not* result in a mutator phenotype in Chinese hamster ovary cells (136). However, overexpression of the gene did result in mismatch repair deficiency in human cell lines (137). This suggests that hMSH2 partitions between available pools of hMSH3 and hMSH6. The binding specificities of the various MutS homologs and the genetic evidence suggests a central role for hMSH2 (hence the large number of HNPCC kindreds). hMSH6 and hMSH3 appear to have partially overlapping functions, with hMutSα (hMSH6) believed to be primarily responsible for initiation of repair of mismatches and hMutSβ (hMSH3) believed to function in repair of most insertion-deletion errors.

Two other MutS homologs have recently been described in humans; hMSH4 and hMSH5 (138 - 140). hMSH5 is expressed in greater amounts in meiotic tissue (141, 142) and based on yeast genetic evidence does not appear to function in mismatch repair (138, 143). In mouse cells, mutations in MSH5 result in meiotic defects (144). In *Saccharomyces cerevisiae*, MSH4 and MSH5 have been shown to be required for crossing-over during meiotic recombination (138, 139, 143). Based on this evidence it appears that hMSH4 and hMSH5 have specialized functions in recombination events, perhaps acting with hMLH1, with which they have been reported to interact (145). A human homolog to the yeast MSH1 mitochondrial mismatch repair protein has not yet been reported (81, 105).

c. Human MutL homologs

The human MutL homologs hMLH1, hPMS2 and hPMS1 are also required for mismatch repair (for reviews see 81). Approximately 61% of HNPCC kindreds contain mutations in the hMLH1 gene (11, 146 - 148), implying a central role for hMLH1 in mismatch repair. Interestingly, hMLH1 promoter hypermethylation has also been detected in spontaneous tumors displaying microsatellite instability (149, 150). This methylation has been shown to correlate with a lack of hMLH1 expression demonstrating that epigenetic events can also lead to aberrant expression of this mismatch repair gene and the mutator phenotype (151, 152). As with the MutS homologs, the MutL homologs appear to function as heterodimeric complexes in 1:1 ratios. Cells mutated in these genes display a similar microsatellite instability and a mutator phenotype and extracts from

such cells are defective in repair of mismatches and small insertion/deletion loops (10, 153 - 157). Unfortunately, as with bacteria very little is known in regards to the exact roles and biochemical functions of the MutL homologs in human cells.

What is known is that a protein fraction consisting of a heterodimer of hPMS2 and hMLH1 is capable of restoring mismatch repair activity in nuclear extracts from human cancer cells that are hMLH1 deficient (158), suggesting the existence of a hMutLα heterodimer of hMSH1 and hPMS2. In addition, a heterodimer of hPMS1 and hMLH1 (hMutLβ) has recently been reported (159). Currently there is one HNPCC family known to harbor a mutation in the hPMS1 gene and two cases linked to mutations in the hPMS2 gene (146, 11). Based on this biochemical and genetic evidence it has been proposed that, as with the MutS homologs, there exists functional redundancies between hPMS2 and hPMS1 with both binding to hMLH1. One obvious possibility would be that one of the MutL heterodimers is primarily responsible for repair of mismatches with hMutSα while another is primarily responsible for repair of insertion-deletion loops with hMutSβ, with some overlap of function. In support of this model, in *S. cerevisiae* the homologue of hPMS1 (confusingly called PMS2) has been shown to interact with MLH1 in the two-hybrid assay (160) and to contribute specifically to repair of a subset of insertion/deletion loops (161). Evidence against such a model comes from genetic studies which have shown the mutator phenotype of hMLH1 deficient cells to be similar to that of cells deficient in hPMS2 or hPMS1 (81). This would not be expected if there was some overlap of function. Clarifying the protein-protein interactions between the

MutL homologs and determining the biochemical functions for these essential proteins is one of the current challenges in the field of mismatch repair.

d. Interactions between the MutS and MutL homologs

Based on the *E. coli* model (see above and Figure 3), it is hypothesized that the MutS and MutL homologs interact in the eukaryotic mismatch repair process. The first study to show this utilized yeast purified proteins (162). In this study it was demonstrated by gel-shift analysis that MSH2, MLH1 and PMS1 (homologous to human PMS2) interact. However, the relevance of this finding is in question as subsequent studies demonstrated that MSH2 does not function primarily as a homodimer, but instead exists as a heterodimer with MSH6 or MSH3. Other studies in yeast using purified proteins have shown that MSH2, MSH6, MLH1 and PMS1 interact in gel-shift studies and that the MLH1-PMS1 complex enhances binding of the MSH2-MSH3 heterodimer to insertion-deletion loops (163, 164). Recently, in human nuclear extracts the hPMS2 and hMSH2 proteins were shown to co-immunoprecipitate with hMLH1 in the presence of heteroduplex DNA (165). Unfortunately this study did not report on the presence of hMSH6 or hPMS1. Therefore, although it appears that the MutS and MutL mismatch repair protein homologs interact with each other, a comprehensive examination has been until now lacking in the literature.

Although the role of ATP binding and hydrolysis has been extensively studied using purified hMutSα, the role of ATP in the eukaryotic MutS/MutL interactions is currently unclear. In the gel-shift studies utilizing yeast purified proteins, MHS2, MLH1

and PMS1 were shown to interact both in the presence and absence of additional ATP (162). Once again the caveat for these studies is that they did not include MSH6 or MSH3. In other studies using yeast purified MSH2, MSH6, MLH1 and PMS1, the higher-order complex only formed in the presence of ATP (163, 164). In human nuclear extracts, the co-immunoprecipitation of hPMS2 and hMSH2 with hMLH1 was observed to occur only in the presence of ATP (165). It has been suggested that the MutL homologs could act to modulate the ATPase activity of the hMutSα heterodimer, similar to how GAP proteins modulate GTP hydrolysis in G-proteins. Alternatively, they could function in steps of DNA mispair correction subsequent to mismatch recognition, such as in strand discrimination, translocation or binding of exonucleases. It is also quite possible that the MutL homologs possess an as yet unidentified ATPase activity, similar to that recently demonstrated in *E. coli* MutL (103, 104).

e. Other proteins involved in eukaryotic mismatch repair

A number of other proteins have been identified as being required for eukaryotic mismatch repair. PCNA appears to be one of these. From biochemical studies it is required both in the early stages of repair and during replication, presumably in this latter case in its usual role in polymerase processivity (166). PCNA mutants display a mutator phenotype similar to those of the mismatch repair protein mutants (167) and PCNA has been shown to co-immunoprecipitate with the mismatch repair proteins in human nuclear extracts (165). As in *E. coli* a number of partially redundant exonucleases also appear to function. One of these is probably exonuclease 1. It has been shown to physically

interact with hMSH2 in human nuclear extracts (168) and in yeast genetic studies mutants in the gene for exonuclease 1 have a weak mutator phenotype that acts in the same epistatic pathway as MSH2 (169, 170). Another candidate for a mismatch repair exonuclease is the yeast FEN1 (RAD27) protein. This has been shown in two-hybrid studies to interact with PCNA (171) and mutants display an increased occurrence of frameshift mutations similar to that seen in MHS2 mutants (171). From fractionation experiments DNA polymerase δ also appears to be required (172). Similarly, immunodepletion and reconstitution experiments have demonstrated that single-stranded binding protein and RPA are required *in vitro* in mismatch repair (173). It also seems likely that RFC will be found to be required as it is generally necessary for PCNA loading onto DNA. This list of required proteins is certainly not complete. For instance, a DNA helicase and a 3' –> 5' exonuclease has yet to be identified, although DNA polymerase δ could possibly provide the latter function. DNA ligase I is also likely to be involved in mismatch repair as it is frequently associated with DNA polymerase δ and PCNA-dependent replication.

f. Strand discrimination

Another as yet unresolved question in the field of mismatch repair is the nature of the strand discrimination signal in eukaryotic cells. In *E. coli* the hemi-methylated state of the DNA that occurs immediately after replication serves as the strand discrimination signal with the MutH-associated endonuclease nicking the newly synthesized, temporarily unmethylated strand (83). Vertebrates and plants also methylate their DNA,

primarily at the 5' position of cytosine in CpG or CpXpG motifs. One report from 1985 (174) suggested that such sites could direct repair. However, a methylation based strand discrimination system seems unlikely as these results have not been duplicated and the patterns of methylation in higher organisms are highly irregular with stretches of up to several kb remaining unmethylated. Attempted mismatch repair in such areas would lead to an unacceptable level of mutation due to undirected repair. As well, many lower eukaryotes such as *S. cervisiae* and *Drosophila melongaster* lack methylation altogether but have functional mismatch repair systems. Finally, MutH-like methylation-sensitive endonucleases have not been found in any of the numerous organisms whose genomes have been or are being studied, even in other microorganisms such as *Streptococcus pneumoniae* (82). It appears that methylation-based strand discrimination, although elegant, is the exception rather than the rule.

What is known is that the mismatch repair process can be directed in all systems (including *E. coli*) by a nick on the strand containing the mismatch (175, 176). Circular substrates containing mismatched nucleotides but lacking a nick have been found to be refractory to strand specific mismatch repair, both *in vitro* (175, 176) and *in vivo* (177, 178). Experiments using human cell extracts have demonstrated that pre-existing nicks on the same strand of DNA as the incorrect base, located either 5' or 3' to the mismatch, can direct repair and that the strand-break can be as many as 1000 base pairs away from the mismatch (175, 176). As such nicks are present in recombination intermediates they could serve to direct repair in this instance. As for post-replicative repair, nicks or gaps that can direct repair will also occur between neighboring Okazaki fragments on the

lagging strand. The leading strand, however, presents a difficulty. Currently a commonly proposed theory is that the mismatch repair proteins are directly associated with the replication apparatus at the replication fork, thus dispensing of the need for a separate strand discrimination signal. Evidence supporting this hypothesis comes from yeast two-hybrid studies where PCNA, a protein known to interact with DNA polymerases, was demonstrated to interact with MLH1 (167). Immunoprecipitation studies using human nuclear extracts have also demonstrated an interaction between hMLH1, hMSH2 and PCNA (165). These findings suggest a model whereby the PCNA homotrimers link the polymerase with the mismatch repair proteins. Also supporting this are studies in yeast which have shown PCNA to be required in a step prior to re-synthesis, and thus to have a role other than its standard role in facilitating processivity of replication (166). It is also possible that mismatch repair functions at times in the cell cycle other than immediately post-replication although potential strand discrimination signals for this are unknown. Hopefully, by clarifying the protein-protein interactions between the mismatch repair proteins and by identifying their biochemical functions the mechanism of strand discrimination in organisms other than *E. coli* will be understood.

g. Other functions of the mismatch repair proteins

A number of studies have suggested that there are links between mismatch repair and transcription-coupled repair. The first study to suggest this demonstrated that in *E. coli* mutations in MutS or MutL abolished transcription-coupled repair of UV photoproducts (179). Subsequent research using human cell lines showed that

transcription-coupled repair of UV damage was abolished in humans cells lacking hMSH2, hPMS2 or hMLH1 and that the repair could be restored by appropriate chromosome transfer (180, 181). Interestingly, the levels of global nucleotide excision repair in the cells studied remained unaffected. When repair of oxidative DNA damage was examined it was found that only hMSH2 mutants (and not hMLH1, hPMS2 or hMSH6) were deficient in transcription-coupled repair (181). Such discrimination in types of damage recognized has led to the suggestion that the mismatch repair enzymes function in the damage recognition steps of transcription-coupled repair. Recently, a physical interaction between MSH2 in yeast and a number of nucleotide excision repair proteins was demonstrated using the two-hybrid screen (182). There appears to be an overlapping of function in the transcription-coupled repair and mismatch repair pathways. Alternatively, components from each pathway could function together in an as yet unknown manner.

The mismatch repair proteins have also been suggested to play a role in damage recognition at the G_2-M checkpoint and in induction of apoptosis. This concept first developed from studies using methylating agents, where it was shown that MSH2 deficient cells display increased survival rates (183, 184). These agents normally trigger an apoptotic response after G_2-M arrest in normal cells. Failure to detect the damage and hence trigger apoptosis would lead to the observed increased survival rates, thus suggesting a role for hMSH2 or more generally the mismatch repair proteins, in apoptosis and the G_2-M checkpoint. It has subsequently been shown that cell lines deficient in hMutSα or hMutLα (but not hMutSβ) fail to elicit a G_2 checkpoint arrest upon treatment

with methylating agents (185 - 187). Response to other DNA damaging agents such as cisplatin, 6-thioguanine and doxorubicin also appears to depend on a functional mismatch repair system (184). One suggestion is that hMutSα may function in recognition of DNA damage prior to cell cycle arrest. In support of this hypothesis, hMutSα has been shown to directly bind to cisplatin lesions, O^6-methylguanine residues, O^4-methylthymine residues, aminofluorene adducts, acetylaminofluorene adducts and pyrimidine dimers, providing physical evidence for a role in damage recognition (188 - 191). It has also been proposed that the sensitivity to DNA damaging agents is caused by futile cycling of mismatch repair. This repair either results in repeated removal of the nucleotide opposite the lesion, and thus futile cycling, or to potentially lethal double-stranded breaks that result in cell cycle arrest (184).

In conjunction with a putative role in damage recognition, the mismatch repair proteins may also have a more direct role in the induction of apoptosis. Studies in knockout mice found that MSH2 is involved *in vivo* in initiation of apoptosis (192). *In vitro*, cells deficient in human MutS or MutL homologs were unable to induce cell death after damage by a variety of chemical carcinogens (193). From genetic analysis in yeast and studies of p53 expression, this appears to be mediated through both a p53-dependent pathway and a delayed p53-independent apoptotic pathway (193, 194). Other researchers have demonstrated that hMutSα and hMutLα are required for phosphorylation of p53 in response to DNA methylation damage, presumably through activation of one or more protein kinase (195). Stabilization of p53 and apoptosis induction can result from overexpression of hMSH2 or hMLH1 (but not hMSH3, hMSH6 or hPMS2) (196). These

results implicate the mismatch repair system in the initial steps of a damage-signaling cascade that can lead to cell cycle arrest or cell death, although this hypothesis has been challenged. This may have significant clinic implications in that hMSH2 deficiencies (and possibly deficiencies in other mismatch repair proteins) can lead to malignancy not only through failure to repair mismatched nucleotides, but also through failure to initiate apoptosis. Therefore, hMSH2 deficient tumors are likely to be resistant to treatment by many standard chemotoxic agents.

Finally, research has suggested roles for the mismatch repair proteins in a number of disparate cellular functions. Studies in *S. cerevisiae* and in transgenic mice have indicated that hMLH1 functions directly in meiotic recombination (145, 197). Repair of branched structures in yeast also appears to require mismatch repair homologs with MSH2, MSH3 and MSH6 shown to be required for certain types of recombination (198, 199). Similarly, deficiencies in hPMS2 were reported to affect the rates of somatic recombination in human cells (200). These studies imply a central role for the mismatch repair protein in DNA metabolic pathways.

C. Hotspots of Mutation and Mismatch Repair

It has been well documented that the frequency and spectra of tumor-associated mutations are not random. Indeed, recent reviews have suggested that a major portion of human gene mutations are found at mutagenic hotspots, similar to the mutational spectra seen in bacteria (201, 202). The *ras* genes are a prime example of this phenomena. The

ras oncogene codes for a G-protein with a central role in at least three different signal transduction cascades controlling cell growth and differentiation (for reviews see 203, 204). When bound to GDP, Ras is in the 'off' state and cannot activate its downstream effectors. When GDP is exchanged for GTP, Ras is 'on' resulting in activation of the signal transduction cascades. This 'on' state is normally transitory as Ras has an intrinsic GTPase activity, which together with external GTPase activating proteins (GAPs) ensures that the signal is rapidly turned off by hydrolyzing the GTP to GDP. Thus the Ras protein functions as a molecular switch for signal transduction. Screening of human tumors has revealed the apparently ubiquitous nature of mutated *ras* genes in cancers and has shown that *ras* mutations are the most common abnormality of a dominant oncogene in human tumors (for reviews see 201, 203, 204). Direct sequence analysis has demonstrated that there are activating mutations in the *ras* oncogene family in nearly 30% of human tumors (203 - 205). Intriguingly, these mutations occur exclusively in codons 12, 13 and 61 (203 - 205). Clearly, a better understanding of the mechanisms responsible for such precise mutagenic targeting is important for our understanding of the processes responsible for cell transformation to the neoplastic phenotype.

Three general hypotheses have been put forward to explain tumor-associated hotspots of mutation. The first hypothesis is that activating mutations are selected for due to the increased survival rates that they confer. Although this may indeed be a causative factor in the prevalence of some activating hotspots of mutation in tumors it does not explain all cases. For example, several additional activating mutations in the *ras* genes besides codon 12, 13 and 61 have been found *in vitro* that have never been found *in*

vivo in human tumors or animal model studies (203 - 205). Therefore, the selective advantage conferred by an activating mutation is not a sufficient explanation for the existence of these tumor-associated hotspots of mutation.

Secondly, hotspots could occur due to an increased susceptibility of specific DNA sequences to damage. A number of studies, both *in vitro* and *in vivo* have shown that precise mutagen targeting does occur (for review see 206). For example, numerous animal model studies have demonstrated correlations between type of chemical exposure and location and type of *ras* activating mutations in resultant tumors (203, 207). As well, recent studies have shown preferential binding by carcinogens and formation of benzopyrene adducts at mutational hotspots in the p53 tumor suppressor gene (208, 209). These studies clearly demonstrate that mutagen induced lesions can be targeted to specific sequences and that some hotspots are particularly susceptible to DNA damage.

A third hypothesis to explain mutagenic hotspots is that there is decreased fidelity of repair and/or inefficiencies in repair at specific sequences. This can occur either during the replication process or afterwards in post-replicative repair. For example, an inability of the DNA polymerases to perform their 3'–> 5' exonuclease proofreading functions at a specific location would affect repair rates. Indeed, primer extension studies have indicated that polymerase α pausing at the H-*ras* codon 12 hotspot of mutation is abolished when the template is mutated, perhaps reflecting an inability of the polymerase to proofread misincorporations at this hotspot (210). Post-replicative repair processes can also vary depending on the location of the damage. A number of studies have clearly demonstrated that there is a heterogeneity in the nucleotide excision repair process at the

gene level (211 - 213). Nucleotide excision repair of pyrimidine dimers and benzopyrene adducts has been shown to occur correctly, but more slowly, at mutational hotspots in the p53 tumor suppressor gene (214, 215). As well, results from studies examining repair of inserted guanine adducts at different positions in codon 12 or 13 of H-*ras* have suggested that nucleotide excision repair rates vary at different locations (216 - 218). These studies indicate that there are site-specific inefficiencies in repair that could result in hotspots of mutation.

These hypotheses attributing different causative events to the process of increased mutation at hotspots are not mutually exclusive. It seems quite likely that hotspots can occur due to an increased propensity to DNA damage and a decreased ability to repair that damage and that they are then found in tumors due to the oncogenic phenotype that they help confer. For example, in p53 several hotspots at activating locations have been shown to be more susceptible to damage and more slowly repaired (208, 209, 216 - 218). Thus, a combination of events can contribute to the significantly increased frequency of mutation observed at specific locations.

Another factor that is believed to influence the frequency of mutation at a particular site is the sequence context surrounding that site. This was initially shown in *E. coli* in studies examining adduct-induced frameshift mutations (219). Once again, mutations can occur due to increased damage at a particular site or due to decreased fidelity or efficiency of repair, both during and after replication. A number of studies have shown that the surrounding sequence context can affect the rate of damage to a site (219 - 222). The surrounding sequence context has also been shown to affect the rate of

mutagenic bypass by DNA polymerase *in vitro* (223 - 225). Finally, post-replicative repair of bulky lesions has also been shown to be influenced by the surrounding nucleotides in both *E. coli* and eukaryotic cells (211, 212, 226). It appears that surrounding sequence context profoundly affects the rate of mutation, regardless of the reason or reasons for a particular hotspot.

The importance of understanding mechanisms of site-specific mutation is demonstrated by the prevalence of hotspots of mutation in naturally occurring tumors. Also, the importance of the mismatch repair system in genome stability and prevention of mutation has been clearly shown, both in spontaneous tumors and in HNPCC kindreds (10, 12, 14). Previous results from our laboratory have indicated differences in mismatch repair rates for various mismatches at the codon 12 hotspot of mutation in H-*ras* (227). We theorized then that there might be an overall decrease in mismatch repair at the codon 12 location as compared to other non-hotspots of mutation. Such defects in mismatch repair in otherwise repair proficient cells could affect the frequency and spectra of mutation. Therefore, the goal of the studies presented here was to determine if inefficient or incorrect repair of mismatches can play a role in mutagenesis at a tumor-associated hotspot in individuals who do not carry germ-line mutations in one of the genes coding for mismatch repair proteins. The exact interactions between the mismatch repair proteins and DNA substrates, both at hotspot locations and at non-hotspots were then systematically determined.

II. Materials and Methods

A. Enzymes, Antibodies and Reagents

All site-specific mismatch, synthetic oligonucleotides were purchased from Operon Technologies Inc. Amplitherm DNA Polymerase was purchased from Epicentre Technologies Corporation. T4 polynucleotide kinase for immunoprecipitation experiments and *Nae*I and *Nar*I restriction endonucleases were purchased from Promega Corporation. *Hind*III, *Afl*III and *Pvu*I restriction endonucleases were purchased from New England Biolabs. *Xho*I and *Kpn*I restriction endonucleases and T4 DNA ligase were purchased from Boehringer Mannheim, Inc. T4 polynucleotide kinase for gel-shift experiments, Shrimp Alkaline Phosphatase (SAP) and Exonuclease I (ExoI) were purchased from USB Corporation. Thermosequenase, dNTPs, Protein-G Sepharose 4 Fast Flow, streptavidin-horseradish peroxidase, anti-mouse immunoglobulin antibody and ECL Western blotting detection kits were purchased from Amersham Pharmacia Biotech. Radioactively labeled nucleotides were purchased from NEN Life Science Products, Inc. SeaKem GTG agarose, SeaPlaque agarose and NuSieve 3:1 agarose were purchased from FMC BioProducts. DH5α competent *E. coli* cells, Dulbecco's Modified Eagle Medium (DMEM; 4.5 g/L glucose), LipofectAMINE transfection reagent, and OptiMEM medium were purchased from Gibco BRL Life Technologies, Inc. NIH 3T3 cells were obtained form the American Type Culture Collection. Bovine calf serum was purchased from HyClone Laboratories, Inc. Hygromycin B was purchased from

Calbiochem-Novabiochem Corporation. BioMax autoradiography film was purchased from Eastman Kodak Corporation. Antibodies against hMSH2 (monoclonal) were purchased from Oncogene Research Products. Antibodies against hMSH6 (polyclonal), hMLH1 (polyclonal) hPMS2 (polyclonal) and hPMS1 (polyclonal) were purchased from Santa Cruz Biotechnology. Sigma-Fluor liquid scintillation cocktail, Sephadex G-25, Sephadex G-50, carbenicillin and all other reagents were purchased from Sigma Chemical Company unless otherwise noted.

B. Plasmid and M13 Constructs

Prior to these studies the following steps were taken to produce the plasmids and M13 bacteriophage constructs used in the mismatched plasmid preparation (227, 228). First, a shuttle vector containing human H-*ras* genomic DNA was constructed by inserting the wild-type (wt) human H-*ras* genomic sequence (*Bam*HI 6.4 kb segment from pbc-N1) into the *Bam*HI site in the polylinker region of the Epstein Barr Virus (EBV) shuttle vector p220.2. Removal of the original *Hind*III site in the polylinker region of p220.pbc was then accomplished by DNA polymerase I (Klenow fragment) 5'–> 3' exonucleolytic digestion and subsequent blunt-end ligation by the standard procedure (229) to produce the p220.pbc-H/B plasmid (see below for description of –H/B). A 2 kb *Bam*HI-*Kpn*I segment of p220.pbc-H/B containing exon 1 was ligated into the polylinker region of bacteriophage M13mp19 and subjected to oligonucleotide-directed mutagenesis to create two new restriction enzyme recognition sites, *Hind*III and

*Bst*98I, 30 basepairs (bp) apart flanking H-*ras* codon 10 and codon 12 in exon 1. Three separate rounds of oligonucleotide-directed mutagenesis were performed with the M13-*ras* plasmid to change a total of four bases: codon 6, G –> T (no amino acid change to create a unique *Hind*III site) and codon 15, GGC –> CTT (Gly –> Leu, both neutral non-polar amino acids to create a unique *Bst*98I site). Restriction digestion and dideoxy sequencing were used to select M13-*ras* clones that contained only the above indicated base changes. The *Bam*HI-*Kpn*I segment containing the new sites was excised from double stranded M13-*ras* DNA and re-inserted into p220.pbc-H/B to replace the original 2 kb H-*ras* segment, producing the modified plasmid p220.pbc+H/B. The 2 kb *Bam*HI - *Kpn*I segment of the H-*ras* gene containing codon 10 and codon 12 was then isolated from the p220.pbc+H/B plasmid and ligated into the polylinker region of pUC19 , M13mp18 and M13mp19 to produce p*ras*BK2.0, M13*ras*18.9 (+ strand contains non-coding sequence from H-*ras*) and M13*ras* 19.1(+ strand contains coding sequence from H-*ras*), respectively.

C. Heteroduplex Preparation for Mismatch Repair Analysis

To create heteroduplex DNA, 100 µg of the p*ras*BK2.0 plasmid was initially digested with 1.5 units enzyme/µg DNA each of *Afl*III (New England Biolabs) and *Pvu*I (New England Biolabs) at a final DNA concentration of 0.20 µg/µl to release a 2.5 kb fragment containing the inserted H-*ras* segment. The products from this reaction were next digested with *Bst*98I (Promega Corporation) in a final DNA concentration of 50

ng/μl using approximately 10 units enzyme/μg DNA. The digest was checked by gel electrophoresis and repeated if the reaction was not judged as complete by the disappearance of the 2.5 kb band and the appearance of a 2.1 kb band. The products from the *Bst*98I digest were then digested with *Hind*III (New England Biolabs) using approximately 10 units enzyme/μg DNA in a final concentration of 50 ng/μl to produce a unique 1.7 kb fragment. The four restriction enzyme digestions selectively excise the 30 bp segment containing codon 10 of H-*ras* from the *ras* containing segment (Figure 4, Step 1).

Mismatch oligonucleotides complementary to the 30 bp region spanning codon 10 were obtained from Operon Technologies Inc. Coding strand oligonucleotides had the sequence of 5'-AGCTTGTGGTGGTGG**G**CGCCGGCGGTGTGC-3' with the bolded G replaced with T to produce T:C mismatches or A to produce A:C mismatches at codon 10. Non-coding strand oligonucleotides had the sequence of 5'-TTAAGCACACCGCCGGCG**C**CCACCACCACA-3' with the bolded C replaced with T to produce G:T mismatches or with A to produce G:A mismatches at codon 10. Oligonucleotides were phosphorylated using T4 polynucleotide kinase (USB Corporation) at a final DNA concentration of 0.125 μg/μl using 16 units enzyme/μg DNA as described by the manufacturer. The reactions were incubated at 37°C for 60 minutes and then spun through a Sephadex G-50 column (Sigma Chemical Company) equilibrated in dH_2O at 300 x g for 3 minutes.

The phosphorylated mismatch oligonucleotides were annealed with the complementary single stranded M13*ras* DNA and the fragments from the

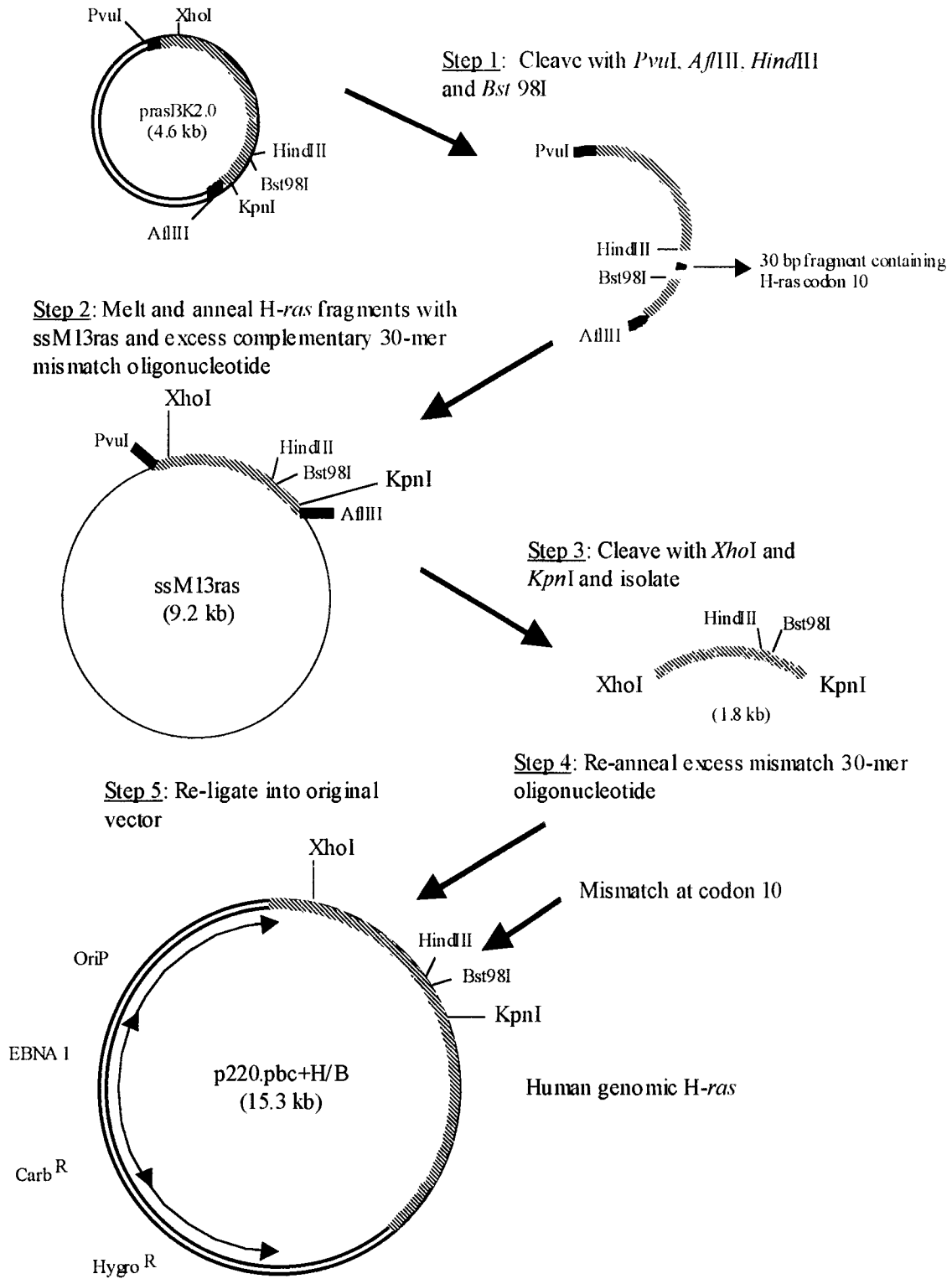

Figure 4 – Mismatch Plasmid Construction. See text for description of processes

*Afl*III/*Pvu*I/*Bst*98I/*Hind*III digested p*ras*BK2.0 at a 50:1:1 molar ratio of oligonucleotides:M13*ras*:fragments (Figure 4, Step 2). This reaction was carried out in a final volume of 50 µl at a final DNA concentration of 45 ng/µl in 40 mM Tris (pH 7.6), 50 mM $MgCl_2$, 50 mM $NaCl_2$. The fragments were heated to 100°C for 8 minutes (min) and then cooled to 80°C over 2 min. During the last 30 seconds of this cooling period the M13*ras*, annealing buffer and mismatch oligonucleotides were added. The reaction was then allowed to cool to 65°C over 30 minutes and held at 65°C for an additional 30 minutes before cooling to 2°C. Generation of heteroduplex DNA was made according to choice of mismatch 30-mer oligonucleotide and single-stranded M13*ras* complementary DNA. Use of single-stranded M13*ras*18.9 (non-coding strand) and the appropriate mismatch-containing oligonucleotide based on the coding strand resulted in T:C and A:C mismatches. Use of single-stranded M13*ras*19.1 (coding strand) and the appropriate mismatch-containing oligonucleotides based on the non-coding strand resulted in G:T or G:A mismatches.

The partially double stranded M13*ras* molecule was next cleaved with *Xho*I and *Kpn*I using 10 units of each enzyme/µg DNA at a final DNA concentration of 100 ng/µl to produce a unique 1.8 kb double stranded fragment (Figure 4, Step 3). The reaction contents were subjected to 1% gel electrophoresis through a SeaPlaque gel (FMC BioProducts) and the 1.8 kb fragment was isolated using the Qiaquick Gel Extraction Kit as described by the manufacturer (Qiagen, Inc.).

To ensure that the mismatch-containing oligonucleotide was indeed present, excess mismatch-containing oligonucleotide was again annealed to the fragment.

Oligonucleotide and the 1.8 kb fragment were mixed together at a 200:1 molar ratio of oligonucleotide:1.8 kb fragment at a DNA concentration of 50 ng/μl in a buffer consisting of 50 mM Tris-HCl (pH 7.6), 10 mM dithiothreitol, 500 μg/ml bovine serum albumin. The mixture was placed in a 2-liter beaker of water at 85°C and allowed to cool overnight to room temperature (Figure 4, Step 4). The 1.8 kb fragment was then ligated to the 13.5 kb *Xho*I-*Kpn*I vector portion of the original p220.pbc-H/B plasmid at a 3:1 molar ratio of fragment:vector using 0.5 units T4 DNA Ligase (Boehringer Mannheim Corporation) per μg DNA as described by the manufacturer. The 13.5 kb vector was produced by digesting p220.pbc-H/B with 10 units/μg DNA each of *Xho*I and *Kpn*I at a final concentration of 100 ng/μl. The digestion reaction products were then run overnight at low voltage on a 0.7% SeaKem GTG gel (FMC BioProducts) and the 13.5 kb band was excised and purified using the Qiaquick Gel Extraction Kit as described by the manufacturer (Qiagen, Inc.). The vector contains the remaining H-*ras* genomic sequence, Epstein-Barr virus (EBV) origin of replication, eukaryotic hygromycin resistance, bacterial carbenicillin resistance and bacterial replication sequences (230). The final ligation step produces a p220pbc+H/B plasmid containing a site- and strand-specific mismatch at H-*ras* codon 10, middle base pair (Figure 4, step 5). This heteroduplex is easily distinguished from any undigested vector (p220.pbc-H/B) by the presence of the *Hind*III and *Bst*98I sites.

D. Cell Lines and Transfection

DH5α competent *E. coli* cells were transformed with 50 ng of mismatch containing plasmid as described by the manufacturer (Gibco BRL Life Technologies, Inc.). Bacteria were grown overnight at 37°C on LB agar plates containing 75 μg/ml carbenicillin. NIH 3T3 cells were grown in DMEM, 10% calf serum at 37°C, 5% CO_2. Cells were seeded at 1 x 10^6 per 100 mm plate in preparation for transfection experiments 16-18 hours (hr) later. For each plate 100 ng of plasmid DNA was added to 670 μl of OptiMEM media (Gibco BRL Life Technologies, Inc.) and 30 μl of LipofectAMINE transfection reagent and incubated for 40 min at room temperature. The cells were placed into OptiMEM media and the plasmid mixture was added evenly to each plate. The plates were then placed at 37°C with gentle rotation for 30 min and then at 37°C, 5% CO_2 for 5 hr 30 min without agitation. At this time the OptiMEM media was removed and replaced with DMEM, 10% calf serum. NIH 3T3 hygromycin resistant cells were subsequently selected for by the addition of 125 units of hygromycin (Calbiochem-Novabiochem Corporation) per ml of media, starting 36 hr after transfection. At the end of 3 weeks, hygromycin resistant colonies on each plate were methanol (97%) fixed and stained using 1% crystal violet, 20% ethanol.

E. Mismatch Repair Analysis

To analyze repair of mismatches *in vivo* in NIH 3T3 cells, DNA was purified from each hygromycin-resistant colony. Cloning cylinders (Bellco Glass, Inc.) were adhered to the culture dish surrounding each colony using sterile silicone vacuum grease. A 100 µl aliquot of lysis buffer (10 mM Tris-HCl (pH 8.3), 50 mM KCl, 0.1 mg/ml gelatin, 0.45% NP-40, 0.45% Tween 20, 2.5 mM $MgCl_2$) containing 12 µg Proteinase K (231) was added to the cloning ring and incubated for 10 min at room temperature. Each solution was then repeatedly aspirated to dislodge remaining cells from the culture plate, transferred into a 0.5-ml microcentrifuge tube and incubated for 1 h at 55°C followed by 10 min at 95°C. Samples were extracted once with 2 volumes (vol) of phenol:chloroform:isoamyl alcohol (25 vol:24 vol:1 vol, Sigma Chemical Company), and precipitated overnight at –20°C with 1/10 vol of 3 M sodium acetate and 2 vol ethanol. The DNA pellets were isolated by centrifugation for 30 min at 1,200 x g and then dried by centrifugation under a vacuum with heat for 20 min. The DNA lysates were then resuspended in 10 µl of sterile dH2O.

To purify DNA from carbenicillin resistant DH5α colonies, cells from each colony were removed from the plates using sterile toothpicks and placed in 0.5-ml microcentrifuge tubes. 100 µl of the lysis buffer (10 mM Tris-HCl (pH 8.3), 50 mM KCl, 0.1 mg/ml gelatin, 0.45% NP-40, 0.45% Tween 20, 2.5 mM $MgCl_2$,12 µg Proteinase K) was added to the microcentrifuge tubes and they were incubated for 1 h at 55°C followed by 10 min at 95°C. Samples were then extracted once with 2 vol of

phenol:chloroform:isoamyl alcohol (25 vol:24 vol:1 vol, Sigma Chemical Company), and precipitated overnight at –20°C with 1/10 vol of 3 M sodium acetate and 2 vol ethanol. The DNA pellets were isolated by centrifugation for 30 min at 1,200 x g and then dried by centrifugation under a vacuum with heat for 20 min followed by resuspension in 10 µl of sterile dH_2O.

A 5-µl aliquot from each DNA lysate was PCR amplified using 2.5 units of Amplitherm enzyme (Epicentre Technologies) per reaction in the supplied buffer plus 0.5-5 mM $MgCl_2$ (optimized for each preparation), 200 µM of each dNTP and 100 ng of each primer in a final volume of 100 µl, with the amplitherm enzyme separated from the other reactants by a wax layer (Chill-Out 14, MJ Research, Inc.). The reactions were heated to 96°C for 3 min followed by 35 cycles of 40 seconds at 96°C, 40 seconds at 62°C and 1 min at 72°C. The samples were then incubated for 7 min at 72°C to allow completion of extension reactions and cooled to 4°C. PCR primers used for DNA amplification were: 5' H-*ras* –> 5'-TGAGGAGCGATGACGGAATAT-3' and 3' H-*ras* –>5'-CAGGCTCACCTCTATAGTGGGGTC-3', yielding an amplified DNA product of 129 bp containing exon 1 of human H-*ras* plus several base pairs of human intronic region surrounding exon 1, thus precluding amplification of NIH 3T3 genomic DNA. Negative controls (no DNA added to PCR amplification reaction) were added to each experiment and correct amplification was checked by electrophoresis on a 2% SeaKem GTG gel (FMC BioProducts) (see Figure 5A).

To confirm that each sample did not result from transfection of undigested vector (p220.pbc-H/B), 20 µl of each PCR amplified product was purified with Qiagen's PCR

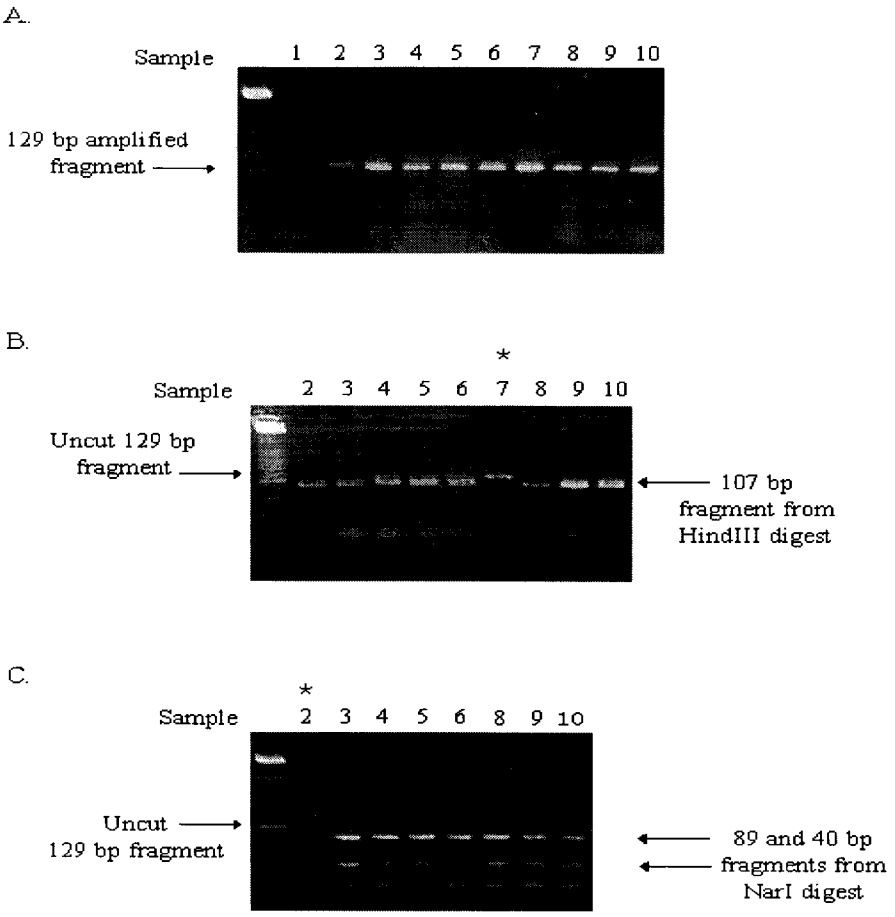

Figure 5 – Example of Agarose Gels from Mismatch Repair Analyses. After transfection of mismatched plasmid, DNA was isolated and PCR amplified from each NIH 3T3 colony as described (Materials and Methods). A 25 bp DNA ladder was run in the initial lane of each gel with the darkest band representing 125 bp. (A) Check of PCR amplification reaction. Lane 1: Negative control with no DNA added, Lanes 2- 10: amplification of 129 base pair fragment. (B) *Hind*III digestion of aliquots from each amplification. Lanes 2-6, 8-10: 107 base pair *Hind*III digested fragment. Lane 7: sample is not digested with *Hind*III and therefore represents transfected p220.pbc-H/B vector. (C) *Nar*I digestion of aliquots from each +H/B sample. Lane 2: partial digest indicates sample is a mixture of wild-type and transformed sequences. Lanes 3-6, 8-10: complete digestion indicates wild-type sequences only.

Purification Kit as described by the manufacturer (Qiagen, Inc.), eluted in 20 µl of dH_2O and then digested with 25 units of *Hind*III (New England Biolabs) overnight at 37°C. The digested samples were electrophoresed on a 4% NuSieve 3:1 gel (FMC BioProducts) and analyzed (see Figure 5B). Any samples which were not digested by the *Hind*III (p220.pbc-H/B instead of +H/B heteroduplex) were eliminated. A 20 µl aliquot of each correctly amplified product was then digested with 5 units of Turbo *Nae I* restriction enzyme (Santa Cruz Biotechnology) for codon 12 analysis or 2.5 units of Turbo *Nar I* (Santa Cruz Biotechnology) for codon 10 analysis in the supplied buffers for 4 hr. The digestion products were electrophoresed on a 4% NuSieve 3:1 gel (FMC BioProducts) and analyzed (see Figure 5C). Only PCR amplified DNA containing wild-type human H-*ras* at the relevant codon is cleaved by these restriction enzymes. If the PCR amplified DNA was not completely cleaved, a 20 µl aliquot was treated with 10 units each of the enzymes SAP (USB Corporation) and ExoI (USB Corporation) and incubated for 15 min at 37°C followed by heat inactivation of the enzymes at 80°C for 15 min. The DNA was then cycle-sequenced as described by the manufacturer (Amersham Pharmacia Biotech), run on a 12% polyacrylamide gel (19:1 acrylamide to bisacrylamide) and exposed overnight to film (Eastman Kodak Corporation) to determine the exact mutation.

F. Preparation of Oligonucleotides for Gel-Shift Assays

For these experiments, 32-mer oligonucleotides were derived from the H-*ras* sequence surrounding codon 10 and 12. These have the sequence of 5'-

GGTGGTGGTGG**X**CGCCG**Y**CGGTGTGGGCAAGA-3' or 5'-GGTGGGCGCCG**Y**CGGTGTGGGCAAGAGTGCGC-3', in which **X** represents the middle base of H-*ras* codon 10 and **Y** represents the middle base of H-*ras* codon 12. Wild-type oligonucleotides were 5'end labeled using [γ-^{32}P] ATP (3,000 Ci/mmol) (NEN Life Science Products, Inc.) and T4 phosphonucleotide kinase (Promega Corporation) at a DNA concentration of 1 pmol/μl for 1 hr as described by the manufacturer. The phosphorylation reaction was quenched by adding 1 μl of 0.5 M EDTA (pH 8.0) and 89 μl of Tris-EDTA (pH 7.5). The oligonucleotides were then purified from non-incorporated nucleotides by filtration through a sephadex G-25 spin column equilibrated in Tris-EDTA, pH 7.5 at 300 x g for 3 min. The 5' [^{32}P]-labeled wild-type single-stranded oligonucleotides were annealed to the complementary oligonucleotides (wild-type or mismatch containing) at a 1:3 molar ratio of labeled wild-type oligonucleotide to unlabeled complementary oligonucleotide at a final DNA concentration of 0.3 pmol/μl and a final volume of 100 μl in a buffer consisting of 1mM Tris-HCl (pH 8.0), 1 mM $MgCl_2$. The solution was heated to 95°C for 5 minutes and then allowed to cool to room temperature over a 2-hr time period prior to rapid cooling to 4°C. Unlabeled wild-type competitor oligonucleotide was prepared similarly. No detectable labeled single-stranded oligonucleotide was found when these substrates were examined by native polyacrylamide electrophoresis. The specific activity of each double-stranded oligonucleotide was determined by liquid scintillation counting in 5 ml of Sigma-Fluor liquid scintillation cocktail (Sigma Chemical Company).

G. Gel-Shift Assays

HeLa nuclear extracts for the nuclear protein-DNA binding reactions were purchased from Promega Corporation and were resuspended in a buffer consisting of 20 mM Hepes (pH 7.9), 20% glycerol, 0.1 M KCl, 0.2 mM EDTA, 0.2 mM PMSF, 0.5 mM DTT. NIH 3T3 nuclear extracts were purchased from Santa Cruz Biotechnology and were resuspended in a buffer consisting of 20 mM Hepes (pH 7.9), 20% glycerol, 0.1 M KCl, 0.2 mM EDTA, 0.5 mM PMSF, 0.5 mM DTT (232). For each reaction involving HeLa nuclear extracts, 10 μg of the protein was first placed in a binding buffer containing 4% glycerol, 1 mM $MgCl_2$, 0.5 mM EDTA, 0.5 mM DTT, 50 mM NaCl, 10 mM Tris-HCl (pH 7.5), and 0.05 μg/ml poly(dI-dC)-poly(dI-dC) and pre-incubated for 40 min at room temperature. For reactions involving NIH 3T3 nuclear extracts, 10 μg of the protein was pre-incubated for 40 min at 4°C in a binding buffer consisting of 10% glycerol, 25 mM Hepes-KOH (pH 8.0), 0.5 mM EDTA, 0.1 mM $ZnCl_2$, 0.5 mM DTT, 0.05 μg/ml poly(dI-dC)-poly(dI-dC). Nuclear protein-DNA binding reactions were then carried out at 4°C in a total volume of 10 μl using 35 fmol of radioactively labeled oligonucleotide and 0.9 pmol of unlabeled double-stranded wild-type competitor (approximately a 1:25 molar ratio). The mismatched oligonucleotide substrate and competitor wild-type oligonucleotide were added simultaneously and the reactions were incubated for a further 30 min at 4°C to allow the proteins to interact with the DNA.

Following nuclear protein-DNA binding, 1 μl of a non-denaturing loading buffer (250 mM Tris-HCl (pH 7.5), 0.2% bromphenol blue, 40% glycerol) was added and the

samples were loaded onto a 6% polyacrylamide non-denaturing gel (39:1 acrylamide to bisacrylamide). Electrophoresis was carried out at 4°C at 100 Volts (10 Volts/cm) in TBE. Gels were then dried and exposed to Biomax film (Eastman Kodak Corporation). Autoradiographs were scanned and analyzed using NIH Image Software. In experiments to assess efficiency of binding to different radioactive substrates, equal amounts of radioactivity were used as determined by liquid scintillation counting. Competition assays using unlabeled mismatched oligonucleotides as competitors were conducted exactly as above except for substitution of unlabeled mismatched oligonucleotide for the unlabeled wild-type oligonucleotide. For antibody binding assays, 1 μg of monoclonal anti-hMSH6 antibody (Santa Cruz Biotechnology, Inc.) was allowed to incubate with the nuclear extracts for 20 minutes prior to addition of the DNA mixture. For ATP inhibition assays, 1 mM ATP was added to the binding buffer prior to addition of nuclear extract and DNA.

H. Preparation of Oligonucleotides for UV Cross-linking, Immunoprecipitation and Western Blotting Assays

A 32-mer oligonucleotide having the sequence of 5'-GGTGGGCGCCG**G**CGGTGTGGGCAAGAGTGCGC-3' (Operon Technologies, Inc.) was used for these assays with the bolded G specifying the location of the mismatch. Wild-type oligonucleotides were 5' end-labeled using [γ-^{32}P] ATP (6,000 Ci/mmol) (NEN Life Science Products, Inc.) and T4 polynucleotide kinase for 1 hr at 37°C as

described by the manufacturer (Promega Corporation). The phosphorylation reaction was quenched by adding 1 µl of 0.5 MEDTA (pH 8.0) and 89 µl of Tris-EDTA (pH 7.5), and the oligonucleotides were then purified from unincorporated nucleotides using a Sephadex G-25 spin column equilibrated in Tris-EDTA (pH 7.5) at 300 x g for 3 min. Aliquots from the same batch of 5' [^{32}P] -labeled wild-type oligonucleotide were annealed to complementary oligonucleotides containing a C (homoduplex), T (heteroduplex, G:T) or A (heteroduplex, G:A) opposite the bolded G, thereby producing double-stranded oligonucleotides with similar specific radioactivities. The annealing was performed at a 1:3 molar ratio of 5' [^{32}P] -labeled to unlabeled oligonucleotide at a final DNA concentration of 0.3 pmol/µl and a final volume of 100 µl in 10 mM Tris-HCl (pH 8.0), 10 mM $MgCl_2$. The solution was heated to 95°C for 5 min and then allowed to cool to 20°C over 2 hr followed by rapid cooling to 4°C. Unlabeled wild-type competitor oligonucleotides were prepared similarly. No detectable labeled single-stranded oligonucleotide was found when these substrates were examined by native polyacrylamide electrophoresis.

I. UV Cross-linking and Immunoprecipitation

HeLa nuclear protein-DNA binding reactions for UV cross-linking and immunoprecipitation experiments were carried out in a binding buffer containing 4% glycerol, 1 mM $MgCl_2$, 0.5 mM EDTA, 0.5 mM DTT, 50 mM NaCl, 10 mM Tris-HCl (pH 7.5), 0.05 µg/ml poly (dI-dC)- poly (dI-dC) and 165 µg of nuclear extract in 10

aliquots with a combined total volume of 200 µl. The nuclear extract was added to the binding buffer and allowed to incubate for 30 min at room temperature. A DNA mixture containing 1.05 pmol of 5' [^{32}P] -labeled double-stranded oligonucleotide (either heteroduplex or homoduplex) and 27 pmol of unlabeled double-stranded homoduplex competitor (an approximately 1:25 molar ratio of 5' [^{32}P] -labeled to unlabeled oligonucleotide) was then added and the reactions were placed on ice for 40 min to allow binding of nuclear proteins to the oligonucleotides. All subsequent steps were performed at 0°C-4°C. Bound proteins were UV cross-linked to the DNA using a 5 min exposure on ice at 254 nm in a UV Stratalinker (Stratagene) at approximately 5 cm from the UV source. 3 µg of the indicated antibody was added and the reactions were placed on a rolling mixer overnight to allow coupling of the antibodies to their antigen. 40 µl of a Protein-G Sepharose 4 Fast Flow slurry (Amersham Pharmacia Biotech) was next added to precipitate the immunoglobulins and the reactions were rotated for a further 3 hr at 4°C. The immunoprecipitates were then recovered by centrifugation (200 x g, 1 min), washed 2 times with a buffer consisting of 10 mM Tris-HCl (pH 8.0), 150 mM NaCl, 0.1% Triton X-100, 0.025% NaN_3 and 0.1% BSA, washed 1 time with a buffer consisting of 10 mM Tris-HCl (pH 8.0), 150 mM NaCl and 0.025 % NaN_3 and then washed 1 time with a buffer consisting of 50 mM Tris-HCl (pH 6.8). Between each wash the samples were centrifuged at 200 X g for 1 min to pellet the beads and the supernatent was aspirated with a fine-tipped Pasteur pipette. After the final wash, approximately 10 µl of the buffer was left in the microcentrifuge tubes and an equal volume of 2X SDS sample buffer (Tris-HCL/SDS (pH 6.8), 4% SDS, 20% glycerol, 2% 2-mercaptoethanol, 10

μg/ml bromphenol blue) was added. The samples were heated for 5 min at 100°C with the caps open, placed on ice and loaded onto a 7.5% discontinuous SDS polyacrylamide gel (stacking gel 30% acrylamide/0.8% bisacrylamide, 4% Tris-HCl/SDS (pH 6.8); separating gel 30% acrylamide/0.8% bisacrylamide, 4% Tris-HCl/SDS (pH 8.8)). Following electrophoresis at 10 mA for 2 hr, gels were dried and exposed to Biomax film (Eastman Kodak Corporation) to detect precipitated labeled oligonucleotide. Assays involving ATP were performed as above except that ATP (Sigma Chemical Company) at 0.1 mM was added immediately prior to the UV cross-linking step.

J. Western Blotting

Nuclear protein was bound to the DNA substrates, UV cross-linked, immunoprecipitated and electrophoresed as above. The resulting gel was then transferred overnight at 10 mA onto a pre-wetted nitrocellulose membrane (Schleicher and Schuell, Inc.) using a Trans-Blot apparatus (Bio-Rad Laboratories) in a transfer buffer consisting of 2.5 mM Tris, 19.2 mM glycine. For Western blotting, membranes were placed in blocking buffer (5% non-fat milk in Tris-buffered saline (pH 7.6), 0.1% Tween 20 (TBS-T) for 1 hr with agitation. The membrane was then washed by rinsing briefly twice in TBS-T, placing the membrane in fresh TBS-T with agitation for 15 min and then placing it again in fresh TBS-T twice for 5 min with agitation. The membrane was next incubated with primary antibody in TBS-T with agitation for 1 hr. The dilution of antibody to TBS-T was 1:200 for hMSH2, hMLH1 and hPMS2, and 1:2000 for hMSH6

and hPMS1. Excess primary antibody was washed from the membrane by rinsing briefly twice in TBS-T, placing the membrane in fresh TBS-T with agitation for 15 min and then placing it again in fresh TBS-T twice for 5 min with agitation. The membrane was then incubated in TBS-T with secondary antibody against the specific primary antibody used. For hMSH2 a horseradish peroxidase (HRP)-conjugated anti-mouse immunoglobulin antibody (Amersham Pharmacia Biotech) was used at a dilution of 1:1000. For hMSH6 an HRP conjugated anti-goat immunoglobulin antibody (Santa Cruz Biotechnology) was used at a dilution of 1:1000. For hMLH1, hPMS2 and hPMS1 a biotinylated anti-rabbit immunoglobulin antibody (Sigma Chemical Company) was used at a dilution of 1:1000. Excess secondary antibody was washed from the membrane again by rinsing briefly twice in TBS-T, placing the membrane in fresh TBS-T with agitation for 15 min and then placing it in fresh TBS-T twice for 5 min with agitation. For hMLH1, hPMS2 and hPMS1 (and when biotinylated molecular weight markers were used, see below) the membrane was then incubated with streptavidin-HRP (Amersham Pharmacia Biotech) for 1 hr in TBS-T with agitation at a dilution of 1:1500 to bind the HRP enzyme to the biotin via streptavidin. Bound antibodies were detected by ECL detection of the HRP enzyme as described by the manufacturer (Amersham Pharmacia Biotech). Between each probe the membrane was stripped of bound antibodies by a 30 min incubation at 55°C in 100 mM 2-mercaptoethanol, 2% SDS, 62.5 mM Tris-HCl (pH 6.7).

K. Molecular Weight Determination

For UV cross-linking and immunoprecipitation experiments high-range molecular weight markers (Bio-Rad Laboratories) were run on each gel. 5 µl of the protein mix was added to 5 µl of 2X SDS sample loading buffer (Tris-HCL/SDS (pH 6.8), 4% SDS, 20% glycerol, 2% 2-mercaptoethanol, 10 µg/ml bromphenol blue) and heated for 5 min at 100°C. The microcentrifuge tubes were then placed on ice and the samples loaded on the gels. After electophoresis the gels were stained with the Zoion Fast Stain Coomasie blue staining kit as described by the manufacturer (Zoion Biotech) to visualize the molecular weight markers. For Western blotting experiments, biotin-conjugated high range molecular weight standards (Bio-Rad Laboratories) were used. An incubation with streptavidin-horseradish peroxidase (Amersham Pharmacia Biotech) was included at a 1:1500 dilution to bind the HRP enzyme to the biotinylated proteins via streptavidin and ECL detection was performed as described by the manufacturer (Amersham Pharmacia Biotech) to visualize the molecular weight markers.

III. Results

A. In Vivo Mismatch Repair Rates

To determine if there is a deficiency in mismatch repair at the H-*ras* hotspot of mutation, repair rates were determined *in vivo* in non-synchronous NIH 3T3 cells for each of the specific mismatches when located at the middle nucleotide of codon 10 of H-*ras*. Previously, *in vivo* rates of repair for specific mismatches at the middle nucleotide position of the H-*ras* codon 12 hotspot of mutation were determined in non-synchronized NIH 3T3 cells (227) (summary of results shown in Figure 6 for comparison). Codon 10 has the same primary sequence as codon 12 (GGC) with the middle nucleotide of each separated by only 6 basepairs. However, codon 10 does not appear to be a hotspot of mutation, as there have not been mutations at this sequence found in any *in vitro* activation assay or *in vivo* in naturally occurring human tumors (203 - 205).

Analysis of *in vivo* mismatch repair by individual cells was performed by transfecting with mismatch-containing plasmid, selecting for the growth of carbenicillin-resistant *E. coli* or hygromycin-resistant NIH 3T3 colonies, isolating the DNA and PCR amplifying a 129 base pair segment from the plasmid containing H-*ras* codon 10. The samples were then analyzed by restriction digest with the *Nar*I enzyme (Promega Corporation) to determine the sequence at codon 10. Any samples not completely digested by *Nar*I were cycle-sequenced to determine the sequence at codon 10 (227, 228). Figure 5 shows an example of the gels resulting from this process.

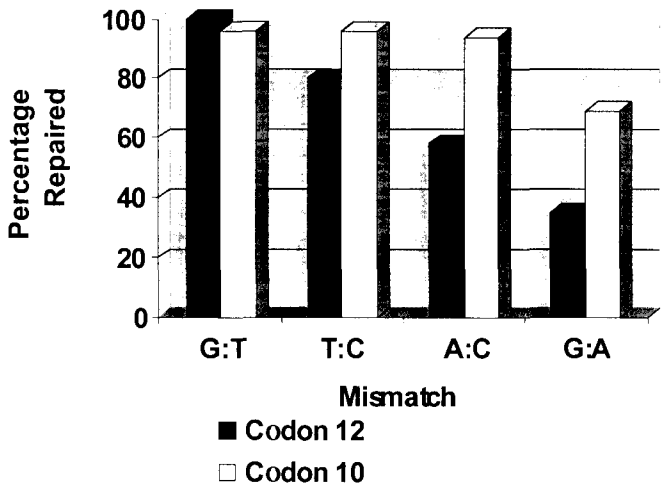

Figure 6 - Comparison of Mismatch Repair Rates for H-*ras* Codon 10 and Codon 12. Repair rates for codon 12 in non-synchronized cells were reported in Arcangeli et. al. (227) and are shown here for comparison (correct repair at codon 12: G:A –> 35%, A:C –> 58%, T:C –>80%, G:T –>100%), correct repair at codon 10 G:A –> 69%, A:C –> 94%, T:C –>96%, G:T –> 96%. Repair percentages include all mismatches repaired correctly to G:C, but not mismatches which are replicated before repair and thus are found as mixtures in the resulting colony.

A number of controls were performed to assess the quality and purity of our mismatched plasmid preparations and repair results. Each mismatch plasmid was prepared at least twice to verify reproducibility of results. Further controls in which mismatch-containing plasmid was transformed into mismatch repair deficient bacteria (NR9161, *mut L*$^-$) yielded only unrepaired mixtures in the resultant colonies (227). Also, control transfections of plasmid containing either the wild-type or mutated sequence were included with each experiment to ensure that analysis of the sequence at codon 12 yielded the expected results after PCR amplification. Finally, all PCR amplified samples were digested with *Hind*III (New England Biolabs) to ensure that the heteroduplex plasmid (+*Hind*III/*Bst*98I, see Materials and Methods) was used for the transfection and not the undigested vector (p220.pbc-H/B) (see Figure 5).

Each mismatch preparation was also transformed into *E. coli* as we have previously demonstrated that *E. coli* is not transformed by gapped plasmid (minus the mismatch oligonucleotide) and that codon 12 of H-*ras* is not a hotspot of mutation in bacteria (227). As seen in Table 2, codon 10 of H-*ras* is also not a hotspot of mutation in *E. coli*. G:A mismatches are the least efficiently repaired, as at the codon 12 location and as observed by other investigators (176, 178, 233 - 235). In *E. coli*, all mismatches that are unrepaired result in a mixture of G:C and T:A or A:T, depending on the mismatch, rather than an incorrectly repaired mismatch (only T:A or only A:T). These mixtures most probably result from replication of the mismatched plasmid in the original transformed cell prior to replication and thus the percent of mixtures reflects the efficiency of repair.

Table 2 - Repair of mismatches at codon 10 of H-*ras* in *E. coli*[a].

Mismatch	Correctly Repaired Mismatch –> G:C (Total Assayed)	Incorrectly Repaired Mismatch –> T:A or A:T (Total Assayed)	Unrepaired Mismatch –> G:C and T:A or A:T (Total Assayed)
G:A	94% (31/33)	0% (0/33)	6% (2/33)
A:C	100% (41/41)	0% (0/41)	0% (0/41)
T:C	98% (59/60)	0% (0/60)	2% (1/60)
G:T	100% (51/51)	0% (0/51)	0% (0/51)

[a]A portion of each mismatch preparation used in NIH 3T3 studies was used to transform mismatch proficient *E. coli* as a control (see Results).

Table 3. Repair of mismatches at codon 10 of H-ras in non-synchronized NIH 3T3 cells [a].

Mismatch	Correctly Repaired Mismatch –> G:C (Total Assayed)	Incorrectly Repaired Mismatch –> T:A or A:T (Total Assayed)	Unrepaired Mismatch –> G:C and T:A or A:T (Total Assayed)
G:A	69% (25/36)	0% (0/36)	31% (11/36)
A:C	94% (47/50)	0% (0/50)	6% (3/50)
T:C	96% (47/49)	0% (0/49)	4% (2/49)
G:T	96% (49/51)	0% (0/51)	4% (2/51)

[a] Codon 10 is not a hotspot of mutation in H-*ras*.

The *E. coli* results also confirm that our mismatched plasmid correctly directs repair to the DNA strand containing the mismatched 30-mer oligonucleotide. The methodology used to prepare the mismatched plasmid does not facilitate hemimethylation d(GATC)-directed mismatch repair by *E. coli*. However, the procedure does produce a pre-ligation total of four nicks on the DNA strand containing the incorrect mismatched nucleotide (each end of the 1.8 kb double-stranded fragment plus each end of the single-stranded 30-mer mismatched oligonucleotide) versus two 'nicks' on the opposite DNA strand (each end of the double-stranded 1.8 kb fragment only) during preparation of mismatched DNA (Figure 4). *In vitro* ligation is highly unlikely to be 100% efficient and therefore, this protocol was determined to be appropriate for biasing the selection for plasmids containing unligated 'nicks' on the strand containing the incorrect nucleotide. The lack of *E. coli* samples where the mismatch plasmid is incorrectly repaired confirms that this procedure correctly directs repair to the strand containing the mismatched oligonucleotide.

As seen in Table 3 and Figure 5, in NIH 3T3 cells there is a significant improvement in correct mismatch repair rates for codon 10 as compared to codon 12 for G:A, A:C and T:C mismatches, while the repair rate for G:T remains at a high level. These results clearly demonstrate that repair of mismatched nucleotides is more efficient at codon 10 than at codon 12 in NIH 3T3 cells, indicating that codon 12 is a hotspot of mutation, at least in part, due to inefficiencies in accomplishing mismatch repair. Furthermore, as both codon 10 and codon 12 have a primary sequence of GGC, the only difference between the mismatches at codon 10 and codon 12 is the surrounding

sequence context. Therefore, these results demonstrate for the first time that deficiencies in mismatch repair can affect mutation rates at a hotspot of mutation and that sequence context can affect mismatch repair efficiency.

B. In Vitro Nuclear Protein Binding to Mismatches at the Codon 12 Hotspot and at Codon 10

Gel-shift nuclear protein-DNA binding assays were used to assess potential differences in mismatch-specific binding to the different mismatches at the codon 12 hotspot and at codon 10. 32-mer double stranded oligonucleotides were constructed based on the human H-*ras* genetic sequence with a specific mismatch located at the middle nucleotide of either codon 12 or codon 10. To ensure that the proximate location of codon 10 or codon 12 to the 3' or 5' end of the oligonucleotide was not affecting binding, an additional set of oligonucleotides were used in which the codon 12 position was identical in relation to the 3' and 5' end as the position of codon 10 in the first set of oligonucleotides, with similar results (Materials and Methods). All experiments were performed with both NIH 3T3 nuclear extracts and with mismatch repair proficient nuclear extracts from the human cell line HeLa (176)(Figure 7A and 7B). In each reaction an excess of unlabelled homoduplex competitor was added to control for non-mismatch-specific interactions as well as an excess of poly(dI-dC)-poly(dI-dC) to control for non-specific DNA binding interactions. Two mismatch-specific bands were observed on non-denaturing polyacrylamide gels when using HeLa nuclear extracts and one band was observed when using NIH 3T3 nuclear extracts. Densitometry measurements were

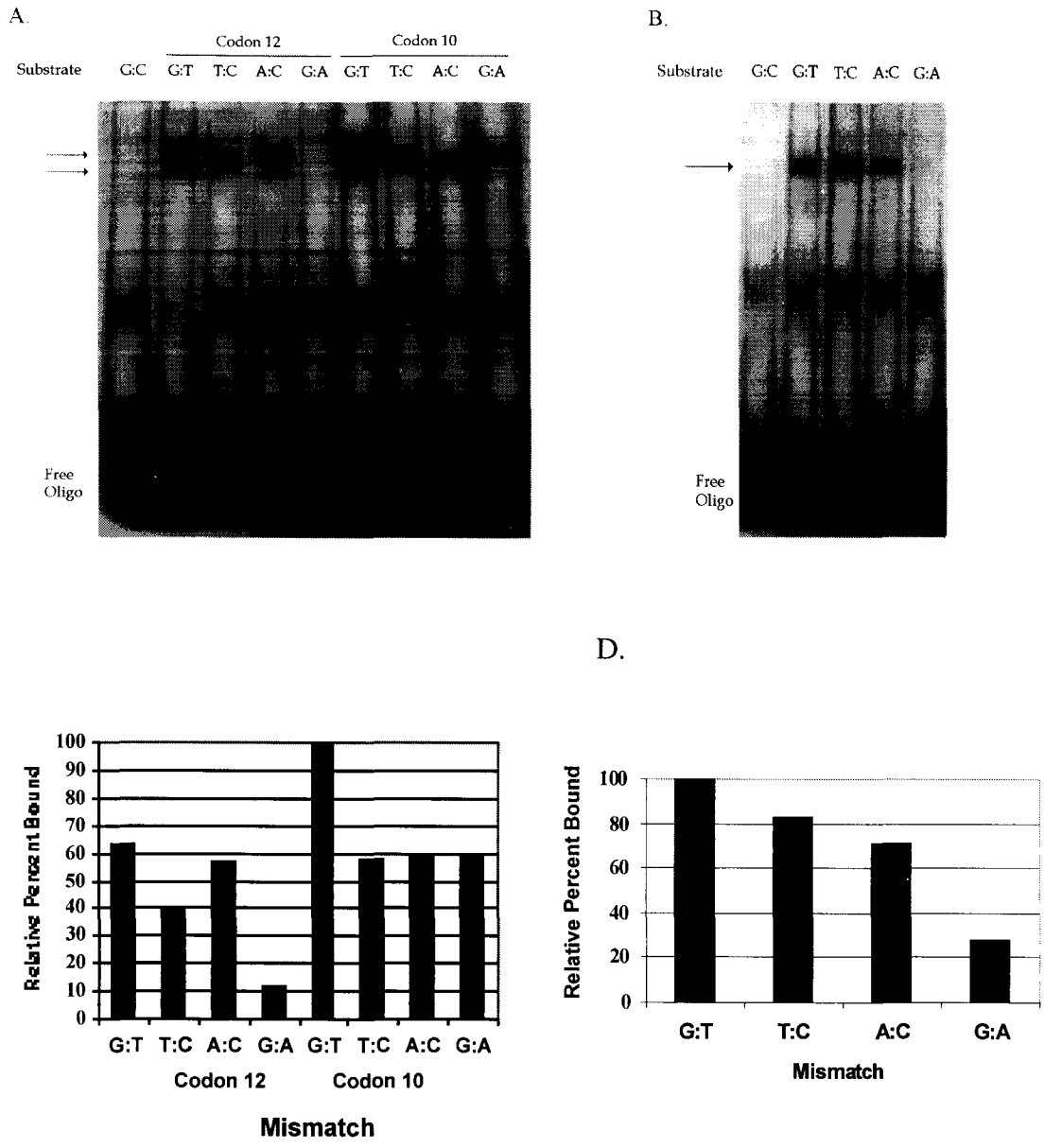

Figure 7 - Relative Amounts of Nuclear Protein Binding to Specific Mismatches at Codon 10 or Codon 12 of H-*ras*. Gel-shift assays were performed using equal amounts of radioactivity for each mismatch. Arrows indicate mismatch specific bands. (A) HeLa nuclear extract binding to mismatches at codon 10 or codon 12. (B) NIH 3T3 nuclear extract binding to codon 12 mismatches. (C) Comparison of the relative amounts of HeLa mismatch specific nuclear extract binding at codon 10 and codon 12. (D) Comparison of the relative amounts of NIH 3T3 mismatch specific nuclear extract binding at codon 12. Autoradiographs were analyzed using NIH Image software. Relative amounts of each mismatch were compared with the amount bound to the G:T containing oligonucleotide which was arbitrarily set at 100%. Averages were determined from three separate experiments.

performed to determine the relative amounts of mismatch-specific protein binding (both bands for HeLa nuclear extracts and the one band for NIH 3T3 nuclear extracts) after incubation of the nuclear extracts with each mismatch tested (Figure 7C and 7D). As shown in Figure 7D, the relative amounts of mismatch-specific binding correlates closely to our observed *in vivo* mismatch repair rates for the H-*ras* codon 12 site. Additionally, as shown in Figures 7A and 7C, there is virtually no mismatch-specific binding to the G:A mismatch located at codon 12, while at codon 10 there are observable levels of binding of just the slower migrating band to this same mismatch. This demonstrates a sequence context effect in binding by the mismatch-specific factors, and is especially intriguing in light of the low levels of repair of G:A mismatches at the codon 12 position and correspondingly higher levels of repair at codon 10.

To determine the identity of the binding factor we included monoclonal antibodies specific for the known DNA binding domain of hMSH6, a component of the hMutSα heterodimer. As seen in Figure 8A, incubation of anti-hMSH6 antibody with HeLa nuclear extract before the addition of mismatch DNA results in a marked decrease in binding by the slower migrating mismatch-specific band to G:T mismatches at codon 10. In additional experiments, ATP was added to the nuclear protein-mismatch DNA incubations, as ATP has been demonstrated to inhibit binding of the hMutSα complex to mismatched DNA (108, 120 - 122). As shown in Figure 8B, 1 mM ATP completely inhibits all mismatch-specific protein binding to the codon 10 G:T mismatched oligonucleotide. This inhibition of binding was also observed for all other specific mismatches at both codons 10 and 12 with either NIH 3T3 or HeLa nuclear extracts

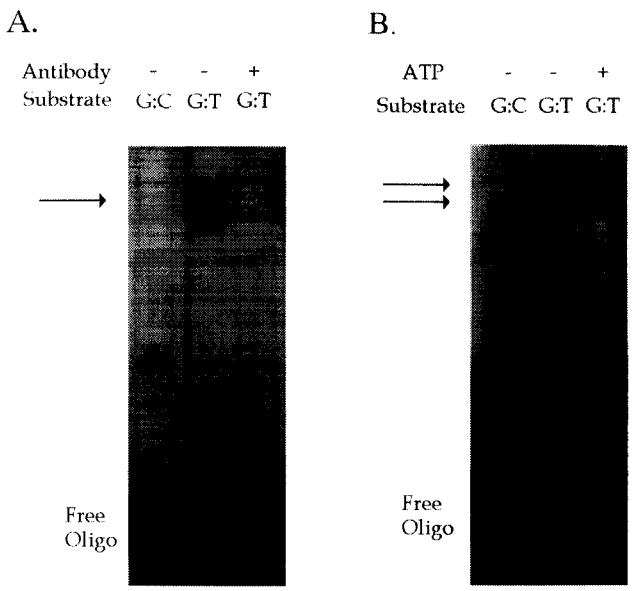

Figure 8 - Effect of anti-hMSH6 Antibody and ATP on Mismatch Specific Binding. Gel-shift assays were performed as described in Materials and Methods using HeLa nuclear extracts. (A) 1 µg of anti-hMSH6 antibody (Santa Cruz Biotechnology, Inc.) was added to nuclear extract prior to addition of oligonucleotides as indicated (+ lane), resulting in a disruption of binding. (B) 1 mM ATP was added to the binding buffer prior to addition of nuclear extract and oligonucleotides as indicated (+ lane), resulting in disruption of all mismatch specific binding.

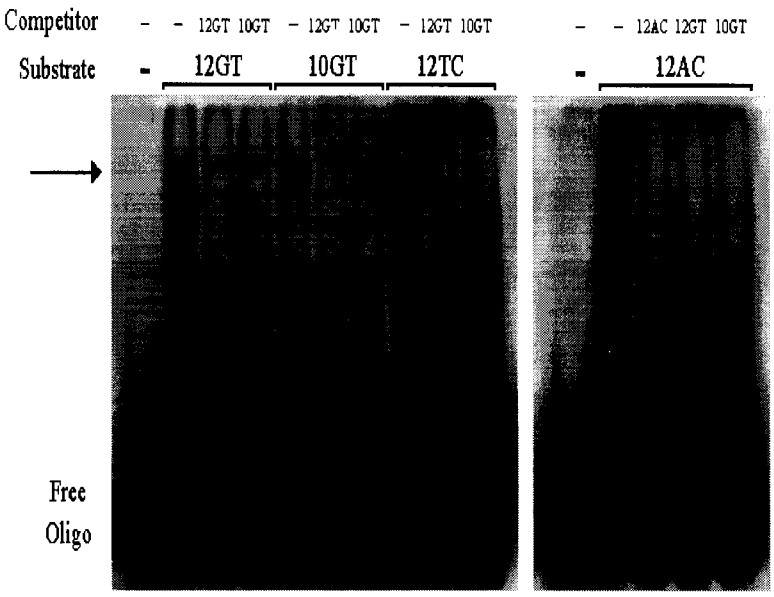

Figure 9 – Competition Assays. Gel-shift assays were performed as described in Materials and Methods with NIH 3T3 nuclear extracts using an excess of unlabeled mismatch-containing oligonucleotide as the competitor. All shown mismatches are able to compete away the mismatch specific band demonstrating that the same binding activity is responsible for the binding, regardless of which mismatch is used as the 5' [^{32}P] - labeled substrate.

(results not shown). Competition assays using an excess of non-radioactively labeled mismatched oligonucleotide demonstrated inhibition of binding between each mismatched competitor oligonucleotide when using either NIH 3T3 or HeLa nuclear extracts (see example in Figure 9). This demonstrates that the same binding factor was responsible for the mismatch-specific binding to each of the mismatches. Taken together the above results indicate that the mismatch-specific binding factor observed for each mismatch in NIH 3T3 cells and the slower migrating band we observe with HeLa nuclear extracts is the hMutSα complex. We cannot conclusively identity the faster migrating band observed with HeLa nuclear extracts, although based on its release from the oligonucleotide substrate upon addition of ATP, it is likely to represent a mismatch repair protein or protein complex. One possibility is that this band is the hMutSβ heterodimer bound to mismatched DNA.

C. In Vitro Mismatch Repair Protein Interactions

1. hMSH6, hMSH2, hMLH1, and either hPMS2 or hPMS1 form a mismatch repair protein complex that interacts specifically with heteroduplex DNA

Immunoprecipitation experiments followed by Western blotting were performed to determine the exact proteins bound to the mismatched oligonucleotides and to determine the nature of the interactions between the mismatch repair proteins and the DNA. HeLa nuclear extracts, which are mismatch repair proficient (176), were incubated

with a mixture of 5' [^{32}P] -labeled DNA substrate (either homoduplex or heteroduplex) mixed with unlabeled homoduplex competitor to control for non-mismatch-specific interactions and poly(dI-dC)-poly(dI-dC) (not a mismatch) to control for non-specific DNA binding interactions. Use of whole nuclear extracts instead of purified proteins enabled the search for novel protein interactions. The sequence of the oligonucleotide substrate used was based on that of H-*ras* with a G:T mismatch located at the middle nucleotide of codon 10. Mutations at this location have not been found in any human tumors (204, 205) and in the previous experiments a high rate of correct repair of G:T mismatches at codon 10 was demonstrated in mammalian cells (236), lending further support to the mismatch repair proficiency of this system.

Nuclear extracts were incubated with the DNA, the bound proteins were UV cross-linked to the oligonucleotides (see below) and immunoprecipitation was performed. The samples were then run on a denaturing polyacrylamide gel, transferred to a nitrocellulose membrane and Western blotting was performed on the resulting membrane. In Figure 10, antibody against hMSH6 was used for immunoprecipitation and the resulting membrane was sequentially probed for hMSH6, hMSH2, hMLH1, hPMS2, and hPMS1, with stripping of bound antibody between each probe. The bands seen in Figure 10B result from chemiluminescent detection of bound antibody. As shown in the hMSH6 Western blot, antibody against hMSH6 is able to immunoprecipitate itself, demonstrating the efficiency of the immunoprecipitation and Western blotting protocols. Antibody against hMSH6 is also capable of co-immunoprecipitating hMSH2, hMLH1, hPMS2 and hPMS1, indicating the existence of a mismatch repair complex or complexes consisting

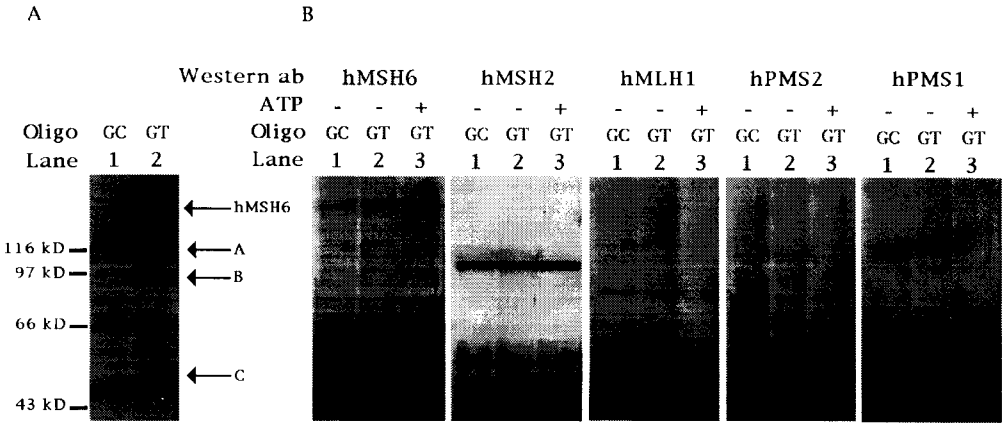

Figure 10 – hMSH6 Immunoprecipitation and Subsequent Autoradiogram and Western Blots. (A) HeLa nuclear extracts were incubated with 5' [^{32}P] -labeled homoduplex DNA (GC, Lane1) or heteroduplex DNA (GT, Lane 2) in the absence of ATP. Bound proteins were UV cross-linked to the DNA, and immunoprecipitated with antibody against hMSH6. An autoradiogram of the SDS-polyacrylamide gel is shown. Bands represent proteins bound to 5' [^{32}P] -labeled oligonucleotides. Arrows indicate mismatch specific binding activities (hMSH6, and proteins that run to the approximate positions of 115 kDa (A), 95 kDa (B) and 50 kDa (C)). (B) HeLa nuclear extracts were incubated with DNA as above in either the absence (Lanes 1 and 2) or presence (Lanes 3) of 0.1 mM ATP. After hMSH6 immunoprecipitation and SDS-poylacrylamide electrophoresis, parallel lanes from the same gel as in (A) were transferred to a nitrocellulose membrane. Western blotting was performed with the indicated antibody probes (Western ab) with stripping of bound antibody between probes. Bands result from chemiluminescent detection of bound antibody. The large dark band at the bottom of all blots results from detection of immunoglobulins used in immunoprecipitation.

of at least these proteins. These protein-protein interactions occur in the absence of additional ATP and occur to an approximately equal extent in the presence of either homoduplex or heteroduplex DNA.

In these same experiments, autoradiography was performed on parallel lanes of the same gel to determine which of the proteins identified above were also capable of becoming UV cross-linked to the 5' [^{32}P] -labeled DNA (and not the unlabelled homoduplex competitor) and thus physically interacts with the DNA. As seen in Figure 10A four bands are observed where proteins bind specifically to 5' [^{32}P] -labeled heteroduplex DNA (Lane 2) and not to the similar 5' [^{32}P] -labeled homoduplex DNA (Lane 1). By comparing the bands seen in Figure 10A to those identified in the Western blots in Figure 10B it can be seen that the highest molecular weight band runs to approximately the same position on the gel as hMSH6. This band has been identified as hMSH6 bound to the mismatched DNA as (1) the size of this band correlates with the predicted molecular weight of 160 kDa for hMSH6, (2) binding to the mismatched DNA is disrupted upon addition of ATP (see Figure 16) and (3) a number of previous studies have indicated the mismatch-specific DNA binding activity of hMSH6 when in the hMutSα complex (117, 120). Therefore, the predominant mismatch-specific DNA binding activity observed within nuclear extracts in these studies is hMSH6. This binding to the DNA occurs only with the mismatched oligonucleotide and is not seen when the 5' [^{32}P] -labeled homoduplex substrate is used. We also observe mismatch-specific DNA binding proteins that run to the approximate positions of 115 kDa (A), 95 kDa (B) and 50 kDa (C) (indicated with arrows). To be observed in Figure 10A, these

proteins must be UV cross-linked to the mismatched oligonucleotide (approximately 10 kDa). Therefore these bands represent proteins of approximately 102 kDa (A) 83 kDa (B) and 37 kDa (C). It is possible that the A, B and/or C proteins are components of the complexes involving hMSH2, hMSH6, hMLH1 and hPMS2/hPMS1. Alternatively, as HeLa nuclear extracts are mismatch repair proficient, these bands may represent proteins that become bound to mismatched DNA in subsequent steps in the repair process.

To confirm that the mismatch repair proteins exist as a complex within HeLa nuclear extracts, the above experiments were repeated using antibody against hMLH1 for the immunoprecipitation (Figure 11). Western blotting was then performed with the membrane probed with antibodies against hMSH6, hMSH2, hMLH1, hPMS2, and hPMS1. Again, the bands seen in the Western blots in Figure 11 result from chemiluminescent detection of bound antibody. As seen in Lanes 1 and 2 of Figure 11, these experiments demonstrate an interaction between hMLH1 and hMSH6, hMSH2, hPMS2, and hPMS1 in the absence of added ATP, confirming the results in Figure 10B. In the absence of ATP, antibody against hMLH1 was able to co-immunoprecipitate each of the other proteins in the presence of both homoduplex and heteroduplex DNA. Similar co-immunoprecipitation of all the mismatch repair proteins in the absence of additional ATP was observed when antibody against hMSH2 was used (Figure 12, Lanes 1 and 3). Interestingly, when antibody against hPMS2 is used for immunoprecipitation hPMS1 does not co-immunoprecipitate (Figure 13). As well, antibody against hPMS1 does not co-immunoprecipitate hPMS2. As co-precipitation of both hPMS2 and hPMS1 is observed when antibodies against hMSH6 (Figure 10), hMLH1 (Figure 11) or hMSH2

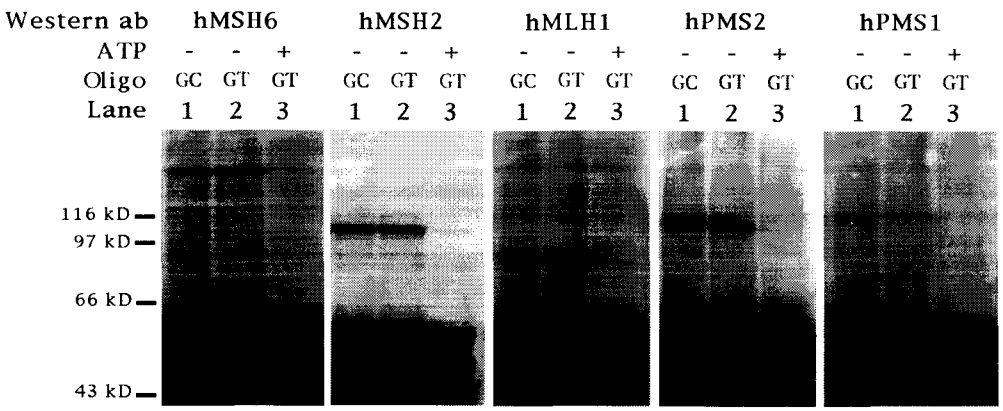

Figure 11 - hMLH1 Immunoprecipitation and Subsequent Western Blotting. HeLa nuclear extracts were incubated with homoduplex (GC, Lane 1) or heteroduplex (GT, Lanes 2 and 3) DNA in the absence or presence of 0.1 M ATP as indicated. Bound proteins were UV cross-linked to the DNA and immunoprecipitation was performed with antibody against hMLH1. Following SDS-polyacrylamide electrophoresis and transfer to nitrocellulose, Western blotting was performed with the indicated antibody probes (Western ab), with stripping of bound antibody between probes. Chemiluminescence was used for detection with sequential stripping of the membrane between probes. Bands result from chemiluminescent detection of bound antibody and do not represent protein bound to 5' [^{32}P] -labeled oligonucleotide.

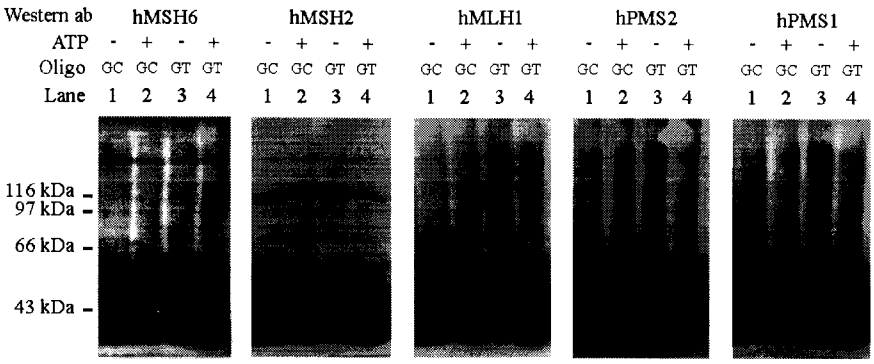

Figure 12 – hMSH2 Immunoprecipitation and Subsequent Western Blotting. HeLa nuclear extracts were incubated with homoduplex (GC, Lanes 1 and 2) or heteroduplex (GT, Lanes 3 and 4) DNA in the absence or presence of 0.1 M ATP as indicated. Bound proteins were UV cross-linked to the DNA and immunoprecipitation was performed with antibody against hMSH2. Following SDS-polyacrylamide electrophoresis and transfer to nitrocellulose, Western blotting was performed with the indicated antibody probes, with stripping of bound antibody between probes (Western ab). Chemiluminescence was used for detection with sequential stripping of the membrane between probes. Bands result from chemiluminescent detection of bound antibody and do not represent protein bound to 5' [^{32}P] -labeled oligonucleotide.

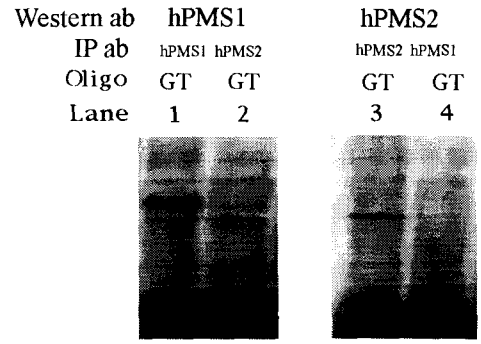

Figure 13 - hPMS1 and hPMS2 Do Not Co-immunoprecipitate Each Other. HeLa nuclear extracts were incubated with heteroduplex DNA in the absence of ATP and immunoprecipitation was performed using antibody against hPMS1 (IP antibody in Lanes 1 and 4) or hPMS2 (IP antibody in Lanes 2 and 3). After SDS-polyacrylamide electrophoresis and transfer to nitrocellulose, Western blotting was performed with the indicated antibody probes (Western ab). Chemiluminescence was used for detection with sequential stripping of the membrane between probes.

(Figure 12) are used for the initial immunoprecipitation, it can be concluded that *either* hPMS2 or hPMS1 exists in the mismatch repair complex but not both together. Therefore two mismatch repair protein complexes exist; one consisting of hMSH6, hMSH2, hMLH1 and hPMS2 and the other consisting of hMSH6, hMSH2, hMLH1 and hPMS1.

The ability of the mismatch repair proteins to interact in solution in the absence of the 32-mer oligonucleotides was also examined. In Figure 14, the nuclear extracts were incubated in the binding buffer without the addition of the 5' [^{32}P] -labeled oligonucleotides. Immunoprecipitation was performed with antibodies against both hMSH2 and hMLH1 and the membrane from the resulting denaturing polyacrylamide gel was probed with antibodies against the various mismatch repair proteins. As can be observed, antibodies against hMSH2 and hMLH1 are capable of co-immunoprecipitating hMSH6, hPMS2 and hPMS1, demonstrating that the mismatch repair proteins exist as a complex in the absence of the 32-mer DNA substrates. However, as it was necessary to include poly (dI-dC)-poly (dI-dC) to bind non-specific DNA binding proteins so that the mismatch-specific bands could be observed, it cannot be conclusively stated whether the complexes are pre-formed in the absence of DNA.

To further determine the nuclear protein-DNA interactions, UV cross-linking experiments were performed. In these experiments nuclear extracts were incubated with 5' [^{32}P] -labeled heteroduplex or homoduplex oligonucleotides, the proteins were UV cross-linked to the DNA, and then antibodies against five of the mismatch repair proteins were used for separate immunoprecipitations. The immunoprecipitated proteins that

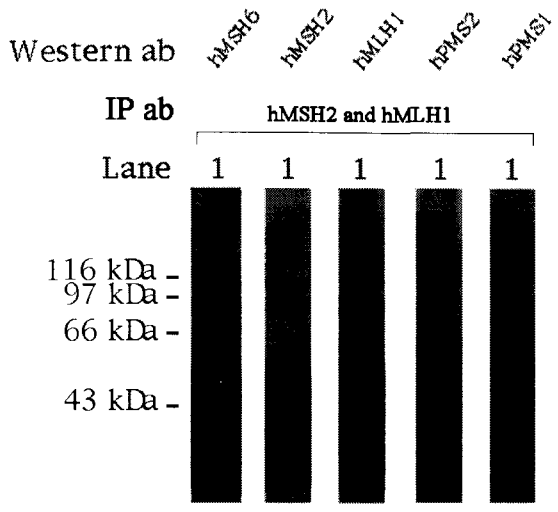

Figure 14 – hMSH2 and hMLH1 Immunoprecipitation in the Absence of 32-mer oligonucleotide DNA. HeLa nuclear extracts were incubated in the absence of 5' [^{32}P] - labeled 32-mer oligonucleotide. Proteins were UV treated and immunoprecipitation was performed with antibody against hMSH2 and hMLH1, simultaneously. Following SDS-polyacrylamide electrophoresis and transfer to nitrocellulose, Western blotting was performed with the indicated antibody probes (Western ab). Chemiluminescence was used for detection with sequential stripping of the membrane between probes.

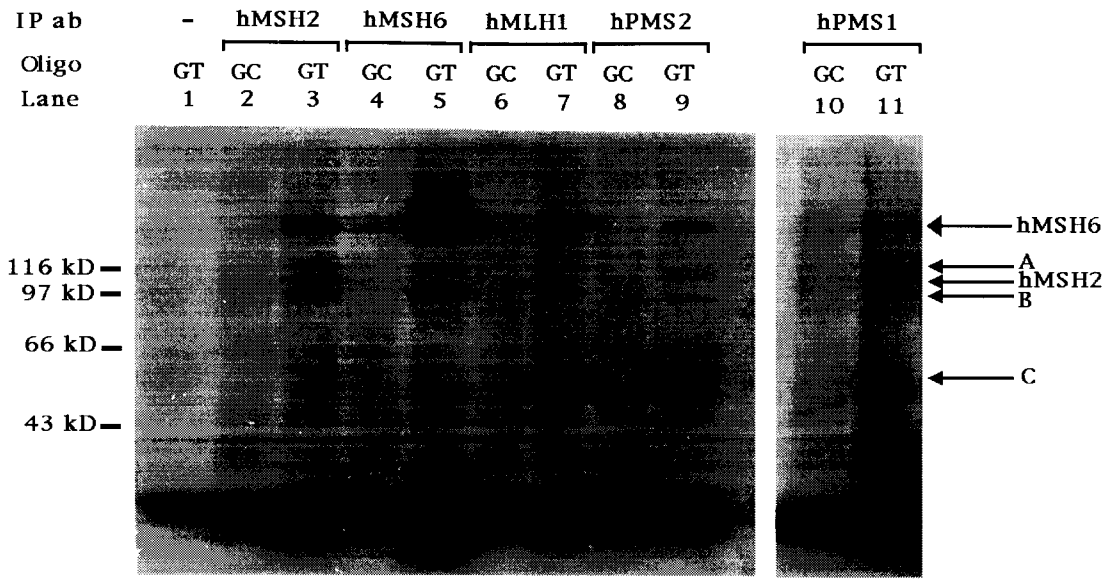

Figure 15 - UV Cross-linking and Immunoprecipitation of Protein-DNA Complexes. The 5' [^{32}P] -labeled 32mer oligonucleotide duplex containing GC (homoduplex) or GT (heteroduplex) was incubated with HeLa nuclear extracts and bound proteins were UV cross-linked to the DNA. Immunoprecipitation was performed with the indicated antibodies (IP antibody) and the immunoprecipitates were electrophoresed on an SDS-polyacrylamide gel. The figure is an autoradiogram of the resulting gels. Arrows indicate the five observed bands (hMSH6, hMSH2 and proteins that run to the approximate position of 115 kDa (A), 95 kDa (B) and 50 kDa (C) bound to 5' [^{32}P]-labeled oligonucleotides.

became UV cross-linked to the 5' [^{32}P] -labeled oligonucleotides were observed by autoradiograph of the resulting denaturing polyacrylamide gel (Figure 15). When antibodies against hMSH2, hMSH6, hMLH1, hPMS2 or hPMS1 were used for immunoprecipitation the same four proteins (hMSH6, A, B, and C) became bound to the mismatched DNA and not to the homoduplex DNA. This is consistent with the binding pattern observed in Figure 10A. The predominant mismatch-specific DNA binding activity is that of hMSH6 as identified in Figure 10, regardless of the antibody used for immunoprecipitation. The degree of binding by hMSH6 is greater when antibody against hMSH6 is used in a direct immunoprecipitation than when hMSH6 is co-immunoprecipitated using antibodies against hMSH2, hMLH1, hPMS2 or hPMS1. This is the expected result as during the co-immunoprecipitations the protein-protein interactions can potentially be easily disrupted, and thus further confirms that this band represents hMSH6. Alternatively, it is possible that the intensity of the hMSH6 band from the hMSH6 immunoprecipitation results from there being hMSH6 homomultimers bound to the oligonucleotides in addition to the larger mismatch repair complexes. However, this is unlikely as studies using purified hMSH6 have shown it to be incapable of binding to DNA when not interacting with hMSH2 in the hMutSα heterodimer (117). The amount of hMSH6 UV cross-linked to the heteroduplex when antibody against hMSH2 is used for immunoprecipitation is greater than that seen when antibody against hPMS2, hPMS1 or hMLH1 is used for immunoprecipitation. This could be because the hMutSα complex alone binds to the mismatched DNA, in addition to binding of the

larger mismatch repair complexes or could reflect the strength of the protein-protein interaction between hMSH2 and hMSH6.

When antibody against hMSH2 is used to immunoprecipitate, in addition to the four bands discussed above a unique band is observed of approximately 110 kDa that runs to approximately the same position as hMSH2 as indicated on the Western Blots in Figure 10, Figure 11 and Figure 12. Other investigators have demonstrated purified hMSH2 to be capable of specifically binding to mismatched DNA when not part of the hMutSα heterodimer (112, 113) and as well the hMutSβ heterodimer (hMSH2 and hMSH3) can bind to mismatched DNA, although this interaction is believed to occur via hMSH3, not hMSH2 (109). As bound hMSH2 cannot be co-immunoprecipitated with antibodies against any of the other mismatch repair proteins it appears that hMSH2 does specifically bind to mismatched DNA, but only when not associated with hMSH6.

2. Protein interactions after addition of ATP

The effects of ATP on the mismatch repair protein interactions were also examined. Nuclear extracts were incubated with 5' [^{32}P] -labeled heteroduplex or homoduplex oligonucleotides and the proteins were UV cross-linked to the DNA as above, except that 0.1 mM ATP was added after incubation of the nuclear extract with the 5' [^{32}P] -labeled DNA, but prior to UV cross-linking. The samples were then run on a denaturing polyacrylamide gel and examined by autoradiography to detect bound proteins. In Figure 16, antibodies against hMSH6 and hMLH1 were used to

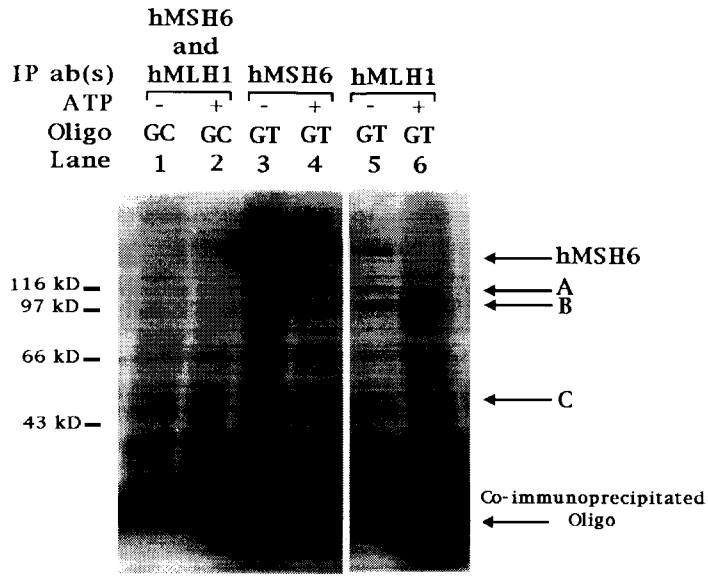

Figure 16 - UV Cross-linking and Immunoprecipitation in the Absence or Presence of ATP. The 5' [^{32}P] -labeled oligonucleotides containing GC (homoduplex) or GT (heteroduplex) were incubated with HeLa nuclear extracts. 0.1 mM ATP was added to samples in Lanes 2, 4 and 6, and bound proteins were UV cross-linked to the DNA. Immunoprecipitation was then performed using antibodies against the indicated proteins (IP antibody). After SDS-polyacrylamide electrophoresis, the resulting gel was dried and exposed to film. Arrows indicate hMSH6 and proteins that run to approximately 115 kDa (A), 95 kDa (B) and 50 kDa (C) bound to 5' [^{32}P]-labeled oligonucleotides and unbound oligonucleotides at the bottom of the gel that have co-immunoprecipitated.

immunoprecipitate proteins UV cross-linked to 5' [^{32}P] -labeled oligonucleotides with and without addition of ATP. When ATP is not added, the same mismatch-specific bands are seen as in Figure 10A and Figure 14 (hMSH6, A, B, and C). The amount of hMSH6 that is bound to the mismatched substrate decreases upon addition of ATP, regardless of the mismatch repair antibody used for immunoprecipitation. This correlates with previous studies that have shown hMutSα to disassociate from oligonucleotide substrates upon binding of ATP to the protein complex (108, 120 - 122). As well, when antibody against hMSH6 is used for immunoprecipitation after the addition of ATP, the amount of binding to the mismatched DNA by the A, B and C proteins also decreases. Binding by hMSH6 does not completely disappear when antibody against hMSH6 is used for immunoprecipitation in these experiments using 0.1 mM ATP. ATP concentrations of 10 mM do, however, completely obliterate hMSH6 binding (results not shown).

Interestingly, a novel interaction between hMLH1 and the heteroduplex DNA is detected when ATP is added to the nuclear extract-DNA incubation. As seen by comparing Figure 16, Lanes 5 and 6, when ATP is added to an hMLH1 immunoprecipitation, the amount of unbound mismatched oligonucleotide that co-precipitates *increases*, as evidenced by the increased amount of oligonucleotide detected at the bottom of the gel. This occurs specifically with the heteroduplex and not the homoduplex oligonucleotide (Lanes 1 and 2). This phenomena does not occur when antibody against any of the other mismatch repair proteins are used (Lanes 3 and 4 and results not shown). hMLH1 itself does not become directly UV cross-linked to the DNA as a band at the expected 80 kDa site is not observed. However, the amount of labeled

DNA bound to the B and C proteins does increase. hMLH1, therefore, participates in an interaction with the heteroduplex DNA after addition of ATP. This interaction appears to include the B and C proteins but does not appear to involve a direct interaction between hMLH1 and the mismatched oligonucleotide.

To compare the protein-protein interactions in the mismatch repair complex after addition of ATP, nuclear extracts were incubated with 5' [^{32}P]–labeled oligonucleotides, 0.1 M ATP was added, bound proteins were UV cross-linked to the DNA and the samples were immunoprecipitated with antibodies against the various mismatch repair proteins. These immunoprecipitates were then run on a denaturing polyacrylamide gel, transferred to a nitrocellulose membrane and blotted with antibodies against the mismatch repair proteins. As seen in each Lane 3 of Figure 10B, when antibody against hMSH6 is used for immunoprecipitation in the presence of ATP, hMLH1, hPMS2 and hPMS1 no longer co-immunoprecipitate with hMSH6. The only protein-protein interaction that remains after addition of ATP is that between hMSH2 and hMSH6 (hMutSα). This is confirmed in Lanes 2 and 4 of the hMSH2 immunoprecipitation shown in Figure 12, where only hMSH6 co-immunoprecipitates after addition of ATP. In Lane 3 of Figure 11 it can be observed that all interactions between hMLH1 and the hMSH6, hMSH2, hPMS2 and hPMS1 mismatch repair proteins are disrupted after addition of ATP. In Figure 12 it can also be seen that the protein interactions observed in the presence of homoduplex DNA are also disrupted after addition of ATP (Lane 2), demonstrating that the presence of a mismatch is not necessary for the conformational changes to occur in the proteins that result in the loss of the protein-protein interactions.

The lack of protein-protein binding seen after addition of ATP in Figures 10, 11, and 12 also confirms that the observed co-immunoprecipitations are the result of specific mismatch repair protein interactions, as ATP is known to bind to and modulate these proteins (108, 120 - 122).

3. Comparison of mismatch repair protein interactions with G:A and G:T mismatches at codons 10 and 12

In the above experiments the binding of mismatch repair proteins was examined for the efficiently repaired G:T mismatch at codon 10 to determine a putative normal pattern of interaction. In the experiments presented here mismatch repair protein binding to oligonucleotide substrates was determined for G:T and G:A mismatches. As well, mismatch repair protein binding was compared at both the codon 10 and 12 location. Oligonucleotides were prepared as described, nuclear extracts were incubated with a mixture containing equal counts per minute of the 5' [^{32}P]-labeled mismatched oligonucleotide together with unlabeled homoduplex competitor, and bound nuclear proteins were UV cross-linked to the DNA substrates. The samples were then immunoprecipitated using antibody against hMSH6 or hMSH2. Immunoprecipitation with antibodies against hMLH1, hPMS2 and hPMS1 is not shown as they generate results similar to (but weaker than) that seen with hMSH6 immunoprecipitation (Figure 15). After immunoprecipitation the samples were run on a denaturing polyacrylamide gel and the gel was dried and exposed to film overnight.

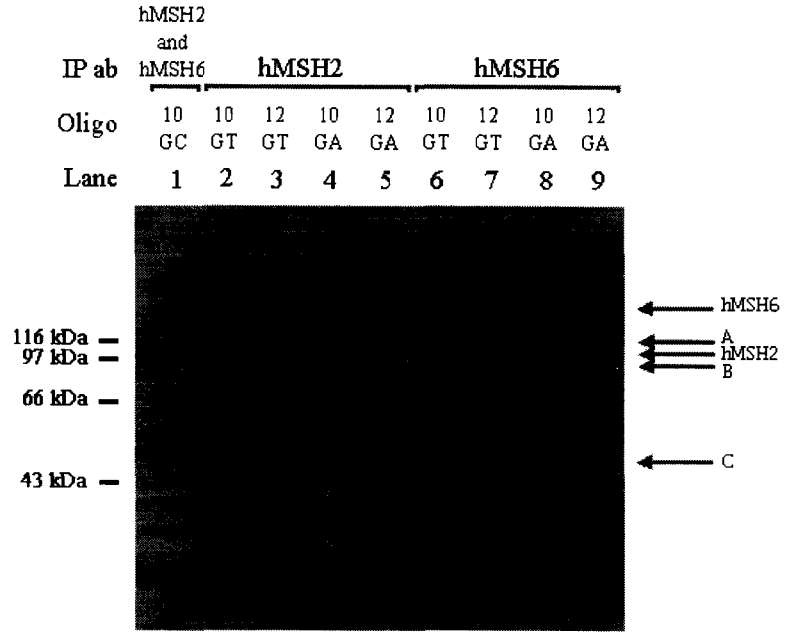

Figure 17 – DNA-Protein UV Cross-linking and Subsequent Immunoprecipitation to G:T and G:A Mismatches at Codon 10 and Codon 12. The 5' [^{32}P] -labeled oligonucleotides containing G:T or G:A mismatches at either codon 10 or codon 12 were incubated with HeLa nuclear extracts. Immunoprecipitation was then performed using antibodies against the indicated proteins (IP antibody). After SDS-polyacrylamide electrophoresis, the resulting gel was dried and exposed to film. Arrows indicate hMSH6, hMSH2 and proteins that run to approximately 115 kDa (A), 95 kDa (B) and 50 kDa (C) bound to 5' [^{32}P]-labeled oligonucleotides.

When antibody against hMSH6 was used for immunoprecipitation (see Figure 17, Lanes 6 - 9) the same four bands (hMSH6, A, B and C proteins) as seen in Figure 15 are detected for G:T mismatches at codon 10, confirming the previous results. As predicted, there is more hMSH6 bound to G:T mismatches at the codon 10 position (Lane 6) than to G:T mismatches at the codon 12 position (Lane 7). As well, the amount of hMSH6 binding seen in Lanes 6 and 7 for G:T mismatches is greater than that detected in Lanes 8 and 9 for G:A mismatches. This is in agreement with the gel-shift experiments and with reports on the binding affinities of purified hMutSα by other investigators (237). Uniquely, there is almost no binding by the B mismatch-specific protein when using an oligonucleotide with a G:T mismatch at the codon 12 position (Lane 7) while this band is seen clearly when using an oligonucleotide with a G:T mismatch at the codon 10 position (Lane 6). This lack of binding by the B protein at codon 12 may possibly reflect an inability to assemble a larger repair protein complex or an inability to proceed to subsequent events in the repair process.

Antibody against hMSH2 was also used for immunoprecipitation after UV cross-linking of bound protein to the oligonucleotide substrates (Lanes 2 - 5). When using oligonucleotides with a G:T mismatch at codon 10, five bands are detected (hMSH6, hMSH2, A, B, and C proteins), as in Figure 15. As seen previously, hMSH2 bound to oligonucleotide is only detected when antibody against hMSH2 is used for direct immunoprecipitation, confirming that although hMSH2 can bind to mismatched DNA, it only does so when not participating in the larger mismatch repair protein complex. When antibody against hMSH2 is used for the immunoprecipitation the amount of hMSH6 and

hMSH2 that is found UV cross-linked to the oligonucleotides with a G:T mismatch at codon 10 is greater than the amount UV cross-linked to oligonucleotides with a G:T mismatch at codon 12 (Lanes 2, 3). This again suggests a general inability of the mismatch repair proteins to bind to and/or recognize mispairs at the codon 12 location. Interestingly, hMSH6 is detected UV cross-linked to oligonucleotides with G:A mismatches at the codon 12 position (Lane 5), but not when the mismatch is located at the codon 10 position (Lane 4). This unusual result was consistently detected when these experiments were repeated. It therefore appears that mismatch repair proteins are able to bind to G:A mismatches at the codon 12 position that are not able to bind to G:A mismatches at the codon 10 position. This result is especially intriguing as hMSH6 UV cross-linked to the oligonucleotide was not detected when antibody against hMSH6 was used for a direct immunoprecipitation with the same mismatched oligonucleotide (Codon 12, G:A) in Lane 9. One possible explanation for these results is that the hMutSα heterodimer binds to oligonucleotides with a G:A mismatch at codon 12 in an unsual configuration. As the anti-hMSH6 antibody used was monoclonal it is possible that this antibody cannot immunoprecipitate hMSH6 if the protein is in a different three-dimensional conformation. This would explain the inability of monoclonal antibody against hMSH6 to directly detect the hMSH6-DNA interaction in Lane 9, as compared to the ability of the polyclonal antibodies against hMSH2 to co-immunoprecipitate bound hMSH6 in Lane 5.

IV. Discussion

Although the existence of hotspots of mutation at oncogenic locations has been well documented, the mechanisms contributing to the increased mutation frequency at these hotspots within human tumors are still in question. The experiments presented here have examined whether inefficiencies and/or inaccuracies in repair of mismatched DNA can contribute to the increased rate of mutation at a hotspot. The relative efficiency of mismatch repair at a non-hotspot of mutation (H-*ras* codon 10) was compared to previously determined repair rates at a nearby oncogenic hotspot of mutation (H-*ras* codon 12). These results demonstrate that for the biologically relevant codon 12 location of H-*ras* there is inefficient repair of specific mismatched base pairs. Furthermore, these experiments demonstrate that the repair rates for mismatched nucleotides vary depending on the precise location and exact composition of the mismatch.

The results for *in vivo* mismatch repair at the middle nucleotide position of codon 10 indicate that G:A, A:C and T:C mismatches at this location are repaired more efficiently than when located at the codon 12 middle nucleotide hotspot of mutation (see Table 3 and Figure 6 for comparison). As the only difference when comparing repair rates for each specific mismatch at these two locations is the sequence context surrounding the codon containing the mismatch, these results indicate for the first time that sequence context can effect a cell's ability to repair mispaired DNA. These results are analagous to studies in which differential nucleotide excision repair at hotspots of mutation has been observed (214, 215, 226). Indeed, in studies examining repair of O^6-

methylguanine adducts opposite thymine a consensus sequence for lack of repair was derived that has significant similarity to the sequence surrounding codon 12 of H-*ras* (226). It is also intriguing that previous primer extension studies have demonstrated that both DNA polymerase β and α to have a strong pause site at the wild-type codon 12 location (210), suggesting stearic hindrance, a difficulty in the gap filling stage of different DNA repair processes, or a general difficulty in enzymatic reactions at this site.

In agreement with previous studies differences in the repair rates were observed when the various mismatches (G:T, T:C, A:C, G:A) were located at the same codon 10 position. This indicates that different mismatches are repaired at different efficiencies, even when at the same location (175, 178, 233 - 235). As seen in Table 3, only 69% of G:A mismatches were correctly repaired at codon 10 in NIH 3T3 cells, while A:C, T:C and G:T were all repaired at a high rate (94%-96%) at this location. Previously, G:A mismatches were found to be repaired at the even lower rate of 35% at codon 12 in NIH 3T3 cells (227). Other investigators have also found G:A to be particularly difficult to repair in both *in vitro* and *in vivo* mismatch repair studies (178, 233 - 235). It appears that there are slower kinetics repair specifically for G:A mismatches. Lack of repair of G:A mismatches at codon 12 in H-*ras* may be biologically relevant, as the resulting T:A transversion is a common activating mutation found at this location in naturally occurring human tumors (203 - 205).

Furthermore, in each case when repair to the wild-type sequence (G:C) did not occur, a mixture of cells within each colony containing G:C and A:T or T:A mutated sequences were observed. Such mixtures most probably result from replication prior to

repair of the single mismatch-containing plasmid in the originally transfected cells. Therefore, in this experimental system there is a decreased efficiency in the kinetics of repair for specific mismatches at specific locations, rather than inaccurate repair leading to mutation.

Gel-shift analysis using nuclear extracts was then performed to determine if binding by specific DNA mismatch repair proteins could be impaired for particular mismatches at codon 10 or codon 12. As seen when comparing Figure 6 and Figure 7C, the relative amount of mismatch-specific binding to each mismatch at codon 12 using NIH 3T3 nuclear extracts correlates with specific mismatch repair abilities. The observed binding in NIH 3T3 nuclear extracts and the slower migrating band in HeLa nuclear extracts is believed to be due to the long-patch mismatch repair hMutSα complex as: (1) this has been shown to be the major mismatch binding activity in HeLa nuclear extracts (80) (2) pre-incubation of nuclear extract with antibody to hMSH6 destroyed this binding (117) and (3) addition of ATP, which has been shown to disrupt binding of the hMutSα complex (108, 120 - 122), resulted in a complete lack of binding by the mismatch-specific factors. Although other mismatch-specific binding factors (DNA topoisomerase I, deoxyinosine 3' endonuclease and human exonuclease I) have been reported (238, 239, 168) these do not bind to DNA with the same sequence specificity and do not exhibit the same sensitivity to ATP.

It is interesting to note that in the gel-shift experiments with HeLa nuclear extracts two mismatch-specific bands were observed (Figure 7A). Although only the slower migrating band was disrupted by pre-incubation with antibody against hMSH6,

both binding activities were disrupted by addition of ATP (Figure 8). A recent paper has demonstrated that hMutSβ releases from DNA upon addition of ATP (135). Binding by purified hMSH2 homodimers is also modulated by ATP (112, 113). As well, both the hMutSβ heterodimer (229 kDa) and an hMSH2 homodimer (204 kDa) would be expected to migrate faster than hMutSα (262 kDa), although migration rates on non-denaturing polyacrylamide gels do not always correlate with molecular weight. It is therefore possible that the faster migrating band in the HeLa gel-shift experiments is the hMutSβ heterodimer or an hMSH2 homodimer bound to the mismatched oligonucleotides. This band was not observed in the gel-shift experiments using NIH 3T3 nuclear extracts. However, somewhat different nuclear extract buffers and binding buffers were used in the experiments involving NIH 3T3 nuclear extracts as compared to the experiments involving HeLa nuclear extracts. Therefore the lack of binding by the second mismatch-specific band in NIH 3T3 nuclear extracts could reflect a difference between murine and human proteins in the different conditions. Alternatively, if the faster migrating band seen when using HeLa nuclear extracts represents hMutSβ bound to the mismatched oligonucleotide, than it could be missing in the experiments with NIH 3T3 nuclear extracts if these cells are lacking a MSH3 activity.

In HeLa nuclear extracts binding by hMutSα (slower migrating band) was observed with oligonucleotides that contain G:A at the codon 10 position but not with oligonucleotides with G:A at the codon 12 position. This demonstrates that the sequence context surrounding a mismatch can effect hMutSα binding. Local sequence context effects on hMutSα binding have also been recently demonstrated for mismatches and one

and two base pair loop structures (237, 240). The observed lack of binding to oligonucleotides containing G:A mismatches at codon 12 correlates with the very low efficiency of repair observed *in vivo* for G:A mismatches at codon 12. Other investigators have demonstrated that hMutSα recognizes and binds to mismatched DNA when in an ADP-bound form and that subsequent ATP binding results in dissociation from or translocation off the mismatched oligonucleotide substrate (121, 125, 126). This had led to the suggestion that repair is modulated by ATP binding rather than mismatch recognition. However, our studies would suggest that at sensitive locations such as the H-*ras* codon 12 hotspot of mutation, there may be deficiencies in recognition of specific mismatches that result in low levels of repair. Recently, deficiencies in hMutSα binding were demonstrated in a number of human lung cancer cell lines that expressed both hMSH2 and hMSH6, indicating that a lack of hMutSα binding may indeed be relevant in tumors (241).

The lower rates of repair for a variety of different mismatches (T:C, A:C, G:A) at codon 12 in NIH 3T3 cells combined with the differential binding by hMutSα implicates an inefficiency in general in the long-patch mismatch repair system at this hotspot, rather than inaccurate repair. There appears to be slower kinetics of recognition and/or repair at codon 12 as compared to codon 10, rather than a completely nonfunctioning long-patch mismatch repair system at this location. Variable kinetics of repair that result in altered *in vivo* repair rates due to plasmid replication before repair have been previously observed in studies using DNA adducts (242). Taken together, the above results suggest

that codon 12 is a hotspot of mutation, at least in part, due to a rate limiting step in recognition and/or binding to mismatches.

In the next phase of these studies UV-crosslinking, immunoprecipitation, and Western blotting were perfomed using HeLa nuclear extracts to identify the proteins bound to the mismatched oligonucleotide substrates and to determine the mismatch repair protein-protein interactions. In these studies protein interactions were observed between the human MutS homologs hMSH2 and hMSH6 and the human MutL homologs hMLH1, hPMS1 and hPMS2. These interactions occur in the absence of ATP, thus ATP binding or hydrolysis is not a pre-requisite for complex formation in HeLa nuclear extracts in these experiments. Although we observe both hPMS2 and hPMS1 in the complex, they do not co-immunoprecipitate each other. Therefore the mismatch repair complex involves either hPMS2 or hPMS1, but not both together (see Figure 18). This is in agreement with a recent publication that describes the hMutLβ complex of hMLH1 and hPMS1 as distinct from the hMutLα complex of hMLH1 and hPMS2 (159). This is also the first report of hPMS1 interaction with the MutS homologs. These results indicate that *either* hMutLα or hMutLβ is capable of interacting with hMutSα and binding to mismatched DNA. If these complexes are at least partially functionally redundant, this would explain the rarity of HNPCC kindreds with mutations in hPMS2 or hPMS1 (11). It has been suggested that the hMutLα heterodimer functions with the hMutSα heterodimer in repair of mismatches and conversely the hMutLβ heterodimer functions with the hMutSβ heterodimer in repair of small insertion-deletion loops. However, in these experiments both the hPMS1 protein (hMutLβ) and the hPMS2 protein (hMutLα)

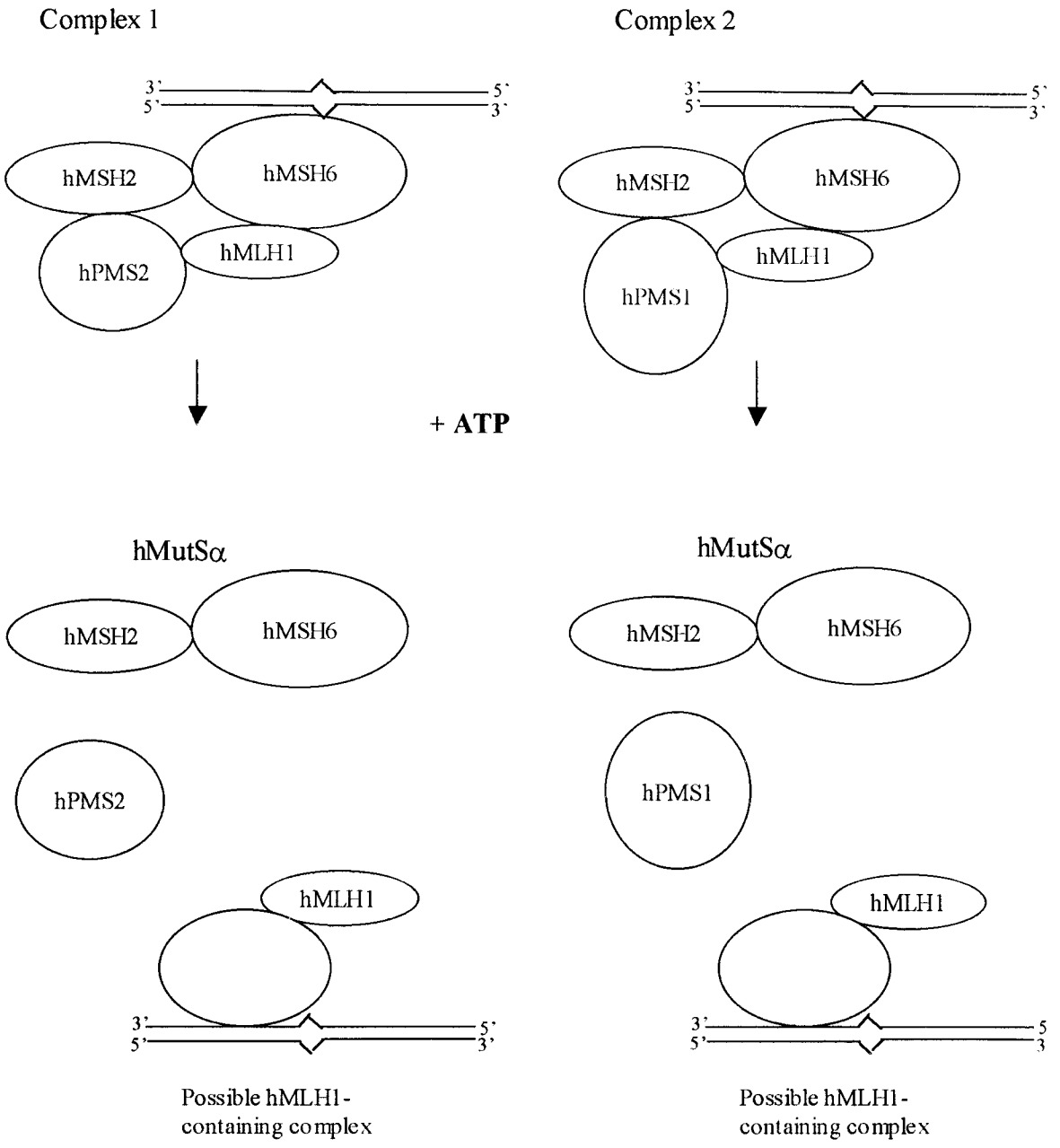

Figure 18 – Proposed Mismatch Repair Protein Interactions.

co-immunoprecipitate with hMSH2 and hMSH6 (hMutSα). Although it is possible that hMutLβ may be able to interact with hMutSα in a manner that is not functionally relevant, it is also possible that the different complexes both interact with hMutSα and have distinct, as yet unknown functions in the repair process. In support of this, the phenotypes of HNPCC patients that carry mutations in hPMS2 or hPMS1 are similar, suggesting that the proteins have distinct roles in the mismatch repair process (8). Possibilities for such functions include translocation, strand discrimination and assembly with endonucleases or other proteins involved in repair of mismatches.

The protein-protein interactions in nuclear extracts occur in the presence of homoduplex and heteroduplex DNA as well as in the absence of the 32-mer oligonucleotides (Figures 10 – 14). However, the protein complex binds specifically only to heteroduplex substrates as detected by UV cross-linking (Figure 10 and Figure 15-17). As previously reported (120), hMSH6 appears to be the predominant DNA binding protein in this complex although binding by the A, B and C proteins was also observed. Interestingly, the position of the A mismatch binding protein is similar to that of hPMS2 and hPMS1 as identified by Western blotting. Further studies are necessary to determine if either hPMS2 or hPMS1 has an as yet unidentified DNA binding activity which allows it to become UV cross-linked to the heteroduplex DNA when in the mismatch repair protein complex or perhaps to function in subsequent steps in the repair process. However, we do not see a stronger A band when either hPMS2 or hPMS1 is used for

direct precipitation (Figure 15, Lanes 9 and 11) as compared to the co-immunoprecipitations (Figure 15, Lanes 3, 5 and 7). If the A band represents either hPMS2 or hPMS1, a stronger band would be expected when using antibody directed specifically against the protein, compared to a co-immunoprecipitation (during a co-immunoprecipitation the non-covalent protein-protein interactions can easily be disrupted). This suggests that the 115 kDa band represents a distinct protein. Other investigators have also identified an unknown protein of approximately 115 kDa cross-linked to heteroduplex DNA (4). The position of the B band may correlate with human exonuclease 1 (94 kDa) (168). This 5' –> 3' exonuclease has previously been shown to physically interact with hMSH2 in human nuclear extracts (168), and genetic studies in yeast have shown the yeast homolog to function in the same epistatic pathway as hMSH2 (169, 170). As well, the B band may represent DNA topoisomerases I, a frequently observed mismatch-specific binding protein of 90 kDa, although this protein has not yet been reported to function in mismatch repair (238). The size of the C band correlates with the reported sizes of RPC II, III, IV and V subunits (37 kDa, 36 kDa, 40 kDa and 38 kDa, respectively) (173). It is also very probable that there will be more proteins identified in the mismatch repair process in humans. For instance, a DNA helicase and a 3' –> 5' exonuclease have yet to be reported as involved in human mismatch repair, yet based on the *E. coli* model it is expected that such proteins will be necessary in human mismatch repair (81). The identification of these three unknown mismatch binding proteins is therefore of great interest in clarifying the proteins involved in mismatch recognition and repair.

hMSH2 is also observed to become UV cross-linked to the heteroduplex DNA, but only when antibody against hMSH2 is used for direct immunoprecipitation (Figure 15). As this mismatch-specific DNA binding activity of hMSH2 does not co-immunoprecipitate with hMSH6, hMLH1, hPMS2, or hPMS1 it can be concluded that hMSH2 is able to bind to mismatched DNA, but only when not participating in the larger mismatch repair protein complexes identified here. One possibility could be that the hMSH2-DNA interaction occurs when hMSH2 is bound to hMSH3 in the hMutSβ heterodimer. Alternatively, as studies with purified hMSH2 have shown it to bind to mismatched oligonucleotides as a homomultimer (112, 113), the observed band could be due to an interaction between hMSH2 homomultimers and the mismatched substrate in nuclear extracts. It is interesting to note that in the gel-shift experiments with HeLa nuclear extracts two mismatch-specific bands were observed (Figure 7A). Immunoprecipitation using antibody against hMSH3 would answer whether the observed activity is hMutSβ or hMSH2 homodimers. Unfortunately, such antibodies are not yet available, although it is expected that they will be in the near future.

After addition of ATP to the mixtures the protein-protein interactions between hMLH1 and hPMS1 or hPMS2 are disrupted as well as the interactions between these proteins and the hMutSα heterodimer (Figures 10 – 13). The only protein-protein interaction that can be observed after addition of ATP is that between hMSH2 and hMSH6 (hMutSα). This is in conflict with yeast studies which have reported that the PMS1, MSH2 and MSH6 complex either remains intact upon addition of ATP (162) or that the protein interactions increase in the presence of ATP (163 - 164). The most

probable explanation for this apparent discrepancy is that the previous studies used purified proteins while these experiments were performed using whole nuclear extracts. In the presence of ATP, the mismatch repair proficient HeLa nuclear extracts can proceed with the repair process resulting in the eventual disruption of the protein-protein interactions. The excess of ATP then prevents re-formation of the protein complex. Although the reactions were maintained at 0°C - 4°C throughout, the reactions were first incubated for 40 minutes and then after UV cross-linking the immunoprecipitations were performed overnight, allowing some time for the mismatch repair processes to occur, even at these sub-optimal conditions. Alternatively, it has been shown in *E. coli* that a mismatch-containing DNA substrate of sufficient size is necessary for MutS and MutL to interact in the presence of ATP (89). In these experiments the relatively small size of the oligonucleotide substrate used (32-mer) could inhibit the ability of the MutS and MutL homologs to form a complex with each other and with the DNA after the addition of ATP. In Figure 16, addition of ATP also decreases the amount of hMSH6 that becomes UV cross-linked to the DNA. This is in agreement with numerous studies involving purified hMSH2 and hMSH6 that have determined that the purified hMutSα heterodimer disassociates from mismatch-containing oligonucleotides upon binding of ATP (108, 120 - 122).

Anytime the proteins interact with the 5' [^{32}P] –labeled DNA, increased amounts of free oligonucleotide will be observed at the bottom of the gel after immunoprecipitation. This is due to the less than 100 % efficiency of the UV cross-linking reactions. Oligonucleotide that interacts with the protein will be co-

immunoprecipitated, and if the DNA is not UV cross-linked to the protein it will become unbound during denaturing gel electrophoresis. Therefore, the amount of free oligonucleotide observed correlates with the protein-DNA interactions (see for example Figure 15). However, in Figure 16 a novel interaction is observed between hMLH1 and the mismatched DNA after addition of ATP. Antibody against hMLH1 is capable of co-immunoprecipitating increased amounts of the 5' [^{32}P] -labeled heteroduplex oligonucleotides (seen free at the bottom of the gel in Lane 6), as compared to the amount of co-immunoprecipitated oligonucleotide observed with 5' [^{32}P] -labeled homoduplex DNA (Lane 2). This occurs even though there is relatively little protein UV cross-linked to the 5' [^{32}P] -labeled oligonucleotide in Lane 6. Therefore, hMLH1 may participate in another mismatch repair protein complex that interacts specifically with mismatched DNA after addition of ATP. This complex does not appear to involve hMSH6, hMSH2, hPMS2 or hPMS1 as antibodies against these proteins do not co-immunoprecipitate increased amounts of the to 5' [^{32}P] -labeled DNA after addition of ATP. hMLH1 does not interact directly with the DNA as it does not become UV cross-linked to the oligonucleotide and 5' [^{32}P] –labeled heteroduplex is found free at the bottom of the gel after denaturing gel electrophoresis. Therefore, hMLH1 appears to participate in a novel protein complex in which other proteins directly interact with the mismatched oligonucleotide (see Figure 18). Other investigators have failed to observe direct interactions between mismatch-containing DNA and the purified hMutLα heterodimer (158). This is understandable if the complex involves additional nuclear proteins which directly interact with the heteroduplex DNA and that have not as yet been identified.

Mismatch-specific binding by the B and C proteins does continue to be observed, making these proteins candidates for participation in this novel complex.

This finding suggests that hMLH1 plays a role in steps in the repair process subsequent to mismatch recognition. Although little is known in regard to the exact biochemical role of hMLH1 in humans, a number of studies in *E. coli* have shed some light on the subject. One suggested role for MutL is to facilitate the interactions between MutS and proteins necessary for subsequent steps in the repair process such as MutH and DNA helicase II (83, 92, 96 - 98). hMLH1's ability to participate in the initial complexes involving hMutSα as well as in the novel complex after addition of ATP suggests that it may have an analogous role in human mismatch repair. As well, recent studies have suggested that MutL acts as a molecular chaperone. This hypothesis arises from MutL's observed homology to the molecular chaperone molecule Hsp90 (102) and recent X-ray crystallography studies which have shown it to bind ATP and have a weak ATPase activity (103, 104). In the crystallography studies the MutL protein was observed to undergo conformational changes upon ATP hydrolysis which are likely to modulate the interactions between MutL and the other components of the repair machinery. With hMLH1, conformational changes upon ATP hydrolysis could result in the different protein-protein and protein-DNA interactions observed in these studies after addition of ATP to the reaction.

Genetic analysis of HNPCC kindreds has demonstrated the importance of the hMLH1 gene product in mismatch repair with approximately 61% of HNPCC kindreds reported as of May 1999 carrying mutations in the hMLH1 gene (11). The central role of

hMLH1 in both the hMutLα and hMutLβ heterodimers (with hPMS2 and hPMS1, respectively) (158, 159) and as observed in these studies in the two mismatch repair protein complexes helps to explain this genetic data. As well, the novel interaction observed in these studies between hMLH1 and heteroduplex DNA after addition of ATP suggests that hMLH1 may have a further unique role in steps in mismatch repair subsequent to mismatch recognition.

These results suggest a model for human mismatch repair whereby the hMutSα heterodimer, either alone or already in a complex with either hMutLα or hMutLβ, recognizes and binds to mispairs (see Figure 18). The formation of these protein-protein complexes occurs in nuclear extracts in the absence of additional ATP. The complex can then stably bind to mismatched DNA, again in the absence of ATP. This protein-DNA complex consists of hMSH2, hMSH6, hMLH1 and either hPMS2 or hPMS1, with possible distinct functions for each complex. In the presence of ATP, conformational changes occur resulting in the eventual release of the protein complex from the heteroduplex oligonucleotides used in these studies and hMLH1's dissociation from hMutSα and hPMS or hPMS1. hMLH1 is then capable of further interaction with the mismatched DNA in a novel manner, presumably playing a role in subsequent steps in the repair process. In this model the hMutSα heterodimer would serve to recognize mismatches and bring the MutL homologs to the site, either as a preformed complex or by recruiting the MutL homologs. After interaction with ATP, a complex involving hMLH1 assembles. hMLH1 would in this model be functioning as a molecular matchmaker between the initial recognition complex that involves hMutSα and the later

protein complex that presumably actuates repair. This is homologous to *E. coli* where it is known that MutL interaction with MutS is necessary to assemble MutH and DNA helicase II in the mismatch repair protein complex (96 - 99).

As a final experiment the mismatch repair protein-DNA interactions were examined for G:A and G:T mismatches located at either codon 10 or codon 12. As predicted from the gel-shift experiments, hMSH6 binds more efficiently to G:T mismatches at the codon 10 position than when the mismatch is located at codon 12 (Figure 17). Also, when antibody against hMSH6 is used for immunoprecipitation, more hMSH6 is found bound to G:T mismatches than to G:A mismatches. This is in agreement with reports from other investigators (237, 240). Once again, the observed degree of binding by hMSH6, and therefore hMutSα, correlates with the efficiency of repair *in vivo* at these locations.

Binding by the B mismatch-specific protein was observed for G:T mismatches at codon 10 but interestingly not for G:T mismatches at codon 12 when antibody against hMSH6 is used for immunoprecipitation (Lane 7). This is surprising as there is detectable binding by hMSH6 and the A and C proteins at the codon 12 site. Therefore, even if mismatch recognition by hMutSα has occurred at the codon 12 location as detected by hMSH6 binding, assembly of the larger mismatch repair protein complex or subsequent steps in the repair process may be in some way impaired. This would be reflected in the lowered efficiency of repair generally seen at the codon 12 location as compared to the codon 10 location. G:T mismatches, however, could still be repaired efficiently due to the separate base excision repair pathway that exists to repair this

mismatch. The identity and function of the B protein will be important in determining if this result reflects an inability to proceed with mismatch repair at H-*ras* codon 12.

hMSH2 binding was also examined by directly immunoprecipitating with antibody against this mismatch repair protein. As seen previously, hMSH2 can become UV cross-linked to the DNA only when not participating in the hMutSα complex as hMSH2 is only seen bound to the mismatched oligonucleotides when antibodies against hMSH2 are used for direct immunoprecipitation. There is more binding by hMSH2 detected for G:T mismatches at codon 10 than at codon 12, similar to the results for hMSH6 binding. This supports the hypothesis that there is a generalized difficulty in recognition and/or binding at the codon 12 location.

Unexpectedly, an increased binding by hMSH6 is observed for G:A mismatches at codon 12 as compared to G:A mismatches at codon 10 (Lanes 4 and 5). Increased amounts of hMSH6 binding to G:A mismatches at codon 12 as compared to codon 10 is observed only when antibody against hMSH2 is used for immunoprecipitation, and not when antibody against hMSH6 is used (compare Lanes 4 and 5 with Lanes 8 and 9). This finding was reproducible when these experiments were repeated. It therefore appears that although binding by hMutSα is possible for G:A mismatches at the codon 12 site, the hMutSα configuration is aberrant in that antibody against hMSH6 cannot detect it. Although the anti-hMSH6 antibody used was polyclonal, it is possible that a conformational change could affect the antibody's ability to bind to the protein. The observed binding by hMSH6 to G:A mismatches at codon 12 could then represent an unusual conformational configuration of the hMutSα heterodimer that the anti-hMSH6

antibody cannot detect. The anti-hMSH2 antibodies are polyclonal and are able to bind to hMSH2. In this way they co-immunoprecipitate hMSH6, as seen in Lane 5. Based on the relatively low efficiency of repair for G:A mismatches at codon 12 *in vivo*, this proposed conformation of hMutSα may represent a dead-end in the repair process.

The importance of understanding mechanisms of site-specific mutation is demonstrated by the prevalence of hotspots of mutation in naturally occurring tumors. In these studies cellular mismatch repair rates for mismatches at a non-hotspot location were determined and compared to previously determined rates of repair for the same mismatches at an oncogenic hotspot of mutation. From these results it can be concluded that H-*ras* codon 12 is a hotspot of mutation, at least in part, due to deficiencies in mismatch repair. It was also shown that surrounding sequence context can effect rates of repair of mismatches. These experiments are the first to demonstrate differential rates of repair at a hotspot of mutation and differential rates of repair for mismatches depending on local sequence context. Differences in binding by hMutSα were then observed *in vitro* both by gel-shift and UV cross-linking methods. These differences in binding generally correlate with mismatch repair efficiency *in vivo*. Importantly, these experiments were performed using two mismatch proficient cell lines, and thus the lack of mismatch repair and mismatch repair protein binding observed may have ramifications for initiation of tumorigenisis in individuals who are not hereditarily predisposed to cancer.

The general mechanisms of long-patch mismatch repair are currently of great interest as it has been shown that these genes are often mutated in spontaneous tumors

and that individuals mutant in the mismatch repair genes are hereditarily predisposed to cancer. The mismatch repair protein-protein and protein-DNA interactions were examined in these studies. Two novel mismatch repair protein complexes were observed, one consisting of at least hMSH2, hMSH6, hMLH1 and hPMS2 and the other consisting of at least hMSH2, hMSH6, hMLH1 and hPMS1. Identification of these protein complexes, their interactions with heteroduplex DNA, and the effect of ATP was then examined. Additionally, a novel complex that forms after addition of ATP and involves hMLH1 was detected. These results add to our rapidly expanding knowledge of the mismatch repair system and hopefully are an essential step in future understanding of the mechanisms involved in tumorigenesis in humans.

V. References

1. Friedberg, E.C., Walker, G.C. and Siede, W. (1995) *DNA repair and Mutatgenesis*. Washington D.C.: ASM Press.

2. Umar, A. and Kunkel, T.A. (1996) DNA-replication fidelity, mismatch repair and genome instability in cancer cells. *Eur. J. Biochem.* **238**, 297-307.

3. Kunkel, T.A. (1992) DNA replication fidelity. *J. Biol. Chem.* **267**, 18251-18254.

4. Jiricny, J. (1998) Replication errors: cha(lle)nging the genome. *EMBO J.* **17**, 6427-6436.

5. Loeb, L.A. (1994) Microsatellite instability: marker of a mutator phenotype in cancer. *Cancer Res.*, **54**, 5059-5063.

6. Loeb, L.A. (1991) Mutator phenotype may be required for multistage carcinogenesis. *Cancer Res.*, **54**, 5059-5063.

7. Eshleman, J.R. and Markowitz, S.D. (1995) Microsatellite instability in inherited and sporadic neoplasms. *Current Opin. Oncol.*, **7**, 83-89.

8. Marra, G. and Boland, C.R. (1995) Hereditary nonpolyposis colorectal cancer (HNPCC): the syndrome, the genes, and historical perspectives. *J. Natl. Can. Inst.*, **87**, 1114-1125.

9. Bocker, T., Ruschoff, J. and Fishel, R. (1999) Molecular diagnostics of cancer predisposition: hereditary non-polyposis colorectal carcinoma and mismatch repair defect. *Biochim. Biophys. Acta.*, **1423**, O1-O10.

10. Boyer, J.C., Umar, A., Risinger, J.I., Lipford, J.R., Kane, M., Yin, S., Barett, J.C., Kolodner, R.D. and Kunkel, T. (1995) Microsatellite instability, mismatch repair deficiency, and genetic defects in human cancer cell lines. *Cancer Res.*, **55**, 6063-6070.

11. Peltomaki, P. and Vasen, H.F. (1997) Mutations predisposing to hereditary nonpolyposis colorectal cancer: database and results of a collaborative study. The International Collaborative Group on Hereditary Nonpolyposis Colorectal Cancer. *Gastroenterology*, **113**, 1146-1158.

12. Kolodner, R.D. (1995) Mismatch repair: mechanisms and relationship to cancer susceptibility. *Trends Biol. Sci.*, **20**, 397-401.

13. Eshelman, J.R., Lang, E.Z., Bowerfind, G.K., Parsons, R., Vogelstein, B., Wilson, J.K.V., Veigl, M.L., Sedgwick. W.D. and Markowitz, S.D. (1995) Increased mutation rate at the *hprt* locus accompanies microsatellite instability in colon cancer. *Oncogene*, **10**, 33-37.

14. Liu, B., Nicolaides, N.C., Markowitz, S., Wilson, J.K.V., Parsons, R.E., Jen. J. Papadopolous, N., Peltomaki, P., de la Chapelle, A., Hamilton, S.R., Vogelstein, B. and Kinzler, K.W. (1995) Mismatch repair gene defects in sporatic colorectal cancers with microsatellite instability. *Nat. Genet.*, **9**, 48-55.

15. Parsons, R., Li, G.-M, Longley, M.J., Modrich, P., Liu, B., Berk, T., Hamilton, S.R., Kinzler, K.W. and Vogelstein, B. (1995) Mismatch repair deficiency in phenotypically normal human cells. *Science*, **268**, 738-740.

16. Sancar, A. (1996) DNA EXCISION REPAIR. *Annu. Rev. Biochem.*, **65**, 43-81.

17. Vaughan, P., Lindahl, T. and Sedgwick, B. (1993) Induction of the adaptive response of *Escherichia coli* to alkylation damage by the environmental mutagen, methyl chloride. *Mutat Res.*, **293**, 249-257.

18. Moore, M.H., Gulbis, J.M., Dodson, E.J., Demple, B. and Moody, P.C.E. (1994) Crystal structure of a suicidal DNA repair protein: the Ada O6-methylguanine-DNA methyltransferase from *E. coli*. *EMBO J.*, **13**, 1495-1501.

19. Fritz, G., Tano, K., Mitra, S. and Kaina, B. (1991) Inducibility of the DNA repair gene encoding O^6-methlyguanine-DNA methyltransferase in mammalian cells by DNA-damaging treatments. *Mol. Cell. Biol.*, **11**, 4660-4668.

20. Fornace, A.J., Nebert, D.W., Hollander, M.C., Luethy, J.D., Papathanasiou, M. Fagnoli, J. and Holbrook, N.J. (1989) Mammalian genes coordinately regulated by growth arrest signals and DNA-damaging agents. *Mol. Cell. Biol.*, **9**, 4196-4203.

21. Laval, F. (1991) Increase of O^6-methylguanine-DNA methyltransferase and N^3-methyladenine glycosylase in rat hepatoma cells treated with DNA-damaging agents. *Biochem. Biophys. Res. Commun.*, **176**, 1086-1092.

22. Krokan, H.E., Standal, R. and Slupphaug, G. (1997) DNA glycosylases in the base excision repair of DNA. *Biochem. J.*, **325**, 1-16.

23. Seeberg, E., Eide, L. and Bjoras, M. (1995) The base excision repair pathway. *TIBS*, **20**, 391-397.

24. Wiebauer, K. and Jiricny, J. (1990) Mismatch-specific thymine DNA glycosylase and DNA polymerase β mediate the correction of G-T mispairs in nuclear extracts from human cells. *Proc. Natl. Acad. Sci. USA*, **87**, 5842-5845.

25. McGoldrick, J.P., Yeh, Y.-C., Solomon, M., Essigmann, J.M. and Lu, A.-L. (1995) Characterization of a Mammalian Homolog of the *Escherichia coli* MutY Mismatch Repair Protein. *Mol. Cell. Biol.*, **15**, 989-996.

26. Parikh, S.S., Mol, D.D., Slupphaug, G., Bharati, S., Krokan, H.E. and Tainer, J.A. (1998) Base excision repair initiation revealed by crystal structures and binding kinetics of human uracil-DNA glycosylase with DNA. *EMBO J.*, **17**, 5214-5226.

27. Waters, T.R. and Swann, P.F. (1998) Kinetics of the action of thymine DNA glycosylase. *J. Biol. Chem.*, **273**, 20007-20014.

28. Waters, T.R., Gallinari, P., Jiricny, J. and Swann, P.F. (1999) Human thymine DNA glycosylase binds to apurinic sites in DNA but is displaced by apurinic endonuclease 1. *J. Biol. Chem.*, **274**, 67-71.

29. Otterlei, M., Warbrick, E., Nagelhus, T.A., Haug, T., Slupphaug, G., Akbari, M., Aas, P.A., Steinsbekk, K., Bakke, O. and Krokan, H.E. (1999) Post-replicative base excision repair in replication foci. *EMBO J.*, **18**, 3834-3844.

30. Graves, R.J., Felzenszwalb, I., Laval, J. and O'Connor, T.R. (1992) Excision of 5'-terminal deoxyribose phosphate from damaged DNA is catalyzed by the Fpg protein of *Escherichia coli*. *J. Biol. Chem.*, **267**, 14429-14435.

31. Dianov, G., Sedgwick, B., Daly, G., Olsson, M., Lovett, S. and Lindahl, T. (1994) Release of 5'-terminal deoxyribose-phosphate residues from incised abasic sites in DNA by the *Escherichia coli* RecJ protein. *Nucleic Acids Res.*, **22**, 993-998.

32. Barzilay, G. and Hickson, I. D. (1995) Structure and function of apurinic/apyrimidinic endonucleases. *Bioessays*, **17**, 713-719.

33. Kubota, Y., Nash, R.A., Klungland, A., Schar, P., Barnes, D.E. and Lindahl, T. (1996) Reconstitution of DNA base excison-repair with purified human proteins: interaction between DNA polymerase beta and the XRCC1 protein. *EMBO J.*, **15**, 6662-6670.

34. Caldecott, K.W., Aoufouchi, S., Johnson, P. and Shall, S. (1996) XRCC1 polypeptide interacts with DNA polymerase beta and possibly poly (ADP-ribose) polymerase, and DNA ligase III is a novel molecular "nick-sensor" *in vitro*. *Nucleic Acids Res.*, **24**, 4387-4394.

35. Matsumoto, Y., Kim, K. and Bogenhagen, D.F. (1994) Proliferating cell nuclear antigen-dependent abasic site repair in *Xenopus laevis* oocytes: an alternative pathway of base excision DNA repair. *Mol. Cell. Biol.*, **14**, 6187-6197.

36. Matsumoto, Y., Kim, K., Hurwitz, J., Gary, R., Levin, D.S., Tomkinson, A.E. and Park, M.S. (1999) Reconstitution of proliferating cell nuclear antigen-dependent repair of apurinic/apyrimidinic sites with purified human proteins. *J. Biol. Chem.*, **274**, 33703-33708.

37. Frosina, G., Fortini, P., Rossi, O., Carrozzino, F., Raspoaglio, G., Cox, L.S., Lane, D.P., Abbondandolo, A. and Dogliotti, E. (1996) Repair of abasic sites by mammalian cell extracts. *J. Biol. Chem.*, **271**, 9573-9578.

38. Wu, X., Li, J., Li, X., Hsih, C.L., Burgers, P.M. and Lieber, M.R. (1996) Processing of branched DNA intermediates by a complex of human FEN-1 and PCNA. *Nucleic Acids Res.*, **24**, 2036-2043.

39. Cooper, P.K., Nouspikel, T., Clarkson, S.G. and Leadon, S.A. (1997) Defective transcription-coupled repair of oxidative base damage in Cockayne syndrome patients from XP group G. *Science*, **275**, 990-993.

40. Klungland, A., Hoss, M., Gunz, D., Constantinou, A., Clarkson, S.G., Doetsch, P.W., Bolton, P.H., Wood, R.D. and Lindahl, T. (1999) Base excision repair of oxidative DNA damage activated by XPG protein. *Mol. Cell*, **3**, 33-42.

41. Osheroff, W.P., Jung, H.K., Beard, W.A., Wilson, S.H. and Kunkel, T.A. (1999) The fidelity of DNA polymerase beta during distributive and processive DNA synthesis. *J. Biol. Chem.* **274**, 3642-3650.

42. Beard, W.A. and Wilson, S.H. (1998) Structural insights into DNA polymerase beta fidelity: hold tight if you want it right. *Chem. Biol.* **5**, 7-13.

43. Bhagwat, A.S., Sanderson, R.J. and Lindahl, T. (1999) Delayed DNA joining at 3' mismatches by human DNA ligases. *Nucleic Acids Res.*, **27**, 4028-4033.

44. Hoss, M., Robins, P., Naven, T.J., Pappin, D.J., Sgouros, J. and Lindahl, T. (1999) A human DNA editing enzyme homologous to the *Escherichia coli* DnaQ/MutD protein. *EMBO J.*, **18**, 3868-3675.

45. Mazur, D.J. and Perrino, F.W. (1999) Identification and expression of the TREX1 and TREX2 cDNA sequences encoding mammalian 3'–> 5' exonucleases. *J. Biol. Chem.*, **274**, 19655-19660.

46. Gorman, M.A., Morera, S., Rothwell, D.G., de La Fortelle, E., Mol, C.D., Tainer, J.A., Hickson, I.D. and Freemont, P.S. (1997) The crystal structure of the human DNA repair endonuclease HAP1 suggests the recognition of extra-helical deoxyribose at DNA abasic sites. *EMBO J.*, **16**, 6548-6558.

47. Lindahl, T. and Wood, R.A. (1999) Quality Control by DNA Repair. *Science*, **286**, 1897-1905.

48. Wilson, D.M. and Thompson, L.H. (1997) Life without DNA repair. *Proc. Natl. Acad. Sci. USA*, **94**, 72754-72757.

49. Ma, L., Hoeijmakers, J.H.J. and van der Eb, A.J. (1995) Mammalian nucleotide excision repair. *Biochim. Biophys. Acta*, **1242**, 137-164.

50. Cleaver, J.E. and Kraemer, K.H (1989) *The Metabolic Basis of Inherited Disease.* New York: McGraw-Hill.

51. Grossman, L. and Thiagalingam, S. (1993) Nucleotide excision repair, a tracking mechanism in search of damage. *J. Biol. Chem.*, **268**, 16871-16874.

52. Araujo, S.J. and Wood, R.D. (1999) Protein complexes in nucleotide excision repair. *Mutat. Res.*, **435**, 23-33.

53. Wood, R.D. (1996) DNA repair in eukaryotes. *Annu. Rev. Biochem.*, **65**, 135-167.

54. Hoeijmakers, J.H.J. (1993) Nucleotide excision repair II: From yeast to mammals. *Trends Genet.*, **9**, 211-217.

55. Sargent R.G., Rolig, R.L., Kilburn, A.E., Adair, G.M., Wison, J.H. and Nairn, R.S. (1997) Recombination-dependent deletion formation in mammalian cells deficient in the nucleotide excision repair gene ERCC1. *Proc. Natl. Acad. Sci. USA*, **94**, 13122-13127.

56. Sugasawa, K., Ng, J.M., Masutani, C., Iwai, S., van der Spek, P.J., Eker, A.P., Hanaoka, F., Bootsma, D. and Hoeijmakers, J.H. (1998) Xeroderma pigmentosum group C protein complex is the initiator of global genome nucleotide excision repair. *Mol. Cell*, **2**, 223-232.

57. Wakasugi, M. and Sancar, A. (1999) Order of Assembly of Human DNA Repair Excision Nuclease. *J. Biol. Chem.*, **274**, 18759-18768.

58. Mu, D., Park, C.H., Matsunaga, T., Hsu, D.S., Reardon, J.T. and Sancar, A. (1995) Reconstitution of human DNA repair excision nuclease in a highly defined system. *J. Biol. Chem.*, **270**, 2415-2418.

59. Mu, D., Hsu, D.S. and Sancar, A. (1996) Reaction mechanism of human DNA repair excision nuclease. *J. Biol. Chem.*, **271**, 8285-8294.

60. Wakasugi, M. and Sancar, A. (1998) Assembly, subunit composition, and footprint of human DNA repair excision nuclease. *Proc. Natl. Acad. Sci. USA*, **95**, 6669-6674.

61. Stefanini, M., Gilliani, S., Nardo, T., Marinoni, S., Nazzaro, R., Rizzo, R. and Trevisan, G. (1992) DNA repair investigations in nine Italian patients affected by trichothiodystrophy. *Mutat. Res.*, **273**, 119-125.

62. Harrington, J.J. and Lieber, M.R. (1994) Functional domains within FEN-1 and RAD2 define a family of structure-specific endonucleases: implication for nucleotide excision repair. *Genes Dev.*, **8**, 1344-1355.

63. O'Donovan, A., Davies, A., Moggs, J.G., West, S.C. and Wood, R.D. (1994) XPG endonuclease makes the 3' incision in human DNA nucleotide excision repair. *Nature*, **371**, 432-435.

64. Wood, R. and Shivji, M. (1997) Which DNA polymerases are used for DNA-repair in eukaryotes?. *Carcinogenesis*, **18**, 605-610.

65. Budd, M.E. and Campbell, J.L. (1997) The roles of the eukaryotic DNA polymerases in DNA repair synthesis. *Mutat. Res.*, **384**, 157-167.

66. Nichols, A.F., Ong, P. and Linn, S. (1996) Mutations specific to the xeroderma pigmentosum group I Ddb-phenotype. *J. Biol. Chem.*, **271**, 24317-24320.

67. Hwang, B.J., Toering, S., Francke, U. and Chu, G. (1998) p48 activates a UV-damaged-DNA binding factor and is defective in xeroderma pigmentosum group E cells that lack binding activity. *Mol. Cell. Biol.*, **18**, 4391-4399.

68. Hwang, B.J., Ford, J.M., Hanawalt, P.C. and Chu, G. (1999) Expression of the p48 xeroderma pigmentosum gene is p53-dependent and is involved in global genomic repair. *Proc. Natl. Acad. Sci. USA*, **96**, 424-428.

69. Batty, D.P. and Wood, R.D. (2000) Damage recognition in nucleotide excision repair of DNA. *Gene*, **241**, 193-204.

70. Otrin, V., McLenigan, M., Takao, M., Levine, A. and Protic, M. (1997) Translocation of a UV-damaged DNA binding protein into a tight association with chromatin after treatment of mammalian cells with UV light. *J. Cell Sci.*, **110**, 1159-1168.

71. Hanawalt, P.C. (1994) Trancription-coupled repair and human disease. *Science*, **266**, 1957-1958.

72. Bohr, V.A., Smith V.A, Okumoto, D.S. and Hanawalt (1985) DNA repair in an active gene: removal of pyrimidine dimers from the DHFR gene of CHO cells is much more efficient than in the genome overall. *Cell*, **40**, 359-369.

73. Mellon, I. and Hanawalt, P.C. (1989) Induction of the *Escherichia coli* lactose operon selectively increases repair of its transcribed DNA strand. *Nature*, **342**, 95-98.

74. Mellon, I., Spivak, G. and Hanawalt P.C. (1987) Selective removal of transcription-blocking DNA damage from the transcribed strand of the mammalian DHFR gene. *Cell*, **51**, 214-249.

75. Venema, J., van Hoffen, A., Karcagi, V., Natarajan, A.T., van Zeeland, A.A. and Mullenders, L.H.F. (1991) Xeroderma pigmentosum complementation group C cells remove pyrimidine dimers selectively from the transcribed strand of active genes. *Mol. Cell. Biol.*, **11**, 4128-4134.

76. Kantor, G.J., Barsalou, L.S. and Hanawalt, P.C. (1990) Selective repair of specific chromatin domains in UV-irradiated cells from xeroderma pigmentosum complementation group C. *Mutat. Res.*, **235**, 171-180.

77. Mu, D and Sancar, A. (1997) Model for XPC-independent transcription-coupled repair of pyrimidine dimers in humans. *J. Biol. Chem.*, **272**, 7570-7573.

78. Selby, C.P. and Sancar A. (1994) Mechanisms of transcription-repair coupling and mutation frequency decline. *Microbiol. Rev.*, **58**, 317-329.

79. Drapkin, R., Sancar, A. and Reinberg, D. (1994) Where transcription meets repair. *Cell*, **77**, 9-12.

80. Modrich, P. and Lahue, R. (1996) MISMATCH REPAIR IN REPLICATION FIDELITY, GENETIC RECOMBINATION AND CANCER BIOLOGY. *Annu. Rev. Biochem.*, **65**, 101-133.

81. Kolodner, R.D. and Marsishky G.T. (1999) Eukaryotic DNA mismatch repair. *Curr. Opin. Genet. Dev.*, **9**, 89-96.

82. Jiricny, J. (1998) Eukaryotic mismatch repair: an update. *Mutat. Res.*, **409**, 107-121.

83. Modrich, P. (1991) Mechanisms and biological effects of mismatch repair. *Annu. Rev. Genet.*, **25**, 229-253.

84. Lahue, R.S., Au, D.G. and Modrich, P. (1989) DNA mismatch correction in a defined system. *Science*, **245**, 160-164.

85. Parker, B.O. and Marinus, M.G. (1992) Repair of DNA heteroduplexes containing small heterologous sequences in *Escherichia coli*. *Proc. Natl. Acad. Sci. USA*, **89**, 1730-1734.

86. Su, S.-S. and Modrich, P. (1986) *Escherichia coli* mutS-encoded protein binds to mismatched DNA base pairs. *Proc. Natl. Acad. Sci. USA*, **83**, 5057-5061.

87. Su, S.-S., Lahue, R.S., Au, K.G. and Modrich, P. (1988) Mispair specificity of methyl-directed DNA mismatch correction *in vitro*. *J. Biol. Chem.*, **253**, 6829-6835.

88. Grilley, M., Welsh, K.M., Su, S.-S. and Modrich, P. (1989) Isolation and characterization of the *Escherichia coli* mutL gene product. *J. Biol. Chem.*, **264**, 1000-1004.

89. Galio, L., Bouquet, C. and Brooks, P. (1999) ATP hydrolysis-dependent formation of a dynamic ternary nucleoprotein complex with MutS and MutL. *Nucleic Acids Res.*, **27**, 2325-2331.

90. Joshi, A., Sen, S. and Rao, B.J. (2000) ATP-hydrolysis-dependent conformational switch modulates the stability of MutS-mismatch complexes. *Nucleic Acids Res.*, **28**, 853-861.

91. Allen, D.J, Makhov, A., Grilley, M., Taylor, J., Thresher, R., Modrich, P. and Griffith, J.D. (1997) MutS mediates heteroduplex loop formation by a translocation mechanism. *EMBO J.*, **16**, 4467-4476.

92. Drotschmann, K., Aronshtam, A., Fritz, H.J. and Marinus, M.G. (1998) The *Escherichia coli* MutL protein stimulates binding of Vsr and MutS to heteroduplex DNA. *Nucleic Acids Res.*, **26**, 948-953.

93. Grilley, M., Griffith, J. and Modrich, P. (1993) Bidirectional excision in methyl-directed mismatch repair. *J. Biol. Chem.*, **268**, 11830-11837.

94. Welsh, K.M., Lu, A.-L., Clark, S. and Modrich, P. (1987) Isolation and characterization of the *Escherichia coli* mutH gene product. *J. Biol. Chem.*, **262**, 15624-15631.

95. Au, K.G., Welsh, K. and Modrich, P. (1992) Initiation of methyl-directed mismatch repair. *J. Biol.Chem.*, **267**, 12142-12148.

96. Hall, M.C. and Matson, S.W. (1999) The *Escherichia coli* MutL protein physically interacts with MutH and stimulates the MutH-associated endonuclease activity. *J. Biol. Chem.*, **274**, 1306-1312.

97. Hall, M.C., Jordan, J.R. and Matson, S.W. (1998) Evidence for a physical interaction between the *Escherichia coli* methyl-directed mismatch repair proteins MutL and UvrD. *EMBO J.*, **17**, 1535-1541.

98. Yamaguchi, M., Dao V. and Modrich, P. (1998) MutS and MutL activate DNA helicase II in a mismatch-dependent manner. *J. Biol. Chem.*, **273**, 9197-9201.

99. Dao, V. and Modrich, P. (1998) Mismatch-, MutS-, MutL- and helicase II-dependent unwinding from the single-strand break of an incised heteroduplex. *J. Biol. Chem.*, **273**, 9202-9207.

100. Lovett, S.T. and Kolodner, R.D. (1989) Identification and purification of a single-stranded-DNA-specific exonuclease encoded by the recJ gene of *Escherichia coli*. *Proc. Natl. Acad. Sci. USA*, **86**, 2627-2631.

101. Chase, J.W. and Richardson, C.C. (1974) Exonuclease VII of Escherichia coli. Mechanism of action. *J. Biol. Chem.*, **249**, 45553-45561.

102. Grenert, J.P., Johnson, B.D. and Toft, D.O. (1999) The importance of ATP binding and hydrolysis by hsp90 in formation and function of protein heterocomplexes. *J. Biol. Chem.*, **274**, 17525-17533.

103. Ban, C. and Yang, W. (1998) Crystal structure and ATPase activity of MutL: implications for DNA repair and mutagenesis. *Cell*, **95**, 541-552.

104. Ban, C., Junop, M. and Yang, W. (1999) Transformation of MutL by ATP binding and hydrolysis: a switch in DNA mismatch repair. *Cell*, **97**, 85-97.

105. Fishel, R. and Wilson, T. (1997) MutS homologs in mammalian cells. *Curr. Opin. Genet. Dev.*, **7**, 105-113.

106. Alani, E., Chi, N.W. and Kolodner, R. (1995) The *Saccharomyces cerevisiae* MSH2 protein specifically binds to duplex oligonucleotides containing mismatched DNA base pairs and insertions. *Genes Dev.*, **9**, 234-247.

107. Haber, L.T. and Walker, G.C. (1991) Altering the conserved nucleotide binding motif in the *Salmonella typhimurium* MutS mismatch repair protein affects both its ATPase and mismatch binding activities. *EMBO J.*, **10**, 2702-2715.

108. Drummond, J. T., Li, G.-M., Longley, M. J. and Modrich, P. (1995) Isolation of an hMSH2-p160 heterodimer that restores DNA mismatch repair to tumor cells. *Science* **268**, 1909-1912.

109. Acharya, S., Wilson, T., Gradia, S., Kane, M.F., Guerrette, S., Marsischky, G.T., Kolodner, R. and Fishel, R. (1996) hMSH2 forms specific mispair-binding complexes with hMSH3 and hMSH6. *Proc. Natl. Acad. Sci. USA*. **93**, 13629-13634.

110. Fishel, R.A., Lescoe, M.K., Rao, M.R.S., Copland, N., Jenkins, N., Garber, J., Kane, M. and Kolodner, R. (1993) The human mutator gene homolog MSH2 and its association with hereditary nonpolyposis colon cancer. *Cell*, **75**, 1027-1038.

111. Palombo, F., Hughes, M., Jiricny, J., Truong, O. and Hsuan, J. (1994) Mismatch repair and cancer. *Nature*, **367**, 417-419.

112. Fishel, R., Ewel, A. and Lescoe, M.K. (1994) Purified human MSH2 protein binds to DNA containing mismatched nucleotides. *Cancer Res.*, **54**, 5539-5542.

113. Fishel, R., Ewel, A., Lee, S., Lescoe, M.K. and Griffith, J. (1994) Binding of mismatched microsatellite DNA sequences by the human MSH2 protein. *Science*, **266**, 1403-1405.

114. Branch, P., Aquilina, G., Bignami, M. and Karran, P. (1995) DNA mismatch binding defects, DNA damage tolorance, and mutator phenotypes in human colorectal carcinoma cell lines. *Cancer Res.*, **55**, 2304-2309.

115. Orth, K., Hung, J., Gazdar, A., Bowcock, A., Mathis, J.M. and Sambrook, J. (1994) Genetic instability in human ovarian cancer cell lines. *Proc. Natl. Acad. Sci. USA*, **91**, 9495-9499.

116. Umar, A., Risinger, J.I., Glaab, W.E., Tindall, K.R., Barrett, J.C. and Kunkel, T.A. (1998) Functional overlap in mismatch repair by human MSH3 and MSH6. *Genetics*, **148**, 1637-1646.

117. Palombo, F., Gallinari, P., Iaccarino, I., Lettieri, T., Hughes, M., D'Arrigo, A., Truong, O., Hsuan, J. J. and Jiricny, J. (1995) GTBP, a 160-kilodalton protein essential for mismatch-binding activity in human cells. *Science*, **268**, 1912-1914.

118. Hughes, M.J. and Jiricny, J. (1992) The purification of a human mismatch-binding protein and identification of its associated ATPase and helicase activities. *J. Biol. Chem.*, **267**, 23876-23882.

119. Alani, E. (1996) The *Saccharomyces cerevisiae* Msh2 and Msh6 proteins form a complex that specifically binds to duplex oligonucleotides containing mismatched DNA base pairs. *Mol. Cell. Biol.* **16**, 5604-5615.

120. Iaccarino, I., Marra, G., Palombo, F. and Jiricny, J. (1998) hMSH2 and hMSH6 play distinct roles in mismatch binding and contribute differently to the ATPase activity of hMutSα. *EMBO J.*, **17**, 2677-2686.

121. Gradia, S., Acharya, S. and Fishel, R. (1997) The human mismatch recognition complex hMSH2-hMSH6 functions as a novel molecular switch. *Cell*, **91**, 995-1005.

122. Alani, E., Sokolsky, T., Studamaire, B., Miret, J.J. and Lahue, R.S. (1997) Genetic and biochemical analysis of Msh2p-Msh6p: role of ATP hydrolysis and Msh2p-Msh6p subunits interactions in mismatch base pair recognition. *Mol. Cell. Biol.*, **17**, 2436-2447.

123. Studamire, B., Quach, T. and Alani, E. (1998) *Saccharomyces cerevisiae* Msh2p and Msh6p ATPase activities are both required during mismatch repair. *Mol. Cell. Biol.*, **18**, 7590-7601.

124. Gradia, S., Acharya, S. and Fishel, R. (2000) The Role of Mismatched Nucleotides in Activating the hMSH2-hMSH6 Molecular Switch. *J. Biol. Chem.*, **275**, 3922-3930.

125. Blackwell, L.J., Martik, D., Bjornson., K.P., Bjornson, E.S. and Modrich, P. (1998) Nucleotide-promoted release of hMutS from heteroduplex DNA is consistent with an ATP-dependent translocation mechanism. *J. Biol. Chem.*, **273**, 32055-32062.

126. Gradia, S., Subramanian, S., Wilson, T., Acharya, S., Makhov, A., Griffith, J. and Fishel, R. (1999) hMSH2-hMSH6 Forms a Hydrolysis-Independent Sliding Clamp on Mismatched DNA. *Mol. Cell*, **3**, 255-261.

127. Blackwell, L.J., Bjornson, K.P. and Modrich, P. (1998) DNA-dependent activation of the hMutSalpha ATPase. *J. Biol. Chem.*, **273**, 32049-32054.

128. Miyaki, M., Konishi, M. Tanaka, K., Kikuchi-Yanoshita, R., Muraoda, M., Yasuno, M., Igari, T., Koike, M., Chiba, M. and Mori, T. (1997) Germline mutation of MSH6 as the cause of hereditary nonpolyposis colorectal cancer. *Nat. Genet.*, **17**, 271-272.

129. Papadopoulos, N., Nicolaides, N.C., Liu, B., Parsons, R., Lengauer, C., Palombo, F., D'Arrigo, A., Markowitz, S., Wilson, J.K., Kinzler, K.W., et. al. (1995) Mutations of GTBP in genetically unstable cells. *Science*, **263**, 1915-1917.

130. Edelman, W., Yang, K., Umar, A., Heyer, J., Lau, K., Fan, K., Liedtke, W., Cohen, P.E., Kane, M.F., Lipford, J.R., Yu, N., Crouse, G.F., Pollard, J.W., Kunkel, T., Lipken, M., Kolodner, R. and Kucherlapati, R. (1997) Mutation in the mismatch repair gene Msh6 causes cancer susceptibility. *Cell*, **91**, 467-477.

131. Genshel, J., Littman, S.J., Drummond, J.T. and Modrich, P. (1998) Isolation of MutSβ from human cells and comparison of the mismatch repair specificities of MutSβ and MutSα. *J. Biol. Chem.*, **273**, 19895-19901.

132. Guerette, S., Wilson, T. Gradia, S. and Fishel, R. (1998) Interactions of human hMSH2 with hMSH3 and hMSH2 with hMSH6: examination of mutations found in hereditary nonpolyposis colorectal cancer. *Mol. Cell. Biol.*, **18**, 6616-6623.

133. Palombo, F., Iaccarino, I., Nakajima, E., Ikejima, M., Shimado, T. and Jicicny, J. (1996) hMutSβ, a heterodimer of hMSH2 and hMSH3, binds to insertion/deletion loops in DNA. *Curr. Biol.,* **6**, 1181-1184.

134. Habraken, Y., Sung, P., Prakash, L. and Prakash, S. (1996) Binding of insertion/deletion DNA mismatches by the heterodimer of yeast mismatch repair proteins MSH2 and MSH3. *Curr. Biol.*, **6**, 1185-1187.

135. Wilson, T., Guerrette, S. and Fishel, R. (1999) Dissociation of Mismatch Recognition and ATPase Activity by hMSH2-hMSH3. *J. Biol. Chem.*, **274**, 21659-21664.

136. Hinz, J.M. and Meuth, M. (1999) MSH3 deficiency is not sufficient for a mutator phenotype in Chinese hamster ovary cells. *Carcinogenesis*, **20**, 215-220.

137. Marra, G., Iaccarino, E., Lettieri, T., Roscilli, G., Delmastro, P. and Jiricny, J. (1998) Mismatch repair deficiency associated with overexpression of the MSH3 gene. *Proc. Natl. Acad. Sci. USA*, **21**, 8568-8573.

138. Hollingsworth, N.M., Ponte, L. and Halsey, C. (1995) MSH5, a novel MutS homolog, facilitates meiotic reciprocal recombination between homologs in *Saccharomyces cerevisiae* but not mismatch repair. *Genes Dev.*, **9**, 975-985.

139. Paquis-Flucklinger, V., Santucci-Darmanin, S., Saunieres, A., Turc-Carel, C. and Desnuelle, C. (1997) Cloning and expression analysis of a meiosis-specific MutS homolog: the human MSH4 gene. *Genomics*, **44**, 188-194.

140. Bocker, T., Barusevicius, A., Snowden, T., Rasio, D., Guerrette, S., Robbins, D., Schmidt, C., Burczak, J., Croce, C.M., Copeland, T., Kovatich, A.J. and Fishel, R. (1999) hMSH5: A Human MutS homologue That Forms a Novel Heterodimer with hMSH4 and Is Expressed during Spermatogenesis. *Cancer Res.*, **59**, 816-822.

141. Winand, N.J., Panzer, J.S. and Kolodner, R. (1998) Cloning and characterization of the human and *Caenorhabditis elegans* homologs of the *Saccharomyces cerevisiae* MSH5 gene. *Genomics*, **53**, 69-80.

142. Her, C. and Doggett, N.A. (1998) Cloning, structural characterization, and chromosomal localization of the human orthologue of *Saccharomyces cerevisiae* MSH5 gene. *Genomics*, **53**, 50-61.

143. Ross-Macdonald, P. and Roeder, G.S. (1994) Mutation of a meiosis-specific MutS homolog decreases crossing over but not mismatch correction. *Cell*, **79**, 1069-1080.

144. Edelmann, W., Cohen, P., Knetz, B., Winand, N., Heyer, J., Kolodner, R., Pollard, J.W. and Kucherlapati, R. (1999) Mammalian MutS homolog 5 is required for chromosome pairing in meiosis. *Nat. Genet.*, **19**, 123-127.

145. Hunter, N. and Borts, R.H. (1997) Mlh1 is unique among mismatch repair proteins in its ability to promote crossing-over during meiosis. *Genes Dev.*, **11**, 1573-1582.

146. Nicolaides, N.C., Papdopoulos, N., Liu, B., Swl, Y.-F, Carter, K.C., Ruben, S.M., Rosen, C.A., Haseltine, W.A., Fleishmann, R.D., Fraser, C.M., Adams, M.D., Venter, J.C., Dunlop, M.G., Hamilton, S.R., Peterson, G.M. de la Chapelle, A., Vogelstein, B. and Kinzler, K.W. (1994) Mutations of two PMS homologues in hereditary nonpolyposis colon cancer. *Nature*, **371**, 75-80.

147. Papadopoulos, N., Nicolaides, N.C., Wei, Y.-F., Ruben, S.M., Carter, K.C., Rosen C.A., Haseltine, W.A., Fleischmann, R.D., Fraser, C.M., Adams, M.D., et. al. (1994) Mutation of a mutL homolog in hereditary colon cancer. *Science*, **263**, 1625-1629.

148. Bronner, C.E., Baker, S.M., Morrison, P.T., Warren, G., Smith, L.G., Lescoe, M.K., Kane, M., Earabino, C., Lipford, J., Lindblom, A., Tannerfard, P., Bollag, R.J., Godwin, A.R., Ward, D.C., Nordenskjold, M., Fishel, R., Kolodner, R. and Liskay, R.M. (1994) Mutation in the DNA mismatch repair gene homologue hMLH1 is associated with hereditary nonpolyposis colon cancer. *Nature*, **368**, 258-261.

149. Yanagisawa, Y., Akiyama, Y., Iida, S., Ito, E., Nomizu, T., Sugihara, K., Yuasa, Y. and Maruyama, K. (2000) Methylation of the hMLH1 promoter in familial gastric cancer with microsatellite instability. *Int. J. Cancer*, **85**, 50-53.

150. Esteller, M., Catasus, L., Matias-Guiu, X., Mutter, G.L., Prat, J., Baylin, S.B. and Herman, J.G. (1999) hMLH1 promoter hypermethylation is an early event in human endometrial tumorigenesis. *Am. J. Pathol.*, **155**, 1767-1772.

151. Deng, G., Chen, A., Hong, J., Chae, H.S. and Kim, Y.S. (1999) Methylation of CpG in a small region of the hMLH1 promoter invariably correlates with the absence of gene expression. *Cancer Res.*, **59**, 2029-2033.

152. Strathdee, G., MacKean, M.J., Illand, M. and Brown, R. (1999) A role for methylation of the hMLH1 promoter in loss of hMLH1 expression and drug resistance in ovarian cancer. *Oncogene*, **18**, 2335-2341.

153. Bhattacharyya, N.P., Skandalis, A., Ganesh, A., Groden, J. and Meuth, M. (1994) Mutator phenotype in human colorectal carcinoma cell lines. *Proc. Natl. Acad. Sci. USA*, **91**, 6319-6323.

154. Eshelman, J.R., Lang, E.Z., Bowerfind, G.K., Parsons, R., Vogelstein, B., Wilson, J.K.V., Veigl, M.L., Sedwick, W.D. and Markowitz, S.D. (1995) Increased mutation rate at the *hprt* locus accompanies microsatellite instability in colon cancer. *Oncogene*, **10**, 33-37.

155. Umar, A., Boyer, J.C. and Kunkel, T.A. (1994) DNA loop repair by human cell extracts. *Science*, **266**, 814-816.

156. Umar, A., Boyer, J.C., Thomas, D.C., Nguyen, D.C., Risinger, J.L, Boyd, J. Ionov, Y., Perucho, M and Kunkel, T.A. (1994) Defective mismatch repair in extracts of colorectal and endometrial cancer cell lines exhibiting microsatellite instability. *J. Biol. Chem.*, **269**, 14367-14370.

157. Risinger, J.I., Umar, A., Barrett, J.C. and Kunkel, T.A. (1995) A hPMS2 mutant cell line is defective in strand-specific mismatch repair. *J. Biol. Chem.*, **270**, 18183-18186.

158. Li, G.M. and Modrich, P. (1995) Restoration of mismatch repair to nuclear extracts of H6 colorectal tumor cells by a heterodimer of human MutL homologs. *Proc. Natl. Acad. Sci. USA*, **92**, 1950-1954.

159. Raschle, M., Marra, G., Nystrom-Lahti, M., Schar, P., and Jiricny, J. (1999) Identification of hMutLβ, a Heterodimer of hMLH1 and hPMS1. *J. Biol. Chem.* **274**, 32368-32375.

160. Pang, Q., Prolla, T.A. and Liskay, R.M. (1997) Functional domains of the *Saccharomyces cerevisiae* Mlh1p and Pms1p DNA mismatch repair proteins and their relevance to human hereditary nonpolyposis colorectal cancer-associated mutations. *Mol. Cell. Biol.*, **17**, 4465-4473.

161. Flores-Rozas, H. and Kolodner, R.D. (1998) The *Saccharomyces cerevisiae* MLH3 gene functions in MSH3-dependent suppression of frameshift mutations. *Proc. Natl. Acad. Sci. USA*, **95**, 12404-12409.

162. Prolla, T.A., Pang, Q., Alani, E., Kolodner, R.D. and Liskay, R.M. (1994) MLH1, PMS1 and MSH2 interactions during the initiation of DNA mismatch repair in yeast. *Science*, **265**, 1091-1093.

163. Habraken, Y., Sung, P., Prakash, L. and Prakash, S. (1998) ATP-dependent Assembly of a Ternary Complex Consisting of a DNA Mismatch and the Yeast MSH2-MSH6 and MLH1-PMS1 Protein Complex. *J. Biol. Chem.*, **273**, 9837-9841.

164. Habraken, Y., Sung, P., Prakash, L. and Prakash, S. (1997) Enhancement of MSH2-MSH3-mediated mismatch recognition by the yeast MSH1-PMS1 complex. *Curr. Biol.*, **7**, 790-793.

165. Gu, L., Hong, Y., McCulloch, S., Watanabe, H. and Li, G.M. (1998) ATP-dependent interaction of human mismatch repair proteins and dual role of PCNA in mismatch repair. *Nucleic Acids Res.*, **26**, 1173-1178.

166. Umar, A., Buermeyer, A.B., Simon, J.A., Thomas, D.C., Clark, A.B., Liskay, R.M. and Kunkel, T.A. (1996) Requirement for PCNA in DNA mismatch repair at a step preceding DNA resynthesis. *Cell*, **87**, 65-73.

167. Johnson, R.E., Kovvali, G.D., Guzder, S.M., Amin, N.S., Hom, C., Habraken,Y., Sung, P., Prakash, L. and Prakash, S. (1996) Evidence for involvement of yeast proliferating cell nuclear antigen in DNA mismatch repair. *J. Biol. Chem.*, **271**, 27987-27990.

168. Schmutte, C., Marinescu, R.C., Sadoff, M.M., Guerrette, S., Overhauser, J. and Fishel, R. (1998) Human exonuclease I interacts with the mismatch repair protein hMSH2. *Cancer Res.*, **58**, 4537-4542.

169. Skankasi, P. and Smith, G.R. (1995) A role for exonuclease I from *S. pombe* in mutation avoidance and mismatch correction. *Science*, **267**, 1166-1169.

170. Tishkoff, D.X., Boerger, A.L., Bertrand, P., Filosi, N., Gaida, G.M., Kane, M.F. and Koldner, R.D. (1997) Identification and characterization of *Saccharomyces cerevisiae* EXO1, a gene encoding an exonuclease that interacts with MSH2. *Proc. Natl. Acad. Sci. USA*, **94**, 7487-7492.

171. Tishkoff, D.X., Filosi, N., Gaida, G.M. and Kolodner, R.D. (1997) A novel mutation avoidance mechanism dependent on *S. cerevisiae* RAD27 is distinct from DNA mismatch repair. *Cell*, **88**, 253-263.

172. Longley, M.J., Pierce, A.J. and Modrich, P. (1997) DNA polymerase delta is required for human mismatch repair *in vitro*. *J. Biol.Chem.*, **272**, 10917-10921.

173. Lin, Y.L., Shivji, M.D., Chen, C., Kolodner, R.D., Wood, R.D. and Dutta, A. (1998) The evolutionary conserved zinc finger motif in the largest subunit of human replication protein A is required for DNA replication and mismatch repair but not for nucleotide excision repair. *J. Biol. Chem.*, **273**, 1453-1461.

174. Hare, J.T. and Taylor, J.H (1985) One role for DNA methylation in vertebrate cells is strand discrimination in mismatch repair. *Proc. Natl. Acad. Sci. USA*, **82**, 7350-7354.

175. Holmes, J.J., Clark, S. and Modrich, P. (1990) Strand-specific mismatch correction in nuclear extracts of human and *Drosophila melongaster* cell lines. *Proc. Natl. Acad. Sci. USA*, **87**, 5837-5841.

176. Thomas, D.C., Roberts, J.D. and Kunkel T.A. (1991) Heteroduplex repair in extracts of human HeLa cells. *J. Biol. Chem.*, **266**, 3744-3751.

177. Brown, T.C. and Jiricny, J. (1987) A specific mismatch repair event protects mammalian cells from loss of 5-methylcytosine. *Cell*, **50**, 945-950.

178. Brown, T.C. and Jiricny, J. (1988) Different base/base mispairs are corrected with different efficiencies and specificities in monkey kidney cells. *Cell*, **54**, 705-711.

179. Mellon, I. and Champe, G.N. (1996) Products of DNA mismatch repair genes *mutS* and *mutL* are required for transcription-coupled nucleotide-excision repair of the lactose operon in *Escherichia coli. Proc. Natl. Acad. Sci. USA*, **93**, 1292-1297.

180. Mellon, I., Rajpal, D.K., Koi, M., Boland, C.R. and Champe, G.N. (1996) Transcription-coupled repair deficiency and mutations in human mismatch repair genes. *Science*, **272**, 557-560.

181. Leadon, S.A. and Avrutskaya, A.V. (1998) Requirement for DNA mismatch repair proteins in the transcription-coupled repair of thymine glycols in *Saccharomyces cerevisiae. Mutat. Res.* **407**, 177-187.

182. Bertrand, P., Tishkoff, D.X., Filosi, N., Dasgupta, R. and Kolodner, R.D. (1998) Physical interaction between components of DNA mismatch repair and nucleotide excision repair. *Proc. Natl. Acad. Sci. USA*, **95**, 14278-14283.

183. de Wind, N., Dekker, M., Berns, A., Radman, M. and te Riele, H. (1995) Inactivation of the mouse Msh2 gene results in mismatch repair deficiency, methylation tolerance, hyperrecombination, and predisposition to cancer, *Cell*, **82**, 321-330.

184. Karran, P. and Hampson, R. (1996) Genomic instability and tolerance to alkylating agents. *Cancer Surveys*, **28**, 69-85.

185. Kat, A., Thilly, W.G., Fang, W.H., Longley, M.J., Li, G.M. and Modrich, P. (1993) An alkylation-tolerant, mutator human cell line is deficient in strand-specific mismatch repair. *Proc. Natl. Acad. Sci. USA*, **90**, 6424-6428.

186. Goldmacher, V.S., Cuzick, R.A. and Thilly, W.G. (1986) Isolation and partial characterization of human cell mutants differing in sensitivity to killing and mutation by methylnitrosourea and N-methyl-N-nitro-N-nitosoguanidine. *J. Biol.Chem.*, **261**, 12462-12471.

187. Hawn, M.T., Umar, A., Carethers, J.M., Marra, G., Kunkel, T.A., Boland, C.R. and Koi, M. (1995) Evidence for a connection between the mismatch repair system and the G2 cell cycle checkpoint. *Cancer Res.*, **55**, 3721-3725.

188. Yamada, M., O'Regan, E., Brown, R. and Karran, P. (1997) Selective recognition of a cisplatin-DNA adduct by human mismatch repair proteins. *Nucleic Acids Res.*, **25**, 491-496.

189. Duckett, D.R., Drummond, J.T., Murchie, A.I.H., Reardon, J.T., Sancar, A., Lilley, D.M.J. and Modrich, P. (1996) Human MutSalpha recognized damaged DNA base pairs containing O6-methylguanine, O4-methlythymine, or the cisplatin-d(GpG) adduct. *Proc. Natl. Acad. Sci. USA*, **93**, 6443-6447.

190. Mello, J.A., Acharya, S., Fishel, R. and Essigmann, J.M. (1996)The mismatch-repair protein hMSH2 binds selectively to DNA adducts of the anticancer drug cisplatin. *Chem. Biol.*, **3**, 579-589.

191. Li, G.M., Wang, H. and Romano, L.J. (1996) Human MutSalpha specifically binds to DNA containing aminoflourene and acetylaminofluorene adducts. *J. Biol. Chem.*, **271**, 24084-24088.

192. Toft, N.J., Winton, D.J., Kelly, J., Howard, L.A., Dekker, M., Riele, H.T., Arends, M.J., Wyllie, A.H., Margison, G.P. and Clarke, A.R. (1999) Msh2 status modulates both apoptosis and mutation frequency in the murine small intestine. *Proc. Natl. Acad. Sci. USA*, **96**, 3911-3915.

193. Wu, J., Gu, L, Wang, H., Geacintov, N.E. and Li, G.M. (1999) Mismatch repair processing of carcinogen-DNA adducts triggers apoptosis. *Mol. Cell. Biol.*, **19**, 8292-8301.

194. Hickman, M.J. and Samson, L.D. (1999) Role of DNA mismatch repair and p53 in signaling induction of apoptosis by alkylating agents. *Proc. Natl. Acad. Sci. USA*, **96**, 10764-10769.

195. Duckett, D.R., Bronstein, S.M., Taya, Y. and Modrich, P. (1999) hMutSα- and hMutLα-dependent phosphorylation of p53 in response to DNA methylator damage. *Proc. Natl. Acad. Sci. USA*, **96**, 12384-12388.

196. Zhang, H., Richards, B., Wilson, T., Lloyd, M., Cranston, A., Thorburn, A., Fishel, R. and Meuth, M. (1999) Apoptosis induced by overexpression of hMSH2 or hMLH1. *Cancer Res.*, **59**, 3021-3027.

197. Kirkpatrick, D.T. and Petes, T.D. (1997) Repair of DNA loops involves DNA-mismatch and nucleotide-excision repair proteins. *Nature*, **387**, 929-931.

198. Sugawara, N., Paques, F., Colaiacovo, M. and Haber, J.E. (1997) Role of *Saccharomyces cerevisiae* Msh2 and Msh3 repair proteins in double-strand break-induced recombination. *Proc. Natl. Acad. Sci. USA*, **94**, 9214-9219.

199. Nicholson, A., Hendrix, M., Jinks-Robertson, S. and Crouse, G.F. (2000) Regulation of mitotic homeologous recombination in yeast. Function of mismatch repair and nucleotide excision repair genes. *Genetics*, **154**, 133-146.

200. Ciotta, C., Ceccotti, S., Aquilina, G., Humbert, O., Palombo, F., Jiricny, J. and Bignami, M. (1998) Increased somatic recombination in methylation tolerant human cells with defective DNA mismatch repair. *J. Mol. Biol.*, **276**, 705-719.

201. Drake, J.W., Charlesworth, B., Charlesworth, D. and Crow, J.F. (1998) Rates of Spontaneous Mutation. *Genetics*, **148**, 1667-1686.

202. Loechler, E.L. (1996) The role of adduct site-specific mutagenesis in understanding how carcinogen-DNA adducts cause mutations: perspective, prospects, and problems. *Carcinogenesis*, **17**, 895-902.

203. Barbacid, M. (1987) *ras* Genes. *Annu. Rev. Biochem.*, **56**, 779-827.

204. Bos, J.L. (1988) The *ras* gene family and human carcinogenesis. *Mutat. Res.*, **195**, 255-271.

205. Kiaris, H. and Spandidos, D.A. (1995) Mutations of ras genes in human tumors. *Int. J. Oncol.*, **7**, 413-421.

206. Dogliotti, E., Hainout, P., Hernandez, T., D'Errico, M. and DeMarini, D.M. (1998) Mutation Spectra Resulting from Carcinogenic Exposure: From Model Systems to Cancer-Related Genes. *Recent Results Cancer Res.*, **154**, 97-124.

207. Balmain, A. and Brown, K. (1988) Oncongene Activation in Chemical Carcinogenesis. *Adv. Cancer Res.*, **51**, 147-182.

208. Denissenko, M.F., Pao, A., Tang, M.-S. and Pfeifer, G.P. (1996) Preferential Formation of Benzo[a]pyrene Adducts at Lung Cancer Mutational Hotspots in p53. *Science*, **274**, 430-432.

209. Chen, J.X., Zheng, Y., West, M. and Tang, M.-S. (1998) Carcinogens Preferentially Bind at Methylated CpG in the p53 Mutational Hot Spots. *Cancer Res.*, **58**, 2070-2075.

210. Hoffman, J.-S., Fry, M., Ji, J., Williams, K.J. and Loeb, L.A. (1993) Codons 12 and 13 of H-*ras* Protooncogene Interrupt the Progression of DNA Synthesis Catalyzed by DNA Polymerase α. *Cancer Res.*, **53**, 2895-2900.

211. Kunala, S. and Brash, D.E. (1992) Excision repair at indivuidual bases of the *Escherichia coli lacI* gene: relation to mutation hotspots and transcription coupling activity. *Proc. Natl. Acad. Sci. USA*, **89**, 11031-11035.

212. Wei, D., Maher, V.M. and McCormick, J.J. (1995) Site specific rates of excision repair of benzo{a}pyrene diol epoxide adducts in the hypoxanthine phosphoribosyltransferase gene of human fibroblasts: correlation with mutation spectra. *Proc. Natl. Acad. Sci. USA*, **92**, 2204-2208.

213. Hanawalt, P.C. (1991) Heterogeneity of repair at the gene level. *Mutat. Res.*, **247**, 203-211.

214. Tornaletti, S. and Pfeifer, G.P. (1994) Slow Repair of Pyrimidine Dimers at p53 Mutation Hotspots in Skin Cancer. *Science*, **263**, 1436-1440.

215. Denissenko, M.F., Pao, A., Pfeifer, G.P. and Tang, M.-S. (1998) Slow repair of bulky DNA adducts along the nontranscribed strand of the human p53 gene may explain the strand bias of transversion mutations in cancers. *Oncogene*, **16**, 1241-1247.

216. Le Page, F., Margot, A., Grollman, A.P., Sarasin, A. and Gentil, A. (1995) Mutagenicity of a unique 8-oxoguanine in a human H-*ras* sequence in mammalian cells. *Carcinogenesis*, **16**, 2779-2784.

217. Pillaire, M., Margot, A., Villani, G., Sarasin, A., Defais, M. and Gentil, A. (1994) Mutagenesis in monkey cells of a vector containing a single d(GpG) cis-diamminedichloroplatinum(II) adduct placed on codon 13 of the human H-ras proto-oncogene. *Nucl. Acids Res.*, **22**, 2519-2524.

218. Bishop, R.E., Pauly, G.T. and Moschel, R.C. (1996) O^6-Ethylguanine and O^6-benzylguanine incorporated site-specifically in codon 12 of the rat H-*ras* gene induced semi-targeted as well as targeted mutations in Rat4 cells. *Carcinogenesis*, **17**, 849-856.

219. Fuchs, R.P. (1984) DNA binding spectrum of the carcinogen N-acetoxy acetyl amino fluorine significantly differs from the mutation spectrum. *J. Mol. Biol.*, **177**, 173-180.

220. Brash, D.E. and Haseltine, W.A. (1982) UV mutation hotspots occur at DNA damage hotspots. *Nature*, **298**, 189-192.

221. Levy, D.D., Magee, A.D., Namiki, C. and Seidman, M.M. (1996) The Influence of Single Base Changes on UV Mutational Activity at Two Translocated Hotspots. *J. Mol. Biol.*, **258**, 435-445.

222. Levy, D.D., Magee, A.D. and Seidman, M.M. (1996) Single Nucleotide Postions Have Proximal and Distal Influence on UV Mutation Hotspots and Coldspots. *J. Mol. Biol.*, **258**, 251-260.

223. Shibutani, S. and Grollman, A.P. (1993) On the mechanism of frameshift (deletion) mutagenesis *in vitro*. *J. Biol. Chem.*, **268**, 11703-11710.

224. Wang, F.J. and Ripley, L.S. (1994) DNA seqence effects on single base deletions arising during DNA polymerization *in vitro* by *E. coli* Klenow fragment polymerase. *Genetics*, 136, 709-719.

225. Kunkel, T.A. (1992) Biological asymmetries and the fidelity of eukaryotic DNA replication. *Bioessays*, **14**, 303-30.

226. Topal, M., Eadie, J.S. and Conrad, M. (1986) O^6-Methylguanine Mutation and Repair Is Nonuniform. *J. Biol. Chem.*, **261**, 9879-9885

227. Arcangeli, L., Simonetti, J., Pongrantz, C. and Williams, K.J. (1997) Site- and strand-specific mismatch repair of human H-*ras* genomic DNA in a mammalian cell line. *Carcinogenesis*, **18**, 1311-1318.

228. Arcangeli, L. and Williams, K.J. (1995) Mammalian assay for site-specific DNA damage processing using the human H-*ras* proto-oncogene. *Nucleic Acids Res.*, **23**, 2269-2276.

229. Sambrook, J., Fritsch, E.F. and Maniatis, T. (1989) *Molecular Cloning: A Laboratory Manual*, 2nd ed. Cold Spring Harbor University Press, Cold Spring Harbor, NY.

230. Yates, J., Warren, N. and Sugden, B. (1985) Stable replication of plasmids derived from Epstein-Barr virus in various mammalian cells. *Nature*, **313**, 812-815.

231. Higuchi, R. (1989) In Erlich, H.A (ed.), *PCR Technology*. Stockton Press, USA. pp. 31-38.

232. Dignum, J.D., Lebovitz, R.M. and Roeder, R.G. (1983) Accurate transcription initiation by RNA polymerase II in a soluble extract from isolated mammalian nuclei. *Nucleic Acids Res.*, **11**, 1475-1489.

233. Varlet, I., Radman, M. and Brooks, P. (1990) DNA mismatch repair in Xenopus egg extracts: repair efficiency and DNA repair synthesis for all single base-pair mismatches. *Proc. Natl. Acad. Sci. USA*, **87**, 7883-7887.

234. David, P., Efrati, E., Tocco, G., Krauss, S.W. and Goodman, M.F. (1997) DNA replication and postreplication mismatch repair in cell-free extracts from cultured human neuroblastoma and fibroblast cells. *J. Neurosci.*, **17**, 8711-8720.

235. Miller, E.M., Hough, H.L., Cho, J.W. and Nickoloff, J.A. (1997) Mismatch Repair by Efficient Nick-Directed and Less Efficient Mismatch-Specific Mechanisms in Homologous Recombination Intermediates in Chinese Hamster Ovary Cells. *Genetics*, **147**, 743-753.

236. Matton, N., Simonetti, J. and Williams, K. (1999) Inefficient *in vivo* repair of mismatches at an oncogenic hotspot correlated with lack of binding by mismatch repair proteins and with phase of the cell cycle. *Carcinogenesis*, **20**, 1417-1424.

237. Marsischky, G.T. and Kolodner, R.D. (1999) Biochemical Characterization of the Interaction between the *Saccharomyces cerevisiae* MSH2-MSH6 Complex and Mispaired Bases in DNA. *J. Biol. Chem.*, **274**, 26668-26682.

238. Yeh, Y.-C, Liu, H.-F, Ellis, C.A. and Lu, A.-L. (1994) Mammalian Topoisomerase I Has Base Mismatch Nicking Activity. *J. Biol. Chem.* **269**, 15498-15504.

239. Yao, M., Hatahet, Z., Melamede, R.J. and Kow, Y.W. (1994) Purification and Characterization of a Novel Deoxyinosine-specific Enzyme, Deoxyinosine 3' Endonuclease, from *Escherichia coli. J. Biol. Chem.*, **269**, 16260-16268.

240. Macpherson, P., Humbert, O. and Karran, P. (1998) Frameshift mismatch recognition by the human MutS alpha complex. *Mutat. Res.*, **408**, 55-66.

241. Zienolddiny, S., Ryberg, D., Gazdar, A.F. and Haugen, A. (1999) DNA mismatch binding in human lung tumor cell lines. *Lung Cancer*, **26**, 15-25.

242. Le Page, F., Guy, A., Cadet, J., Sarasin, A. and Gentil, A. (1998) Repair and mutagenic potency of 8-oxoG:A and 8-oxoG:C base pairs in mammalian cells. *Nucleic Acids Res.*, **26**, 1276-1281.